Gut-blood vessel interactions: short-chain fatty acids and protease-activated receptors

by

Erika L. Poitras

A thesis submitted in partial fulfillment of the requirements for the degree of

Master of Science

Department of Pharmacology
University of Alberta

Abstract

Background: Gut microbiota and diet, specifically fiber rich diets, have been associated with blood pressure regulation and cardiovascular health. Gut microbiota metabolize fiber into short-chain fatty acids (SCFAs) of which, acetate is the most abundant, followed by propionate and butyrate. It has been reported that these SCFAs cause a reduction in blood pressure *in vivo* and that this may be due to their direct vasorelaxation effect on blood vessels. My goal is to further understand gut to blood vessel interactions, specifically by investigating the effect of these SCFAs on blood vessels and the mechanism through which they may mediate their effects. In my research I aimed to address the hypothesis that **SCFAs have direct vasodilator actions on resistance arteries mediated through endothelium-dependent mechanisms.** In addition to this, I also aimed to investigate blood vessel to gut interactions with focus on regulation of gut motility. Gut motility is influenced by many factors including hormones, neural inputs, and pacemaker interstitial cells of Cajal (ICC). These pacemaker ICC express a receptor tyrosine-protein kinase, known as c-kit, that allows them to differentiate and develop and can be used as a cell surface marker for ICC. Previous work in our lab has shown that activation of protease-activated receptor 2 (PAR-2) by serine protease, trypsin, inhibits ICC initiated spontaneous contractile activity of colonic smooth muscle. Serine proteases that can activate PAR-2 such as trypsin, factor VIIa, and factor Xa are transported in the blood. My goal with this section of my research was to further elucidate blood vessel to gut interactions, focusing on how PAR-2 activation may influence ICC activity in the rat mid-colon. I aimed to address the hypothesis that **PAR-2 protein is located on c-kit+ ICC and influences gut motility through direct action on ICC in the rat mid-colon.**

Methods: To address the first hypothesis, investigation of the direct effects of SCFAs on vascular tone was done by constructing cumulative concentration-response curves to SCFAs in isolated

mesenteric arteries mounted in a wire myograph and pre-stimulated with phenylephrine (PE). To determine the effects of SCFAs within the mesenteric vascular bed, nerve-evoked vasoconstriction was used to construct frequency-response curves to perivascular nerve stimulation in a perfused mesenteric bed in the presence and absence of SCFAs. Pharmacological inhibitors were used to investigate the mechanism of action of SCFAs. In order to address my second hypothesis, sections of rat mid-colon were collected and prepared for immunofluorescence staining using antibodies to PAR-2, α smooth muscle actin, and c-kit prior to imaging.

Results: In isolated arteries, sodium acetate (0.3 - 100 μM), sodium propionate (3 - 100 μM) and sodium butyrate (0.3 – 100 μM) caused reductions in PE-evoked tone. These effects were differentially inhibited by combinations of the pharmacological inhibitors of nitic oxide synthase and endothelial Ca^{2+}-activated K^{+} channels. In the perfused mesenteric bed, nerve-evoked vasoconstriction was not altered by SCFAs at μM concentrations. However, at a concentration of 30 mM, sodium acetate and sodium propionate did attenuate responses. The PAR-2 immunofluorescence imaging presented staining of PAR-2, α smooth muscle actin and c-kit in the intestinal wall but no apparent overlapping of PAR-2 and c-kit staining was present in the intestinal wall of the rat mid-colon.

Conclusion: These data indicate that SCFAs may cause direct vasorelaxation in mesenteric resistance arteries via activation of endothelium-dependent pathways. SCFAs did not have a significant effect on the perfused mesenteric vascular bed at μM concentrations but did have a significant effect at mM concentrations. Immunofluorescence images of the rat mid-colon indicate that PAR-2 is present in the intestinal wall, but it is not located on ICC. This suggests that it is improbable that PAR-2 activation inhibits ICC-mediated spontaneous smooth muscle contractile activity through direct action on ICC. Future studies are required to determine how PAR-2

activation may influence ICC activity. Overall, this work presents examples of the complex interaction between the gastrointestinal tract and the cardiovascular system. However, further research is required to better explain how SCFAs may be influencing blood pressure regulation and how PAR-2 activation may influence gastrointestinal motility.

Preface

All animal use was approved by the Animal Care and Use Committee (ACUC HS1; AUP 312) according to the guidelines of the Canadian Council on Animal Care and presented in accordance with the principles defined by Grundy (2015).

Acknowledgements

Firstly, I wish to express my gratitude to my supervisors Dr. Frances Plane and Dr. Paul Kerr for guiding me through my research and for supporting my personal growth throughout my studies. Thank you.

I would like to thank Dr. Darren DeLorey for being a member of my supervisory committee and for providing feedback and advice that was invaluable to the progress and completion of my studies.

I would also like to thank Dr. Alister McNeish for providing his expertise and time as examiner of my thesis defense.

I wish to thank Parnian Alavi for her time, patience, and for providing her expertise in all matters of immunofluorescence staining and imaging.

I am thankful to my friend and fellow graduate student, Alexia Maheux, for all her optimism, support and contributions to this work.

Finally, I would also like to express my gratitude to my parents and to Chris for believing in me and encouraging me every step of the way.

Table of Contents

List of Tables

List of Figures

Chapter 1: Introduction to gut-blood vessel interactions

Chapter 2: Materials and methods

Chapter 3: Vascular effects of short-chain fatty acids on small mesenteric arteries

Chapter 4: Introduction to blood vessel-gut interactions

Chapter 6: Expression of PAR-2 in the rat mid-colon

Abbreviations

ACh	acetylcholine
ANO1	anoctamin-1
ANOVA	analysis of variance
ATP	adenosine 5'-triphosphate
BH_4	(*6R*-)5,6,7,8,-tetrahydrobiopterin
Ca^{2+}	calcium
cAMP	cyclic adenosine monophosphate
cGMP	cyclic guanosine monophosphate
Cl^-	chloride
CO_2	carbon dioxide
DAG	diacylglycerol
DAPI	4′,6-diamidino-2-phenylindole
DASH	Dietary Approaches to Stop Hypertension
EDH	endothelium-dependent hyperpolarization
eNOS	endothelial nitric oxide synthase
FRC	frequency-response curve
GPCR	G-protein coupled receptor
GPR41	G-protein coupled receptor 41
GTP	guanosine 5'-triphosphate
H^+	hydrogen ion (proton)
ICC	interstitial cells of Cajal
IK_{Ca}	intermediate conductance calcium-activated potassium channel
IP_3	inositol 1,4,5-triphosphate
IP_3R	inositol 1,4,5-triphosphate receptor
K^+	potassium
L-NAME	N^G-nitro-L-arginine methyl ester
L-Type VGCC	long lasting (L)-type voltage-gated calcium channel
MCT1	monocarboxylate transporter 1
MLCK	myosin light-chain kinase
MLCP	myosin-light chain phosphatase
NA	noradrenaline
Na^+	sodium
NADPH	nicotinamide-adenine-dinucleotide phosphate
NHE	sodium-proton exchanger (Na^+/H^+ exchanger)
NO	nitric oxide
O_2	molecular oxygen (dioxygen)
Olfr78	olfactory receptor 78
$P2X_1$	purinergic receptor P2X 1
PAR-2	protease-activated receptor 2
PDGFRα	platelet-derived growth factor receptor α
PE	phenylephrine

PIP_2	phosphatidylinositol 4,5-bisphosphate
PKG	protein kinase G
PLC	phospholipase C
RyR	ryanodine receptor
SCFA	short-chain fatty acid
SEM	standard error of the mean
SERCA	sarco/endoplasmic reticulum calcium-ATPase
sGC	soluble guanylyl cyclase
SK_{Ca}	small conductance calcium-activated potassium channel
TRAM-34	triarylmethane
TRPV1	transient receptor potential vanilloid 1 channel
TRPV4	transient receptor potential vanilloid 4 channel
T-type VGCC	transient (T)-type voltage-gated calcium channel

Part 1

This thesis addresses interactions between gut and blood vessel function and is composed of two arms that will be addressed and discussed separately. The first arm focuses on the interaction between gut-derived small molecules and vasomotor control of small mesenteric resistance arteries. The second arm focuses on interactions between serine proteases, that circulate in the blood, and activate protease-activated receptors located in the gastrointestinal wall and influences gut motility.

Chapter 1: Introduction to gut-blood vessel interactions

Over the past 30 years, studies have revealed an association between diet and blood pressure regulation (Appel et al., 1997; Chiu et al., 2016; Dolmatova et al., 2018; Kaye et al., 2020; Mills et al., 2020; Najjar et al., 2018; Nardocci et al., 2019; Rabi et al., 2020; Rouse et al., 1984; Saneei et al., 2014; Schwingshackl et al., 2019). Fiber-rich diets have been reported to be beneficial for the treatment and prevention of hypertension (Appel et al., 1997; Najjar et al., 2018). A by-product of interest of fiber-rich diets are short-chain fatty acids (SCFAs), which are produced through anaerobic fermentation of indigestible fibers in the lower intestine. These SCFAs may be able to affect blood pressure through their direct vasorelaxation effect on blood vessels, that has been reported by many investigators (Aaronson et al., 1996; Knock et al., 2002; Mortensen et al., 1990; Natarajan et al., 2016; Nutting et al., 1991; Pluznick et al., 2013). In the body, blood pressure is tightly controlled through by regulation of blood vessel diameter which can be influenced by sympathetic nerve output and endogenous molecules released from cells of the blood vessel wall such as endothelin (Brain et al., 1988) and prostacyclin (Moncada et al., 1976), as well as molecules released from cells external to the blood vessel such as angiotensin II (Batenburg et al., 2005) and bradykinin (Danser et al., 2000). An imbalance of these endogenous regulators and

inappropriate maintenance of blood vessel diameter can lead to high blood pressure. Further study on how SCFAs may be involved in influencing blood vessel diameter is the focus of the first part of my thesis. I investigated the effects of these gut derived SCFAs on blood vessel function *in vitro.* I aimed to further elucidate the extent of their effects and the possible mechanisms by which these SCFAs may alter vasodilation and vasoconstriction of blood vessels. A greater understanding of the possible influence of SCFAs on blood vessels may provide insight on their role in diet influenced blood pressure regulation.

1.1 Hypertension

Loss of appropriate blood pressure regulation through an imbalance of vasoconstriction and vasodilation can lead to increases in blood pressure known as hypertension. Hypertension of the systemic circulatory system, also known as systemic hypertension, affects about a third of adults around the world (Mills et al., 2020; Padwal et al., 2016). Chronic systemic hypertension increases the risk of other major cardiovascular pathologies, including stroke and myocardial infarction, making it the leading risk factor of premature deaths globally (Mills et al., 2016; Padwal et al., 2016). In North America, development of hypertension is largely influenced by the consumption of Western pattern diets (Dolmatova et al., 2018) that include plenty of processed foods (Nardocci et al., 2019). Systemic hypertension is often managed through pharmacological intervention such as the use of angiotensin-converting enzyme (ACE) inhibitors and angiotensin II receptor blockers (ARB) that can reduce vascular tone and, thus, blood pressure (I. A. M. Brown et al., 2018; Schiffrin, 2004). However, drugs may not always provide effective or lasting management of hypertension, therefore patients are also encouraged to change their health behaviour in addition to pharmacological intervention (Najjar et al., 2018; Rabi et al., 2020). Changes in diet have been recommended, often following Dietary Approaches to Stop

Hypertension (DASH), to promote consumption of fiber-rich diets, including plenty of fruits, vegetables, whole grains, plant-based proteins, and low-fat dairy products (Appel et al., 1997; Mills et al., 2020; Rabi et al., 2020). Changes in diet and health behaviour have been reported to support long term treatment and to be beneficial when accompanying current pharmacological interventions for systemic hypertension (Najjar et al., 2018).

1.2 Portal hypertension

Systemic hypertension is not the only manifestation of adverse of blood pressure regulation. An increase in vascular tone within specific vascular beds can lead to development of localized hypertension within an organ or system, such as pulmonary hypertension and portal hypertension (Iwakiri, 2014; Schermuly et al., 2011). Although they may not affect the entire circulatory system, these localized hypertensions can have serious complications, such as those seen in portal hypertension (reviewed by Iwakiri, 2014). Liver cirrhosis (scarring of the liver) can lead to the development of portal hypertension (Iwakiri, 2014). Cirrhosis causes structural changes in the liver that alter endothelial cell integrity within hepatic arteries (Iwakiri, 2014). This results in endothelial dysfunction that can lead to a significant decrease in production of nitric oxide (NO), a potent vasodilator, within these arteries which increases vascular tone due to increased vasoconstriction (Iwakiri, 2014) (described in section **1.6 Vasomotor control**). Increased hepatic vascular tone then results in an increase in portal pressure, which is considered clinically significant portal hypertension once portal pressure is greater than 10 mmHg (Iwakiri, 2014; Nair et al., 2016).

Portal hypertension can eventually lead to the development of collateral vessels in an attempt to compensate for the increase in portal pressure (Iwakiri, 2014). The splanchnic circulation comprises blood flow coming from the spleen and the vasculature surrounding the

gastrointestinal tract, including the mesenteric vascular bed, that eventually feeds into the liver (McConnell & Iwakiri, 2018). An increase in splanchnic vasodilation occurs in response to blood flowing into these collateral vessels which leads to an increase in blood flow to the portal vein and can worsen portal hypertension (**Figure 1.1**) (Iwakiri, 2014; McConnell & Iwakiri, 2018; Nair et al., 2016). Therefore, approaches to treatment for portal hypertension may require different changes in diet compared to systemic hypertension, as an increase in vasodilation of the mesenteric arteries would exacerbate this condition.

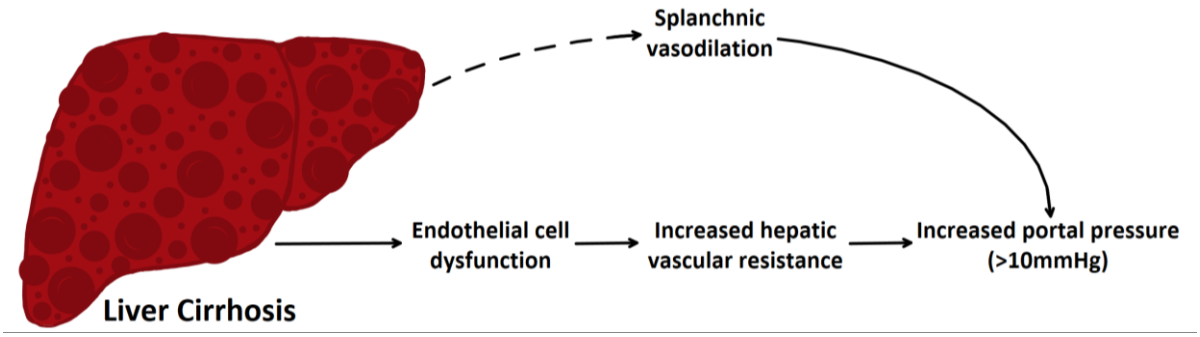

Figure 1.1 Pathogenesis of portal hypertension. Liver cirrhosis results in endothelial cell dysfunction and indirectly causes splanchnic vasodilation due the development of collateral vessels. Both increased hepatic vascular resistance and splanchnic vasodilation contribute to an increase in portal pressure. Clinically significant portal hypertension is defined as an increase in portal pressure of 10 mmHg or greater. Adapted from Figure 1 presented in Nair et al. (2016).

1.3 Diet, gut health and blood pressure

1.3.1 Diet and blood pressure

Clinical research has highlighted the possible impact of high fiber diet on blood pressure in humans. One clinical trial on Dietary Approaches to Stop Hypertension (DASH) aimed to determine how blood pressure may be influenced by diet (Appel et al., 1997). Appel et al. (1997) reported that consumption of diets containing large amounts of fruits and vegetables, thus, plenty

of fiber, were associated with a decrease in blood pressure within two weeks when compared to a typical American diet (Appel et al., 1997). These results were independent of any changes to sodium intake or alcohol consumption, suggesting that DASH diets could supplement other efforts to reduce blood pressure through reduction of sodium and alcohol consumption (Appel et al., 1997). Meta-analysis of these trials have supported the association between DASH diets and a reduction in blood pressure (Saneei et al., 2014). In addition to this, treatment of hypertension through the use of blood pressure medications and plant-based DASH diets have been shown to support blood pressure reduction (Najjar et al., 2018). This suggests that changes in diet to increase fruits, vegetables and fiber intake may be useful in preventative or supportive treatment for systemic hypertension (Appel et al., 1997; Chiu et al., 2016; Saneei et al., 2014).

1.3.2 Microbiota and cardiovascular health

Cardiovascular health is further supported by the gastrointestinal tract's ability to digest and obtain nutrients from high fiber diets. The break down of food in the gut, although mostly reliant on mechanical and enzymatic digestion, can also be facilitated by our gut microbiota which is made up of bacteria, fungi and archaea (Flint et al., 2015; Illiano et al., 2020; Turnbaugh et al., 2008). The presence and diversity of gut microbiota can impact a food's apparent nutritional value, while the types of food consumed can also influence the composition and diversity of gut microbiota (Flint et al., 2015; Turnbaugh et al., 2008). Over the past several decades, the importance of diet and the diversity of gut microbiota in maintenance of good health has been emphasized (Appel et al., 1997; Gibson & Roberfroid, 1995; Kaye et al., 2020; O'Neil et al., 2014; Sekirov et al., 2010). The gut microbiota can influence many physiologic systems including immune, metabolic, and cardiovascular systems (Appel et al., 1997; Schwiertz et al., 2010; Sekirov et al., 2010). *Firmicutes* and *Bacteroidetes* are the most common gut bacterial phyla,

making up 90% of bacteria in the gut (Eckburg et al., 2005). Dysbiosis of gut microbiota, in which there are adverse changes in composition, amount and/or function of gut microbiota, has been associated with the development of hypertension (Chang et al., 2020; Durgan et al., 2016; Gomez-Arango et al., 2016; Toral et al., 2019; Yang et al., 2015). The ratio of *Firmicutes:Bacteriodetes* can be altered in hypertensive states, indicating the importance of maintaining microbial diversity in cardiovascular health (Gomez-Arango et al., 2016; Hu et al., 2017).

The bacteria in the *Bacteriodetes* and *Firmicutes* phyla enable fermentation of indigestible dietary fiber to produce short-chain fatty acids (SCFA) (Duncan et al., 2002; Ganesh et al., 2018; Gomez-Arango et al., 2016). Germ-free animals, that lack commensal microbiota, are reported to have minimally detectable SCFA plasma levels (Perry et al., 2016). Gomez-Arango et al. (2016) reported that altered SCFA production due to a reduction in a SCFA-producing bacteria, *Odoribacter*, from the *Bacteriodetes* phylum, was associated in elevated blood pressure in overweight and obese pregnant women (Gomez-Arango et al., 2016). In pregnant women with preeclampsia, dysbiosis was observed with a decrease in fecal SCFA levels compared to pregnant women without preeclampsia (Chang et al., 2020). Another study done by Shi et al. (2021) reported that intermittent fasting altered gut microbiota and shifted the microbial diversity of hypertensive rats closer to that of wild-type control rats. This shift in microbial diversity was associated with a reduction in blood pressure in the hypertensive rat model (Shi et al., 2021). In a rat model with disruptive sleep apnea, Ganesh et al. (2018) reported that the development of dysbiosis resulted in a decrease in cecal concentration of the SCFA, acetate, furthermore, the model subsequently developed epithelial dysfunction, hypertension, and neuroinflammation (Ganesh et al., 2018). These studies suggest that altering gut microbiota through diet and/or

antibiotics and, therefore bacterial by-products, may be associated with changes in blood pressure regulation.

1.4 Short-chain fatty acids

Over the past three decades, there has been some focus on the possible effect of SCFAs on blood vessels and cardiovascular health (Aaronson et al., 1996; Knock et al., 2002; Mortensen et al., 1990; Natarajan et al., 2016; Nutting et al., 1991; Pluznick et al., 2013). SCFAs are by-products of anaerobic fermentation of indigestible polysaccharides, such as starch and pectin, by bacteria in the lower intestine (Bugaut, 1987; Titgemeyer et al., 1991). These fibers are considered indigestible as they contain β-glycosidic linkages that cannot be hydrolyzed by digestive enzymes produced by the body, but can be fermented by anaerobic bacteria (Louis & Flint, 2017; T. L. Miller & Wolin, 1996; Stumpff, 2018; Zhang et al., 2018). SCFAs are carboxylic acids containing a short, saturated carbon side chains of up to 6 carbons in length. The most prevalent and physiologically relevant SCFAs are acetate, propionate, and butyrate (**Figure 1.2**) (Adak & Khan, 2019; Bugaut, 1987). Production of SCFAs is dependent on the fermentability of the fiber ingested, therefore the type of mono- and polysaccharides ingested, as well as the duration of transit of the carbohydrates through the colon, and the presence and diversity of the anaerobic bacteria responsible for fermentation (Flint et al., 2015; Morrison & Preston, 2016; Titgemeyer et al., 1991). These three SCFAs are produced at a fairly constant molar ratio of 60:25:15 (acetate:propionate:butyrate), however, SCFA production and molar ratios are influenced by the fiber's composition and, thus, could be altered through changes in diet (Bugaut, 1987; Cummings et al., 1987; Louis & Flint, 2017; T. L. Miller & Wolin, 1996; Titgemeyer et al., 1991).

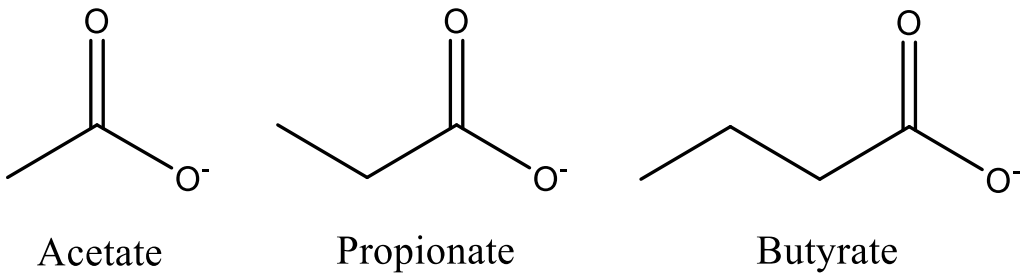

Figure 1.2 Structure of short-chain fatty acids, acetate, propionate, and butyrate.

1.4.1 SCFA transport

Once formed, these SCFAs are taken up into epithelial cells in the large intestine via diffusion of undissociated SCFAs and through monocarboxylate transporter 1 (MCT1) which provides cotransport across the apical membrane of dissociated SCFAs, acetate$^-$, propionate$^-$ and butyrate$^-$ ($SCFA^-$) and protons (H^+) from the lumen (Bugaut, 1987; Fleming et al., 1991; Rübsamen & von Engelhardt, 1981; Stumpff, 2018). This cotransport of $SCFA^-$ and H^+ also facilitates transport of sodium (Na^+) into the cell from the lumen through Na^+/H^+ exchanger (NHE), resulting in the promotion of Na^+ uptake with the uptake of $SCFA^-$ from the lumen (Musch et al., 2001; Rübsamen & von Engelhardt, 1981; Stumpff, 2018; Zaharia et al., 2001). Once absorbed into the epithelial cell these SCFAs can be metabolized by these cells, as is the case for butyrate as it is largely used up as an energy source for colonocytes (Bugaut, 1987; Donohoe et al., 2011). The remaining SCFAs are transported into the mesenteric circulation through the basolateral membrane and driven by efflux of Na^+ through Na^+/K^+-ATPase (Bachmann et al., 2011; Stumpff, 2018; Stumpff et al., 2011). These two ions, Na^+ and $SCFA^-$, appear to be charge-coupled and therefore drive the movement of one another across the epithelial cell membranes in order to maintain electroneutrality of the cell (Stumpff, 2018). $SCFA^-$ are transported out of the epithelial cell through anion transporting proteins, such as MCT1, allowing dissociated SCFAs to exit the cell

and enter the blood stream (Adak & Khan, 2019; Stumpff, 2018). Once in the circulation, SCFAs can then interact with receptors (described in **Section 1.4.3 Endogenous SCFA receptors**), including those found in the vasculature (Bugaut, 1987; Natarajan et al., 2016; Pluznick et al., 2013).

Physiological concentrations of SCFAs in the blood are reported to decrease as circulation continues from the portal vein through the liver and into the peripheral circulation (Bloemen et al., 2009; Cummings et al., 1987; Morrison & Preston, 2016). SCFAs can be metabolized by the liver and, therefore, their concentration decreases into the peripheral circulation (Morrison & Preston, 2016). In a recent study, Tian et al. (2020) reported that SCFA concentrations in peripheral blood samples taken from healthy individuals appear to be much higher than what was previously reported by Cummings et al. (1987) and Bloemen et al. (2009) presented in **Table 1.1** (Bloemen et al., 2009; Cummings et al., 1987; Tian et al., 2020). This may be explained by the methods used to analyze blood samples. Tian et al. (2020) used gas chromatography-mass spectrometry which may be better optimized to measure these molecules compared to the liquid chromatography-mass spectrometry and gas-liquid chromatography methods used by Bloemen et al. (2009) and Cummings et al. (1987), respectively (Bloemen et al., 2009; Cummings et al., 1987; Moreau et al., 2003; Tian et al., 2020).

Table 1.1 Physiological SCFA concentration in blood (μM)			
	Portal	**Hepatic**	**Peripheral**
Acetate	258-294 (Bloemen et al., 2009; Cummings et al., 1987)	115-242 (Bloemen et al., 2009; Cummings et al., 1987)	70-192 (Bloemen et al., 2009; Cummings et al., 1987)
Propionate	36-88 (Bloemen et al., 2009; Cummings et al., 1987)	8-21 (Bloemen et al., 2009; Cummings et al., 1987)	5-2843 (Bloemen et al., 2009; Cummings et al., 1987; Tian et al., 2020)
Butyrate	29-35 (Bloemen et al., 2009; Cummings et al., 1987)	12-15 (Bloemen et al., 2009; Cummings et al., 1987)	4-2700 (Bloemen et al., 2009; Cummings et al., 1987; Tian et al., 2020)

Table 1.1 Physiological SCFA concentrations in human blood, as reported by Cummings et al. (1987); Bloemen et al. (2009), and Tian et al. (2020).

1.4.2 SCFAs and blood pressure

In vivo studies have reported that supplementation of SCFAs in animal diets, and intracolonic and intravenous administration of SCFAs are associated with reduced blood pressure in animal models. Kaye et al. (2020) found that addition of SCFA to diet lead to a reduction in blood pressure in hypertensive mice (Kaye et al., 2020). In a rat model of obstructive sleep apnea, pre- and probiotic treatment, as well as direct infusion of acetate into the rat cecum, were also reported to have prevented hypertension (Ganesh et al., 2018). Skrzypecki et al. (2018) found that intraperitoneal butyrate injection (500mg/kg dose) reduced blood pressure in normotensive and spontaneously hypertensive rats (Skrzypecki et al., 2018). This finding was supported by Onyszkiewicz et al. (2019) that reported that intracolonic and intravenous administration of butyrate to rats induced a transient decrease in blood pressure (Onyszkiewicz et al., 2019). In addition to the three SCFAs mentioned above, a SCFA less commonly produced in the gut, valerate, has also been reported to reduced blood pressure in a dose-dependent and transient manner in rats with intravenous and intracolonic infusions (Onyszkiewicz et al., 2020; Skrzypecki et al., 2020). These studies demonstrate that SCFAs could influence blood pressure regulation in these animal models.

Ample work has also been done to investigate the effect of SCFAs in blood vessels directly (Aaronson et al., 1996; Knock et al., 2002; Mortensen et al., 1990; Natarajan et al., 2016; Nutting et al., 1991; Onyszkiewicz et al., 2019; Pluznick et al., 2013). In 1990, Mortensen et al. reported that all three SCFAs, acetate, propionate and butyrate, induced relaxation of human colonic resistance arteries in a concentration-dependent manner (0.1-30 mM) (Mortensen et al., 1990). This concentration-dependent relaxation effect of SCFAs was supported by studies done in isolated rat arteries by Nutting et al. (1991) and Aaronson et al. (1996) (Aaronson et al., 1996;

Nutting et al., 1991). These earlier studies proposed that SCFA-induced vasorelaxation was mediated through endothelium independent mechanisms in rat mesenteric arteries and human colonic arteries, as removal of the endothelium did not appear to significantly diminish the effect of these SCFAs at higher concentrations (Aaronson et al., 1996; Mortensen et al., 1990). Later studies also supported the finding that SCFAs cause vasorelaxation in isolated arteries (Knock et al., 2002; Natarajan et al., 2016; Onyszkiewicz et al., 2019). However, Knock et al. (2002) and Natarajan et al. (2016) reported that removal of the endothelium significantly attenuated this effect at lower concentrations and proposed that the endothelium does play a role in mediating the effect of SCFAs at ≤10 mM (Knock et al., 2002; Natarajan et al., 2016). Although there is some division on the extent of the role of endothelium-dependent mechanisms in mediating the effect of SCFAs, it appears that they may not work through either endothelium-dependent or independent mechanisms exclusively. Together these studies provide evidence that SCFAs, acetate, butyrate, and propionate, can cause vasorelaxation in isolated resistance arteries. It has been further suggested by Natarajan et al. (2016) and Onyszkiewicz et al. (2019) that this effect may be mediated through the activation of an endogenous SCFA receptor (Natarajan et al., 2016; Onyszkiewicz et al., 2019).

1.4.3 Endogenous SCFA receptors

These three SCFAs have been shown to act on several endogenous receptors throughout the body (reviewed by Kimura et al., 2020). Two of these endogenous receptors have been implicated in blood pressure regulation: GPR41 and Olfr78 (Natarajan et al., 2016; Pluznick et al., 2013). These receptors have been located to the vasculature and may play a role in mediating vasorelaxation and, thus, blood flow and blood pressure regulation (Natarajan et al., 2016; Pluznick et al., 2013).

Olfr78

Olfr78 is a G-protein coupled receptor (GPCR) that responds to two SCFAs, acetate and propionate (**Table 1.2**) (Pluznick et al., 2013). It has been located to the vascular smooth muscle cells of small resistance arteries and has a particularly high expression in renal blood vessels (Pluznick et al., 2013). Within the kidney, Olfr78 receptors have been found in the renal juxtaglomerular apparatus from which renin is synthesized and secreted (Chen et al., 2007; Hackenthal et al., 1990; Pluznick et al., 2013). Stimulation of Olfr78 by an endogenous ligand, acetate or propionate, activates G_s protein to induce adenylate cyclase activity and increase intracellular cyclic adenosine monophosphate (cAMP) (Chen et al., 2007; Pluznick et al., 2013). Pluznick et al. (2013) reported that propionate stimulation of Olfr78 on the renal juxtaglomerular apparatus resulted in elevated intracellular cAMP levels and prompted renin secretion (Pluznick et al., 2013). Renin release induces the vasoconstrictive renin-angiotensin system and increases mean arterial pressure (Ferro et al., 2006; Hackenthal et al., 1990). Furthermore, Pluznick et al. (2013) reported that Olfr78 knockout mice had lower plasma renin levels and lower blood pressure compared to wild-type mice fed the same diet, indicating Olfr78 receptor may play a role in elevating blood pressure (Pluznick et al., 2013). It should be noted that the concentration of SCFA necessary to activate Olfr78 is likely quite high as Olfr78 has a large half maximal effective concentration (EC_{50}) for these ligands (**Table 1.2**) (Pluznick et al., 2013).

Table 1.2 EC_{50} of SCFAs at Endogenous Receptors		
Short-Chain Fatty Acid	**EC_{50} (μM)**	
	GPR41/FFAR3	**Olfr78**
Acetate	820-3162 (A. J. Brown et al., 2003; Hudson et al., 2012; Le Poul et al., 2003)	2350 (Pluznick et al., 2013)
Propionate	5-141 (A. J. Brown et al., 2003; Hudson et al., 2012; Le Poul et al., 2003)	920 (Pluznick et al., 2013)
Butyrate	33-193 (A. J. Brown et al., 2003; Hudson et al., 2012; Le Poul et al., 2003)	-

Table 1.2 SCFAs and their EC_{50} at endogenous receptors. EC_{50} for GPR41 was measured in transfected HEK293, Flp-In T-REx 293, and CHO cells through changes in GTPγS binding (A. J. Brown et al., 2003) and cAMP concentration (Hudson et al., 2012; Le Poul et al., 2003); EC_{50} for Olfr78 was measured in HEK293 cells through changes in cAMP (Pluznick et al., 2013). This table was modified and adapted to include Olfr78 from "Table 3. Affinity of fatty acids for FFAR3 and FFAR2" presented in Kimura et al. (2020) which is licensed under CC BY 4.0 (Kimura et al., 2020).

GPR41

Originally an orphaned GPCR, GPR41 was deorphanized in 2003 when it was first shown that this receptor responds to SCFAs (A. J. Brown et al., 2003; Le Poul et al., 2003). Due to the nature of its endogenous ligand, GPR41 is also known as free fatty acid receptor 3 (FFAR3). GPR41 is sensitive to pertussis toxin inhibition indicating it couples with $G_{i/o}$ protein (A. J. Brown et al., 2003; Le Poul et al., 2003). This receptor has been located to several tissues and cell types including the epithelial and enteroendocrine cells of the colonic mucosa (Samuel et al., 2008; Tazoe et al., 2009), adipocytes (A. J. Brown et al., 2003), regulatory immune cells (A. J. Brown et al., 2003), pulmonary smooth muscle cells (Mizuta et al., 2020), and more recently in smooth muscle cells and endothelial cells of small resistance arteries (Natarajan et al., 2016; Pluznick et

al., 2013). Expression of GPR41 in resistance arteries may provide an explanation for how SCFAs may be mediating their vasorelaxation effect, as suggested by Pluznick et al. (2013) and Natarajan et al. (2016) (Natarajan et al., 2016; Pluznick et al., 2013). Furthermore, the presence of GPR41 in the vascular tissue further supports the possibility that SCFAs may play a role in blood pressure regulation (Natarajan et al., 2016; Pluznick et al., 2013).

GPR41 knockout mice have been reported to develop systolic hypertension compared to wild-type mice which led Natarajan et al. (2016) to propose that GPR41 is involved in maintaining blood pressure (Natarajan et al., 2016). Intravenous administration of propionate to these GPR41 knockout mice produced a moderate hypertensive response suggested to be through Olfr78 signalling and activation of the renin-angiotensin system to increase blood pressure (Natarajan et al., 2016; Pluznick et al., 2013). However, in GPR41 heterozygous mouse models, administration of propionate resulted in a hypotensive effect proposed to be mediated by vasodilation of resistance arteries through GPR41 signalling (Pluznick et al., 2013). Taken together, this suggests that SCFAs and GPR41 may play a role in maintaining blood pressure through vasodilation.

1.5 Blood pressure and flow

Maintenance of blood pressure is crucial for ensuring appropriate perfusion of tissues and organs throughout the body. Mean arterial blood pressure is determined by cardiac output, the volume of blood ejected from the heart, and by peripheral vascular resistance, which is largely regulated by small resistance arteries (Kenner, 1988; Mulvany & Aalkjaer, 1990). Changes in diameter of these resistance arteries can modulate blood pressure and blood flow. The diameter of these arteries is controlled by the contraction and relaxation of the smooth muscle cells located in the vascular wall. Even small changes in the diameter of these vessels can have large impacts

on resistance as can be described mathematically with Hagen-Poiseuille's equation: (Pugsley & Tabrizchi, 2000; Schiffrin, 2004; Touyz et al., 2018)

$$R = \frac{8L\eta}{\pi r^4}$$

R = resistance, L = vessel length, η = blood viscosity, r = arterial radius

A small increase in the radius can significantly decrease resistance and pressure, therefore, increase blood flow through these arteries. Conversely, a small decrease in radius can significantly increase resistance and pressure and, thus, reduce blood flow. It is necessary that the diameter of these vessels be tightly regulated to ensure appropriate blood flow to tissues and organs in the body.

1.6 Vasomotor control

Resistance artery diameter depends on a balance between vasoconstriction and vasodilation. Vasoconstriction is primarily driven by sympathetic output, in which activation of sympathetic neurons initiates the release of noradrenaline (NA), a neurotransmitter, that activates α_1-adrenergic receptors and increases intracellular calcium (Ca^{2+}) in smooth muscle cells to initiate smooth muscle contraction (Bao et al., 1990) (described in **section 1.6.2 Regulation of Vascular Tone**). Vasodilation is primarily mediated by endothelium-dependent mechanisms including the production of nitric oxide (NO) and endothelium-dependent hyperpolarization (EDH). These mechanisms are activated in response to several substances including acetylcholine (ACh) (Cowan et al., 1993) and adenosine 5'-triphosphate (ATP) (Vuorinen et al., 1992) as well as the mechanical stimulation of flow on the endothelium (Ballermann et al., 1998; Joannides et al., 1995; Sprague et al., 2010). Vasomotor control can vary between different types of blood vessels due to their structure and the predominant mechanisms of vasoconstriction and vasodilation.

1.6.1 Vascular structure

The circulatory system is made up of arteries, arterioles, capillaries, venules, and veins. These vessels have varying diameters and distinct characteristics that enable them to efficiently transport blood throughout the body and maintain blood pressure (**Table 1.3**). Blood vessels are made of up to three cell layers: the *tunica intima*, the *tunica media*, and the *tunica adventitia* (Pugsley & Tabrizchi, 2000). All vessels have a single layer of endothelial cells that line the lumen that make up the *tunica intima* (Takano et al., 2005). Within this layer there is also connective tissue which provides stability to the *tunica intima* (Pugsley & Tabrizchi, 2000). The narrowest blood vessels, the capillaries, are made up of only the *tunica intima*, the basement membrane and pericytes (Pugsley & Tabrizchi, 2000).

The *tunica media* is made up mostly of smooth muscle cells and elastin fibers and is found in arteries, arterioles, venules and veins (Pugsley & Tabrizchi, 2000). Arteries and arterioles that lead into the capillaries from the heart have the thickest *tunica media* layer. In larger conducting arteries, such as the aorta or common carotid arteries, the *tunica media* predominantly contains elastic tissue allowing these vessels to accommodate the pulsation of blood flow from the heart (Pugsley & Tabrizchi, 2000). Smaller resistance arteries, such as mesenteric arteries, have a *tunica media* made up mostly of vascular smooth muscle enabling them to mediate changes in resistance through smooth muscle contraction and narrowing of the vessel lumen (**Figure 1.3**) (Chilian et al., 1986; Pugsley & Tabrizchi, 2000; Schiffrin, 2004). The venules and veins that lead away from the capillaries and toward the heart have a thinner *tunica media* containing some vascular smooth muscle but much less than that found in arteries (Pugsley & Tabrizchi, 2000).

The *tunica adventitia*, also known as *tunica externa*, the surrounds all blood vessels, except for the capillaries, and is made up of collagen and elastic connective tissue. This layer is innervated

with autonomic nerves and, in larger vessels, contains the *vaso vasorum* which are small blood vessels that provide blood supply to the larger vessels to ensure cellular homeostasis (Pugsley & Tabrizchi, 2000). The structure and characteristics of blood vessels has been reviewed by Pugsley and Tabrizchi (2000) (Pugsley & Tabrizchi, 2000). The distinct characteristics of blood vessels throughout the body provide the ability to adapt to pulsatile flow and to regulate vascular resistance through a balance between vasoconstriction and vasodilation. These characteristics are necessary to maintain blood pressure and blood flow throughout the systemic and pulmonary circulation.

Table 1.3 Blood vessel structure and characteristics		
Blood Vessel	**Internal diameter**	**Composition**
Conducting artery (ex: Aorta)	>300 μm (Schiffrin, 1992)	*Tunica intima* *Tunica media* - Largely made up of elastic tissue *Tunica adventitia*
Resistance artery (ex: Mesenteric arteries)	150 – 300 μm (Chilian et al., 1986; Mortensen et al., 1990; Mulvany & Aalkjaer, 1990; Schiffrin, 1992)	*Tunica intima* *Tunica media* - Largely made up of vascular smooth muscle *Tunica adventitia*
Arteriole	50 - 150 μm (Jensen et al., 2004; Schiffrin, 1992)	*Tunica intima* *Tunica media* - Largely made up of vascular smooth muscle *Tunica adventitia*
Capillary	~5 μm (Bosman et al., 1995)	*Tunica intima*
Venule	15 – 180 μm (Bishop et al., 2000; Shoukas & Bohlen, 1990)	*Tunica intima* *Tunica media* *Tunica adventitia*
Vein (ex: saphenous vein)	>180 μm (Raffai et al., 2008; Seitz et al., 2016; Staszyk et al., 2003)	*Tunica intima* *Tunica media* *Tunica adventitia*

Table 1.3 Blood vessel type with their respective internal diameter and structural composition.

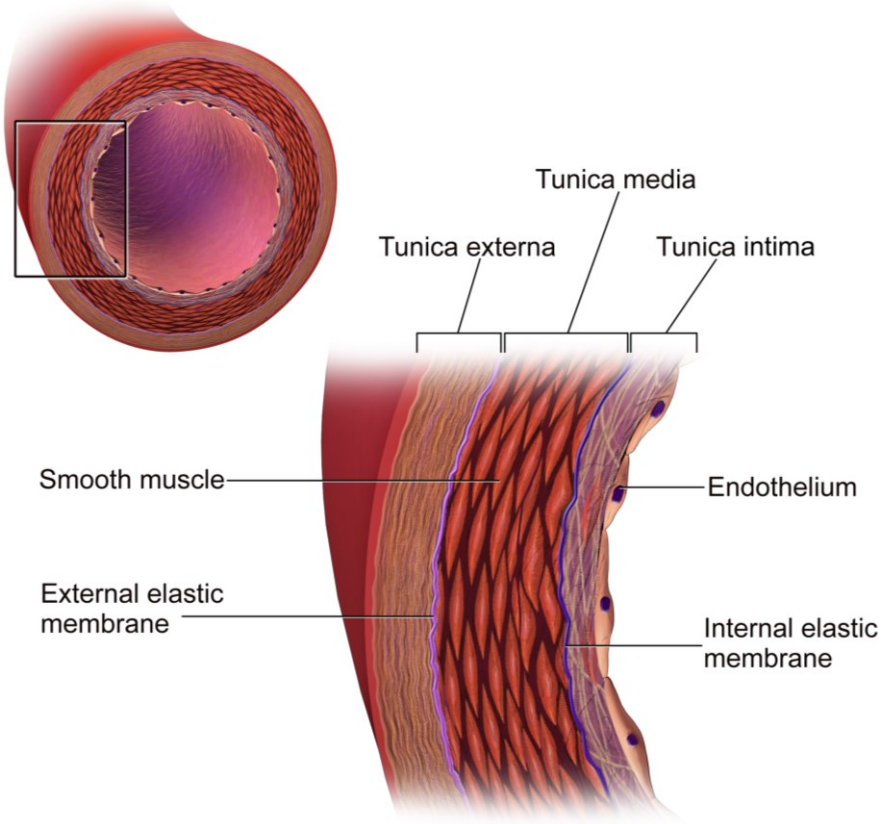

Figure 1.3 Resistance artery structure. The resistance artery *tunica media* is predominantly made up of smooth muscle. This image was cropped to focus on the artery structure from the original "Blausen 0055 ArteryWallStructure" created by BruceBlaus which is licensed under CC BY 3.0 (Blausen.com staff, 2014).

1.6.2 Regulation of vascular tone

Vascular smooth muscle regulates the diameter of arteries and the flow of blood. Vasoconstriction, narrowing of the vessel lumen, through smooth muscle contraction decreases blood flow. Smooth muscle contraction is tightly regulated by the intracellular concentration of Ca^{2+}, where an increase in intracellular Ca^{2+} enables actin-myosin cross-bridge cycling and contraction (reviewed by Tykocki et al., 2017). An increase in intracellular Ca^{2+} is mediated by an influx of Ca^{2+} into the cytoplasm through the opening of Ca^{2+} channels on the cell membrane including long lasting (L)-type voltage-gated Ca^{2+} channels (L-Type VGCCs) and transient (T)-

type VGCCs (Bean et al., 1986; Braunstein et al., 2009; Jensen et al., 2004; VanBavel et al., 2002) and activation of transient receptor potential vanilloid 1 (TRPV1) channels (Phan et al., 2020; Pórszász et al., 2002). Depolarization of the smooth muscle cell increases the open-state probability of VGCCs, thus changing the membrane permeability of Ca^{2+} and allowing an influx of Ca^{2+} ions (Bean et al., 1986; Braunstein et al., 2009; Jensen et al., 2004; VanBavel et al., 2002). Ca^{2+} influx can also be mediated by activation of receptor-operated channels such as inositol 1,4,5-triphosphate receptors (IP_3Rs) (Kobayashi et al., 1989) and ryanodine receptors (RyRs) (Zheng et al., 2008) located on the sarcoplasmic reticulum, an organelle that provides intracellular Ca^{2+} storage.

An increase in cytosolic Ca^{2+} promotes binding of Ca^{2+} to calmodulin to form a calmodulin/Ca^{2+} complex which then activates myosin light-chain kinase (MLCK) (Allen & Walsh, 1994). Activated MLCK phosphorylates myosin light-chain allowing for myosin-actin interactions leading to ATP-dependent cross-bridge cycling necessary for muscle contraction (Touyz et al., 2018). In a non-contractile state, Ca^{2+} concentrations are kept below the necessary threshold to bind to calmodulin and activate MLCK. The resting membrane potential and Ca^{2+} electrochemical gradient across the plasma membrane of smooth muscle cells are maintained with ion pumps, including sarco/endoplasmic reticulum Ca^{2+}-ATPase (SERCA) that pumps Ca^{2+} into the sarcoplasmic reticulum to regulate cytosolic Ca^{2+} concentration (Colyer, 1998; Furukawa et al., 1989; Paul, 1998). To terminate contraction, the myosin light-chain is dephosphorylated by myosin light-chain phosphatase (MLCP), preventing the myosin-actin interactions and, therefore, muscle contraction (**Figure 1.4**) (Cole & Welsh, 2011).

Myosin light-chain phosphorylation can also be regulated independently of Ca^{2+} which allows for the maintenance of contraction as Ca^{2+} concentration decreases, this is known as Ca^{2+}

sensitization (Ratz & Miner, 2009). Agonist induced G-protein coupled receptor signaling can influence phosphorylation of myosin light-chain through activation of the secondary messenger, phospholipase C (PLC) (Ratz & Miner, 2009). PLC hydrolyzes phosphatidylinositol 4,5-bisphosphate (PIP_2) forming inositol 1,4,5-triphosphate (IP_3) and diacylglycerol (DAG) (Hepler & Gilman, 1992). DAG can then activate protein kinase C (PKC) which leads to activation of a MLCP inhibitor (Ratz & Miner, 2009). Ca^{2+} sensitization can also be mediated by Rho-associated kinase, a serine-threonine kinase, that activates a MLCP inhibitor (Behuliak et al., 2017; Uehata et al., 1997). Inhibition of MLCP increases the probability that myosin light-chain remains phosphorylated and active and allows for continued cross-bridge cycling.

The primary driver for smooth muscle contraction is sympathetic outflow. Contraction of smooth muscle cells is initiated by sympathetic outflow via the release of neurotransmitters that act as agonists at G-protein coupled receptors (GPCRs) (Bao et al., 1990; Bradley et al., 2003). Peripheral blood vessels are innervated with sympathetic nerves that can regulate blood flow by influencing arterial diameter allowing the autonomic system to control blood flow to tissues in high demand of oxygen and nutrients while maintaining blood pressure, such as skeletal muscles during exercise (DeLorey et al., 2006; Just et al., 2016). Sympathetic nerve endings form a mesh-like network containing bulbs known as varicosities that surrounds vascular smooth muscle cells (Bennett, 1998). Sympathetic firing through these varicosities initiates the release of neurotransmitters, including noradrenaline (NA), adenosine triphosphate (ATP) and neuropeptide Y (Bao et al., 1990; Bradley et al., 2003). These neurotransmitters generate vasoconstriction by acting on their respective receptors on the vascular smooth muscle (Bao et al., 1990; Bradley et al., 2003). NA is an adrenergic neurotransmitter that binds to α_1-adrenergic receptors, a GPCR coupled to $G_{q/11}$ G-protein (reviewed by Docherty, 2019; Bao et al., 1990). Binding of NA induces

a conformational change in the α_1-adrenergic receptor to promote the dissociation of the $G_{q/11}$ protein from the receptor, (reviewed by Hepler & Gilman, 1992) leading to phosphorylation of PLC. PLC then hydrolyzes PIP_2 forming IP_3, which then binds to IP_3R on the sarcoplasmic reticulum and increases cytosolic Ca^{2+} (Hepler & Gilman, 1992; Kobayashi et al., 1989; Tykocki et al., 2017). Agonists at α_1-adrenergic receptors can also increase L-type VGCC open-probability through DAG mediated activation of PKC, which then activates a tyrosine-protein kinase that increases L-type VGCC activity (Callaghan et al., 2004; Keef et al., 2001; Lepretre et al., 1994; Mironneau & Macrez-Leprêtre, 1995). ATP acts as an agonist to purinergic receptor P2X 1 ($P2X_1$) on vascular smooth muscle cells (Bao et al., 1990). $P2X_1$ receptors act as ligand-gated cation channels for both Na^+ and Ca^{2+} allowing influx of both cations and leading to depolarization and an increase in intracellular Ca^{2+}(reviewed by Burnstock, 2018). Neuropeptide Y potentiates the effects of NA or ATP through neuropeptide Y receptors (Bao et al., 1990; Gonzalez-Montelongo & Fountain, 2021).

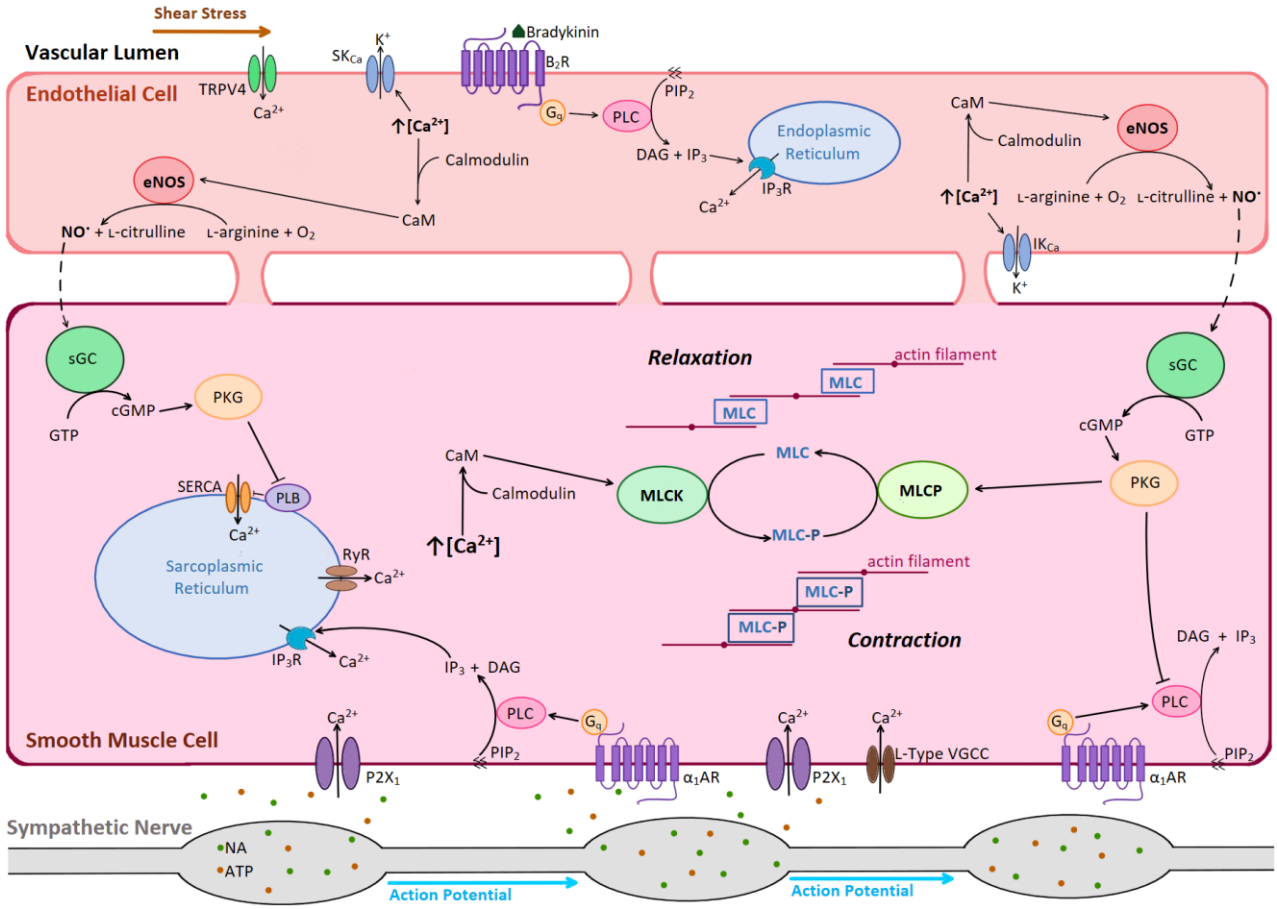

Figure 1.4 Regulation of vascular tone. Endothelium-dependent relaxation is mediated by an increase in intracellular Ca^{2+} evoked by shear stress and agonists at endothelial GPCRs as described in the text (section **1.6.3 Endothelium-dependent control of arterial diameter**). Smooth muscle cell contraction is also tightly regulated by cytosolic Ca^{2+} concentration (section **1.6.2 Regulation of vascular tone**). Release of neurotransmitters, NA and ATP, from sympathetic nerve varicosities are the primary drivers of smooth muscle contraction. NA activates G_q coupled α_1-adrenergic receptors (α_1AR) and ATP activates $P2X_1$ receptors allowing for influx of cations such as Ca^{2+}. Ca^{2+}/calmodulin complex is abbreviated to CaM in this diagram.

1.6.3 Endothelium-dependent control of arterial diameter

Appropriate vasomotor control requires that vasoconstriction be balanced with vasodilation. Vasodilation is primarily mediated by endothelium-dependent mechanisms including nitric oxide (NO) production and endothelium-dependent hyperpolarization (EDH). The endothelium is made of a single layer of endothelial cells that line the lumen of all blood vessels (Pugsley & Tabrizchi, 2000; Takano et al., 2005). It plays a significant role in regulating blood pressure in response to endocrine and paracrine signals, such as bradykinin (Danser et al., 2000) and prostacyclin (Moncada et al., 1976), and in response to the mechanical stimulation of shear stress, the frictional force that blood applies as it flows across endothelial cells (Dewey et al., 1981; Joannides et al., 1995; Korenaga et al., 1994; Vanhoutte et al., 2017). Shear stress is the parallel force applied over a given area (Sprague et al., 2010). Therefore, small arterioles experience the greatest mean shear stress due to their diameter and the incoming blood flow rate to these small vessels (Ballermann et al., 1998; Sprague et al., 2010). *In vivo* and *in vitro* studies have shown that shear stress mediates vasodilation through prostacyclin production and NO release (Ballermann et al., 1998; Joannides et al., 1995; Korenaga et al., 1994; Russell-Puleri et al., 2017; Sprague et al., 2010). This is achieved, at least in part, through shear stress stimulation of apical ion channels found on the endothelial cell, such as transient receptor potential vanilloid 4 (TRPV4) channels (**Figure 1.4**) (Ballermann et al., 1998; Mendoza et al., 2010). TRPV4 channels are cation channels that may be also activated by agonists, such as arachidonic acid (Watanabe et al., 2003), and once open, TRPV4 channels allow the influx of Ca^{2+} into the endothelial cell (Mendoza et al., 2010; Sukumaran et al., 2013). In addition to this, a layer of polysaccharides and glycoproteins, called the glycocalyx, coats the luminal surface of the endothelium (VanTeeffelen et al., 2007). Sialic acids and proteoglycans that are associated with glycosaminoglycans make up these

glycoproteins (Pahakis et al., 2007). They are involved in transduction of shear stress on the endothelium that ultimately induce NO production (Pahakis et al., 2007; VanTeeffelen et al., 2007; Wang et al., 2020). Disruption of the glycocalyx has been reported to attenuate shear stress induced NO release (Florian et al., 2003; Pahakis et al., 2007; VanTeeffelen et al., 2007).

Similar to smooth muscle cell signalling, endothelium-dependent vasodilation pathways can also be mediated by increased intracellular Ca^{2+} concentration (reviewed by Tran et al., 2000). Initiation of Ca^{2+} entry into the endothelial cell by bradykinin, for example, begins with the activation of bradykinin type 2 (B_2) receptor, a $G_{q/11}$ coupled GPCR (Danser et al., 2000; Faussner et al., 2009). Activation of B_2 receptors promotes the dissociation of $G_{q/11}$ protein and begins the signalling cascade (described in section **1.6.2 Regulation of vascular tone**), ultimately leading to an increase in intracellular Ca^{2+} through IP_3R on the endoplasmic reticulum in the endothelial cell (Hepler & Gilman, 1992).

Endothelial nitric oxide synthase and nitric oxide

Mechanical stimulation as well as mediators such as bradykinin (Danser et al., 2000) and histamine (H. Jin et al., 2006), can stimulate endothelial nitric oxide synthase (eNOS) and initiate the production of NO, a potent vasodilator (Palmer et al., 1987; Vanhoutte et al., 2017). eNOS is constitutively expressed in endothelial cells and is activated by Ca^{2+}/calmodulin complex (**Figure 1.4**), therefore, requiring an increase in intracellular Ca^{2+} (reviewed by Marletta, 1993). Ca^{2+}/calmodulin binds to eNOS between the enzyme's two domains: the C-terminal reductase domain and the N-terminal oxygenase domain (Förstermann & Münzel, 2006; Marletta, 1993). The reductase domain binds electron donor nicotinamide-adenine-dinucleotide phosphate (NADPH) and electron transporter flavins: flavin adenine dinucleotide (FAD) and flavin mononucleotide (FMN) (Förstermann & Münzel, 2006; Marletta, 1993). The oxygenase domain

binds the co-factor (*6R*-)5,6,7,8,-tetrahydrobiopterin (BH_4) and a prosthetic heme (Förstermann & Münzel, 2006; Marletta, 1993). Binding of Ca^{2+}/calmodulin to an eNOS monomer enables eNOS activity by assisting electron transfer from the reductase domain to the oxygenase domain (**Figure 1.5**) (Förstermann & Münzel, 2006). However, eNOS must first form a homodimer in order to properly bind its substrate, L-arginine and cofactor BH_4 (Förstermann & Münzel, 2006). Once the Ca^{2+}/calmodulin is bound and the eNOS homodimer is formed, electrons can then be transferred from the reductase domain to the oxygenase domain allowing the enzyme to convert molecular oxygen and L-arginine into NO and L-citrulline (Förstermann & Münzel, 2006). eNOS activity can be inhibited by L-arginine analogues including N^G-nitro-L-arginine methyl ester (L-NAME) that competes with L-arginine for the substrate binding site of eNOS (Rees et al., 1990).

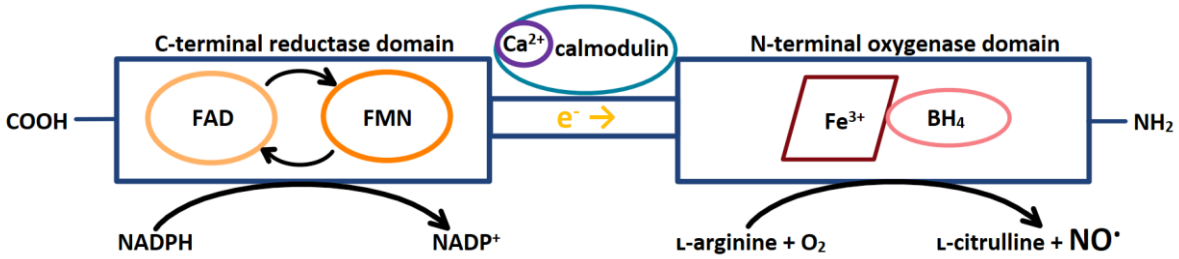

Figure 1.5 eNOS structure. The C-terminal reductase domain of the eNOS enzyme contains electron transporter flavins (FAD and FMN) which enables electron transfer from NADPH. Binding of the Ca^{2+}/calmodulin complex to eNOS allows the movement of electrons to the N-terminal oxygenase domain that contains a prosthetic heme and binds co-factor BH_4. L-arginine and molecular oxygen are then converted to L-citrulline and NO by the N-terminal oxygenase domain. This figure was modified to include the Ca^{2+}/calmodulin complex from the original "Figure 1. Schematic view of NOS" presented in Marletta, 1993 which is licensed under CC BY 4.0.

NO, previously known as an endothelium-derived relaxing factor, is a free radical that plays a role in regulation of basal vasodilation in small resistance arteries, as well as reactive vasodilation in response to paracrine signals and physical stimuli on the endothelial cells (Danser et al., 2000; H. Jin et al., 2006; Joannides et al., 1995; Palmer et al., 1987; Rees et al., 1989). Once produced in the endothelium by eNOS, NO diffuses into the vascular smooth muscle cell and activates soluble guanylyl cyclase (sGC) by binding to the regulatory subunit (Négrerie et al., 2001; Underbakke et al., 2014). Activated sGC then catalyzes guanosine 5'-triphosphate (GTP) into cyclic guanosine monophosphate (cGMP) which acts as a secondary messenger (Négrerie et al., 2001). cGMP activates protein kinase G (PKG) to elicit smooth muscle relaxation through many pathways including promoting MLCP activity resulting in dephosphorylation of myosin light-chain (Etter et al., 2001; Nakamura et al., 2007), inhibition of IP_3 production (Tertyshnikova et al., 1998; Xia et al., 2001), and inhibition of IP_3-mediated Ca^{2+} release through phosphorylation of IP_3R Ca^{2+} channels (Komalavilas & Lincoln, 1996; Murthy & Zhou, 2003; Schlossmann et al., 2003; Tertyshnikova et al., 1998). In addition to this, PKG also phosphorylates phospholamban (PLB), a regulatory molecule that inhibits SERCA uptake of Ca^{2+} into the sarcoplasmic reticulum (**Figure 1.4**) (Colyer, 1998; Paul, 1998). Phosphorylation of PLB attenuates its inhibition of SERCA and allows for Ca^{2+} uptake into the sarcoplasmic reticulum (Colyer, 1998; Paul, 1998). Ultimately, NO-induced increases in cGMP reduces cytosolic Ca^{2+} and inhibits the resulting smooth muscle contraction (described in section **1.6.2 Regulation of vascular tone**).

Endothelium-dependent hyperpolarization

In addition to NO production and the resulting vasorelaxation, the endothelium can also induce relaxation independently of NO release through the activation of endothelium-dependent hyperpolarization (EDH) (Edwards et al., 2010). EDH is produced through the activation of

endothelial cell small and intermediate conductance Ca^{2+}-activated potassium (K^+) channels, SK_{Ca} and IK_{Ca}, respectively (reviewed by Edwards et al., 2010). SK_{Ca}, also known as $K_{Ca}2.3$ channels, and IK_{Ca}, also known as $K_{Ca}3.1$ channels, have both been located to the vascular endothelium with distinct distribution, in which SK_{Ca} has been localized to endothelial cell gap junctions and luminal caveolae, and IK_{Ca} has been localized to the endothelial-smooth muscle interface and adjacent to myoendothelial gap junctions (**Figure 1.4**) (Edwards et al., 1998; Kerr et al., 2012, 2015; Sandow et al., 2006). SK_{Ca} and IK_{Ca} have six transmembrane domains and constitutively bind calmodulin at their C-terminal domain (B. M. Brown et al., 2020; Wulff & Köhler, 2013). When Ca^{2+} binds to calmodulin it initiates a conformational change in calmodulin which then stabilizes the open state of the channel (B. M. Brown et al., 2020). These open channels allow for the efflux of K^+ from the cell resulting in hyperpolarization (Edwards et al., 1998). SK_{Ca} can be inhibited by a polypeptide toxin produced by bees, apamin, that binds to and blocks SK_{Ca} channels via an allosteric mechanism (Lamy et al., 2010). IK_{Ca} can be inhibited by the synthetic selective inhibitor, 1-[(2-chlorophenyl)diphenylmethyl]-1H-pyrazole (TRAM-34) (Wulff et al., 2000).

Endothelial hyperpolarization then spreads to the vascular smooth muscle cell through myoendothelial gap junctions (Mishra et al., 2016). Hyperpolarization of the vascular smooth muscle reduces the probability of L-type VGCC opening (Tykocki et al., 2017). This limits the influx of Ca^{2+} into the cell that would provide the increase in intracellular Ca^{2+} necessary to initiate smooth muscle contraction, as described in section **1.6.2 Regulation of vascular tone**. Absence of the necessary charged residues on the S4 segment make these SK_{Ca} and IK_{Ca} channels insensitive to voltage changes which allows them to remain open as the cell hyperpolarizes (Wulff & Köhler, 2013).

Appropriate vasomotor control and blood pressure regulation requires a balance between vasodilation and vasoconstriction. When this balance is lost, for example due to endothelial cell dysfunction, blood pressure regulation can be jeopardized and the development of hypertension can occur. In hypertensive conditions, drugs can be used to re-establish a balance between vasodilation and vasoconstriction.

To summarize, high fibre diets have been associated with influencing beneficial blood pressure regulation (Appel et al., 1997; Najjar et al., 2018) and recent investigations have focused on SCFAs and their possible role in influencing vasomotor control and blood pressure regulation (Aaronson et al., 1996; Knock et al., 2002; Mortensen et al., 1990; Natarajan et al., 2016; Nutting et al., 1991). SCFAs have previously been shown to induce vasorelaxation in *in vitro* studies, however the mechanism through which they mediate this effect is not yet known. Therefore, much is still to be uncovered with regards to the mechanisms of action of SCFAs and how they may influence blood pressure.

1.7 Hypothesis and research aims

With this in mind, my goal with this arm of my research is to investigate the mechanism underlying the effect of SCFAs in small mesenteric resistance arteries and to test the following hypothesis:

SCFAs have direct vasodilator effects in resistance arteries mediated through endothelium-dependent mechanisms.

To address this hypothesis, I aimed to determine the effects of SCFAs in small mesenteric resistance arteries by investigating their impact on agonist-induced tone in isolated third order mesenteric arteries and on nerve-evoked increases in perfusion pressure in the intact mesenteric

vascular bed. I also aimed to determine the mechanisms through which SCFAs influence small mesenteric resistance arteries with the use of pharmacological tools.

Chapter 2: Methods and materials

2.1 Ethics approval

All animal care and use were approved by the University of Alberta Animal Care and Use Committee for Health Sciences 1 (AUP 312) and followed guidelines presented by the Canadian Council on Animal Care. Description of care and use is described below following Grundy's principles and standards (Grundy, 2015).

2.2 Animal care and use

Male Sprague-Dawley rats (250-300g; Charles River Canada) were housed by the University of Alberta Health Sciences Laboratory Animal Services providing these animals with an enriched environment. These animals were fed standard chow and fresh water *ad libitum* and kept in rooms maintained at an average temperature of 23°C with a 12:12-hour light to dark cycle. Euthanasia was performed by isoflurane inhalation followed by decapitation prior to dissection and collection of the mesenteric vascular bed. All tissues were kept in ice-cold Krebs buffer solution until used.

2.3 Tissues

The mesenteric vascular bed, which surrounds the gastrointestinal tract, is largely made up of small resistance arteries. These small resistance arteries play a large role in blood pressure regulation as they can adjust the diameter of their lumen in response to various stimuli through vasoconstriction and vasodilation (described in **Section 1.6**) making these vessels ideal for investigating the effects of vasoactive agents. The mesenteric vascular bed was either kept intact for mesenteric perfusion experiments (**Figure 2.1**) or further dissected to isolate third order resistance arteries for wire myography experiments.

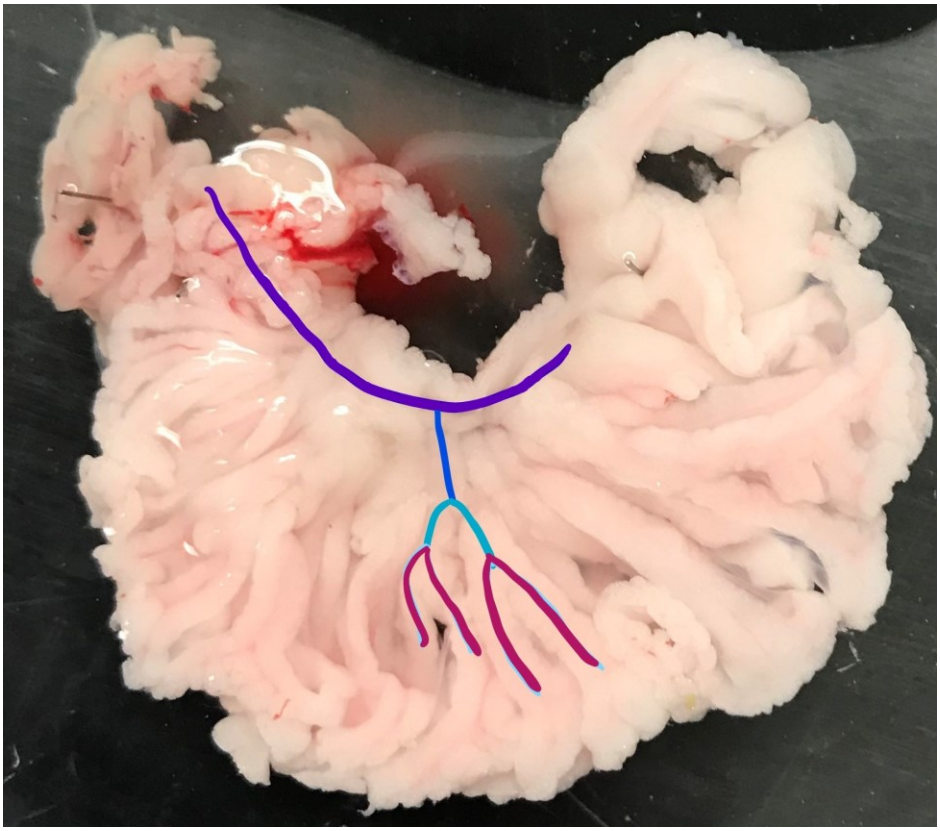

Figure 2.1 Rat mesenteric vascular bed. Lined in dark purple is the superior mesenteric artery. A first order mesenteric artery is lined in dark blue; second order mesenteric arteries are lined in light blue; and third order mesenteric arteries are lined in magenta.

2.4 Experimental procedures

2.4.1 Wire-myography

Third order mesenteric resistance arteries isolated from the mesenteric vascular bed were placed in a petri-dish filled with ice-cold Krebs buffer. Further dissection of the artery was done under a dissecting microscope to remove all adhering perivascular adipose and connective tissue. Once the excess tissue was removed, the artery was then cut into four segments that were each threaded with two gold-plated tungsten wires (25 μM diameter; Goodfellow Cambridge Limited, U.K.). These segments were then mounted in a Mulvany-Halpern myograph (Model 610M, Danish Myo Technology, Aarhus, Denmark) (**Figure 2.2**). Each wire myograph bath was filled with 7 ml

of Krebs buffer solution, oxygenated with 95% O_2/5% CO_2 and kept at 37°C. Once mounted in the myograph, the segments were then stretched until the tension of 5 mN was reached. This is the pre-determined optimal resting tension for these vessels. The segments were left to equilibrate for 20 mins prior to testing endothelial function of the segments with a control acetylcholine (ACh) relaxation curve. These control cumulative-concentration-response curves were constructed by first increasing tone with phenylephrine (PE; 3 μM). Once PE-induced tone stabilized, ACh (10 μM) was added to induce relaxation. The endothelium was considered intact when >90% reduction in PE-induced tone was achieved. Artery segments that did not have >90% reduction in agonist-induced tone were discarded.

To investigate the effect of SCFAs on the segments with intact endothelium, cumulative concentration-response curves were constructed to sodium acetate, sodium propionate and sodium butyrate in the presence and absence of a combination of inhibitors: L-NAME (100 μM), TRAM-34 (1 μM) and apamin (50 nM). To determine the mechanisms through which these SCFAs may be affecting these arteries cumulative concentration-response curves for each SCFA were done under four treatments: 1) time control, 2) L-NAME, 3) TRAM-34 and apamin, and 4) TRAM-34, apamin and L-NAME. All inhibitors were added 20 mins prior to PE stimulation to allow for equilibration. Representative traces of propionate time control and of propionate with all three inhibitors together are presented in **Figure 3.1**. Wire myograph data was recorded with Powerlab 4/25 (AD Instruments, Colorado) and LabChart 8 software (AD Instruments, Colorado).

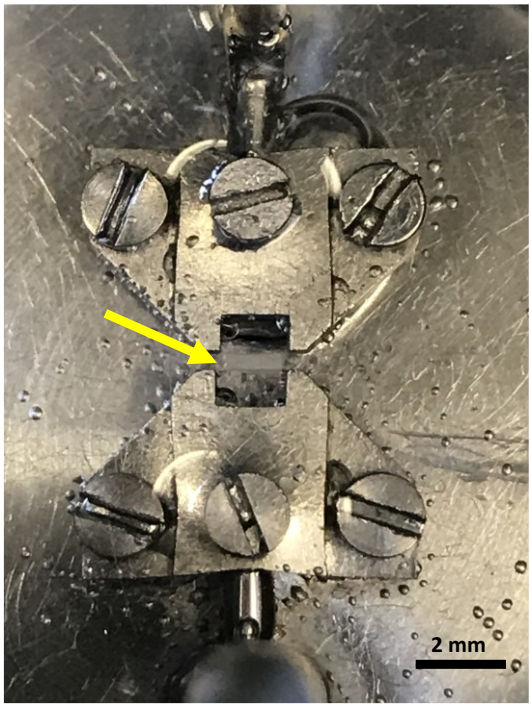

Figure 2.2. A third order mesenteric artery mounted in a Mulvany-Halpern wire myograph. Scale bar is 2 mm.

2.4.2 Perfusion of the mesenteric vascular bed

The intact mesenteric vascular bed was set up as previously described by Narang et al. (2014) (Narang et al., 2014). In brief, a blunted 20 G hypodermic needle was inserted into the superior mesenteric artery of the mesenteric bed and secured with suture thread (Black Braided Silk, Ethicon). The mesenteric bed was flushed with Krebs buffer solution to remove the blood from the vascular bed prior to it being placed on a wire mesh and inserted into a warm water jacket. Once the wire mesh was secured in the water jacket, the needle was then connected to the perfusion apparatus. The mesenteric bed was then perfused with oxygenated (95% O_2/5% CO_2) Krebs buffer (37°C) at a constant flow rate of 5 $mlmin^{-1}$, previously determined to be the optimal perfusion rate to maintain viability of the tissue without increasing the baseline perfusion pressure. The vascular bed was then left to equilibrate for 20 mins. Electrodes were attached to the blunted needle inserted into the vascular bed and the wire mesh to allow for electrical field stimulation of the mesenteric

bed. An in-line pressure transducer was used to measure changes in perfusion pressure in response to electrical field stimulation every 10 mins at 1-40 Hz (90 V, pulse width 1 msec, 30 secs) to create a frequency-response curve. Changes in pressure were recorded with PowerLab 2/20 (AD Instruments, Colorado) and Chart 5.0 software (AD Instruments, Colorado).

2.5 Reagents

Krebs buffer solution was composed of NaCl 118.0 mM, $NaHCO_3$ 25.0 mM, KCl 4.7 mM, $MgSO_4$ 1.2 mM, KH_2PO_4 1.18 mM, glucose 11 mM, and $CaCl_2$ 2.5 mM in distilled water. For perfusion experiments, the effects of SCFAs (30 mM) were investigated under two conditions. The first in which there was equimolar substitution for NaCl with 30 mM SCFAs in the Krebs buffer. Second, 30 mM of the SCFAs were added to the Krebs buffer without equimolar substitution of NaCl.

Table 2.1 Reagents Table

Reagent	Source	Mechanism of action	Solvent
Acetylcholine (ACh)	Sigma-Aldrich	Agonist at muscarinic receptors (Broadley & Kelly, 2001)	Distilled water
Apamin	Tocris	Inhibits SK_{Ca} channels (Blatz & Magleby, 1986; Pease & Wemmer, 1988)	Distilled water
L-NAME	Sigma-Aldrich	Inhibits nitric oxide synthase (Rees et al., 1990)	Distilled water
L-Phenylephrine hydrochloride (PE)	Sigma-Aldrich	Agonist at α_1-adrenoreceptors (Timmermans et al., 1980)	Distilled water
Sodium acetate	Sigma-Aldrich	Not yet known	Distilled water or Krebs buffer
Sodium butyrate	Sigma-Aldrich	Not yet known	Distilled water or Krebs buffer
Sodium propionate	Sigma-Aldrich	Not yet known	Distilled water or Krebs buffer
TRAM-34	Tocris	Inhibits IK_{Ca} channels (Wulff et al., 2000)	Dimethyl Sulphoxide (DMSO)

2.6 Statistical analysis

2.6.1 Wire myography data analysis

Each data point represents a third order resistance artery collected from the mesenteric vascular bed of one animal (n = 1). Data is presented as the mean ± Standard Error of the Mean (SEM) for n animals. Two-way, repeated measures Analysis of Variance (ANOVA) was used to compare multiple measurements. Tukey's post hoc test was done on ANOVA analysis of three comparisons or more, α value was set at 0.05 for all analyses completed. All statistical analyses were performed with GraphPad Prism 6.

2.6.2 Mesenteric perfusion data analysis

Each data point represents one intact mesenteric vascular bed taken from one animal (n = 1). Data is presented as the mean ± SEM for n animals. Analysis was done with two-way, repeated measures ANOVA to compare multiple measurements. Tukey's post hoc test was done on ANOVA analysis of three comparisons or more, and Sidak's post hoc test was done on ANOVA for two comparisons, α value was set at 0.05 for all analyses completed. All statistical analyses were performed with GraphPad Prism 6.

Chapter 3: Vascular effects of short-chain fatty acids on small mesenteric arteries

Several studies have investigated the effects of short-chain fatty acids (SCFAs) on blood vessels (Aaronson et al., 1996; Knock et al., 2002; Mortensen et al., 1990; Natarajan et al., 2016; Nutting et al., 1991; Pluznick et al., 2013). These studies have provided some useful insight; however, they often focused on the actions of a single SCFA at a single concentration and only used one method to investigate their effects. Therefore, the mechanism of action of these SCFAs has not yet been fully elucidated. In my research, I aimed to determine the mechanism of action of these small, gut-derived molecules in influencing vascular tone to address the hypothesis that these SCFAs have direct effects in small resistance arteries mediated through endothelium-dependent mechanisms, using two different preparations. The first focuses on the effect of cumulative concentration of SCFAs in isolated arteries and the second focuses on the effects of a single concentration of SCFAs in the intact mesenteric vascular bed in the presence of flow.

3.1 Results

3.1.1 Effect of SCFAs on agonist-induced tone in isolated mesenteric arteries

The effects of SCFAs on vascular tone in isolated resistance arteries were investigated using wire myography in which segments of a third order mesenteric artery were mounted in the baths of the apparatus, as described in **Chapter 2**. Once mounted, cumulative concentration-response curves were constructed to sodium acetate, sodium propionate, and sodium butyrate, individually, in the absence and presence of pharmacological inhibitors of endothelium-dependent vasodilation. These inhibitors include an inhibitor of NOS, L-NAME, a SK_{Ca} channel inhibitor, apamin, and an IK_{Ca} channel inhibitor, TRAM-34. These inhibitors were used to determine the possible mechanism through which these SCFAs affect vasomotor control in these arteries.

Inhibitors were added to their designated bath 20 mins prior to the addition of phenylephrine (PE) to allow for equilibration. PE (3-10 μM) was added to the baths to induce tone in the artery segments mounted in the wire myograph. Once tone was established, SCFAs were added to the bath at increasing, cumulative concentrations (100 nM – 100 μM).

SCFAs, acetate, propionate, and butyrate, induced a concentration-dependent reduction in tone. Butyrate produced the greatest reduction in tone, followed by propionate and acetate (**Table 3.1** and **Figure 3.2c**). The reduction in tone initiated by these SCFAs was differentially attenuated in the presence of the inhibitors. L-NAME (100 μM) significantly attenuated the effects of acetate (0.3 – 1 μM) and butyrate (0.3 – 10 μM), but not propionate (**Figure 3.2**). TRAM-34 (1 μM) and apamin (50 nM), together, significantly attenuated the effects of propionate (10 μM) and butyrate (0.3 – 10 μM), but not that of acetate (**Figure 3.2**). The greatest attenuation was seen when all inhibitors were present, with significant attenuation of the effects of acetate (0.3 – 3 μM), propionate (10 -30 μM) and butyrate (0.3 – 10 μM; **Figure 3.2**).

These SCFAs have a main effect of evoking a reduction in PE-induced tone in isolated rat mesenteric arteries. However, these SCFAs appear to vary in their effects. Butyrate produced the greatest reduction in tone, an effect that was attenuated by all combinations of inhibitors, suggesting that butyrate may mediate its effects through NO production and opening of SK_{Ca} and IK_{Ca} channels. Propionate and acetate evoked reductions in tone were attenuated by all three inhibitors, together, indicating that endothelium-dependent mechanisms may be involved in mediating their effects at lower concentrations (≤30 μM). Acetate's effects were also attenuated by L-NAME alone, suggesting NO production may play a significant role in mediating its effect. Propionate, however, was partially attenuated by TRAM-34 and apamin, together, and was attenuated to a greater extent by all three inhibitors together. Therefore, the effects of propionate

may not be meaningfully mediated by NO production under these conditions. All together, this suggests that the SCFA-evoked loss in tone works, at least in part, through endothelium-dependent vasodilation mechanisms in isolated rat mesenteric arteries.

Table 3.1 Maximum relaxation produced by SCFAs			
Condition	**Short-chain fatty acid**		
	Acetate	**Propionate**	**Butyrate**
Control	31.6 ± 8.3%	32.7 ± 7.0% (9)	47.3 ± 9.2% (8)
L-NAME	24.8 ± 9.0%	28.7 ± 8.9%	25.0 ± 8.1%
TRAM-34 + apamin	24.2 ± 8.1%	16.0 ± 5.3%	19.6 ± 3.7%
TRAM-34, apamin + L-NAME	15.0 ± 3.0%	12.2 ± 5.0%	19.7 ± 11.5% (8)

Table 3.1. Maximum relaxation produced by SCFAs in the absence and presence of inhibitors. These values are expressed as % of maximum relaxation of PE-induced tone, data for a given treatment is presented as mean ± SEM, n=7 unless otherwise specified; *data contributed by Alexia Maheux.*

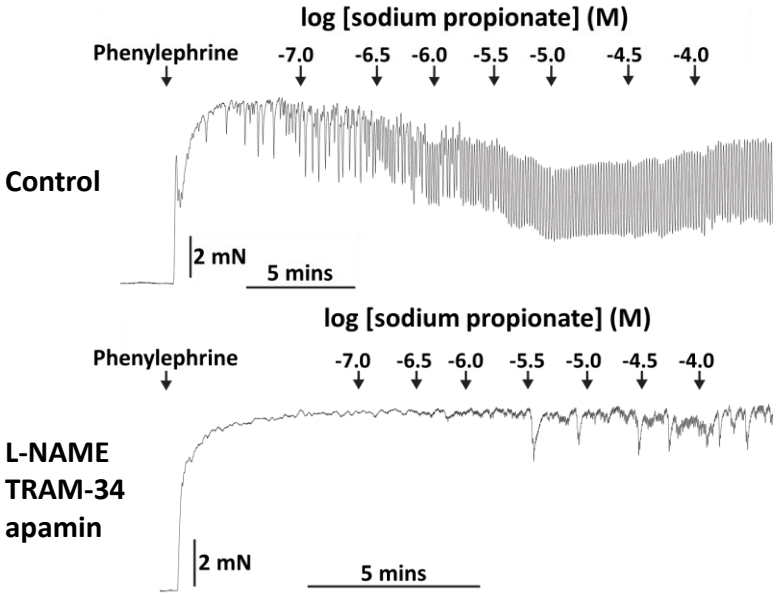

Figure 3.1 Representative traces of cumulative concentration-response curves. Presented are two representative cumulative concentration-response curves to sodium propionate on PE-induced tone on segments of a rat mesenteric resistance artery in the absence and presence of inhibitors L-NAME (100 μM), TRAM-34 (1 μM) and apamin (50 nM); *data contributed by Alexia Maheux.*

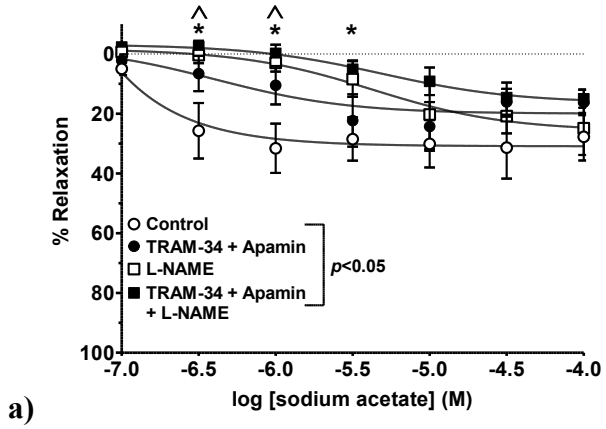

a)

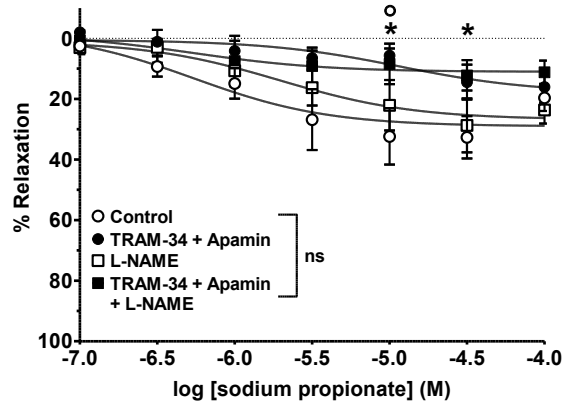

b)

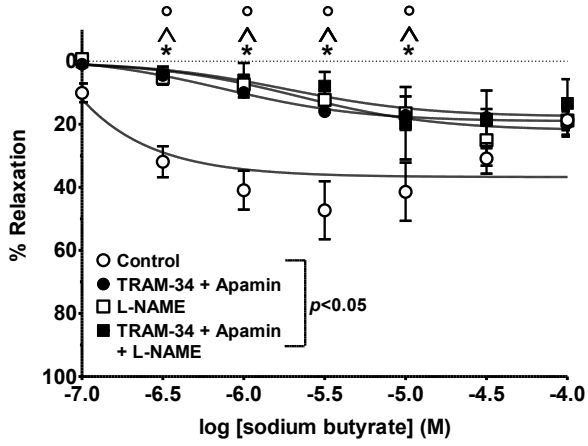

c)

Figure 3.2 Cumulative concentration-response curves presenting the effect of SCFAs in isolated mesenteric resistance arteries. These graphs display mean data of cumulative concentration-response curves to **a)** sodium acetate **b)** sodium propionate (control n=9) and **c)** sodium butyrate (control n=8, TRAM-34 + apamin + L-NAME n=8) as % relaxation of PE-induced tone. All data are presented as mean ± SEM, n=7 unless otherwise specified; ^denotes $p<0.05$ for treatment of L-NAME compared to control; ○ denotes $p<0.05$ for treatment of TRAM-34 and apamin compared to control; *denotes $p<0.05$ for treatment of TRAM-34, apamin and L-NAME compared to control; *data contributed by Alexia Maheux.*

3.1.2 Effect of SCFAs on nerve-evoked increases in perfusion pressure in the rat mesenteric vascular bed

Wire myography data confirms and further supports the finding that SCFAs do affect vasomotor control in isolated rat mesenteric arteries, even at lower concentrations than previously investigated. Therefore, I moved on to determining the effects of SCFAs in the intact mesenteric vascular bed in the presence of flow. To begin, I investigated the effect of SCFAs, acetate and propionate at peripheral physiological concentrations in order to determine the possible effect of these SCFAs at μM concentrations. I then investigated the effect of these SCFAs at a higher concentration (30 mM) with equimolar substitution of NaCl in the Krebs buffer with either 30 mM sodium acetate or 30 mM sodium propionate. It has previously been reported that changes in osmolarity can influence vasodilation (Aalkjær, 2002; F. N. Miller et al., 1981; Steenbergen & Bohlen, 1993; Zakaria et al., 2005). SCFA absorption is coupled with Na^+ absorption from the intestinal lumen into the blood (as described in **section 1.4.1 SCFA transport**). Therefore, to determine if an increase osmolarity influences the effects of SCFAs, I carried out perfusion experiments with the addition of 30 mM sodium acetate or 30 mM sodium propionate to the Krebs buffer without equimolar substitution of NaCl. The presence of flow applies shear stress to the vessel wall that can drive endothelium-dependent vasodilation mechanisms, including NO production and the opening of Ca^{2+}-activated K^+ channels (described in **Chapter 1**). To determine the mechanisms mediating the effects of SCFAs under these conditions, I then investigated the effects of SCFAs on nerve-evoked increases in perfusion pressure in the perfused mesenteric vascular bed in the absence and presence of pharmacological inhibitors to identify the possible role of endothelium-dependent mechanisms.

In the perfused intact rat mesenteric vascular bed, nerve-evoked increases in perfusion pressure are frequency-dependent responses. Under control conditions, in which only Krebs buffer is perfused, the overall mean values of the frequency-response curves did not change significantly over time, however there was significant attenuation at 15 Hz and augmentation at 30 and 40 Hz of frequency-dependent responses over time (**Figure 3.3b)**. In the presence of L-NAME (100 μM), an inhibitor of NOS, the frequency-dependent response was enhanced significantly at stimulation frequencies of 15 to 40 Hz (**Figure 3.3c)**. In the presence of TRAM-34 (1 μM) and apamin (50 nM), inhibitors of IK_{Ca} and SK_{Ca} channels, the frequency-dependent response was also significantly enhanced at stimulation frequencies of 20 to 40 Hz (**Figure 3.3c)**.

Effect of SCFAs, acetate and propionate at physiological peripheral μM concentrations did not significantly change the mean values of the frequency-response curves, therefore no significant main effect was observed (**Figure 3.4**). However, there was a significant attenuation of the frequency-dependent response at 15 and 20 Hz in the second frequency-response curve with sodium propionate (5 μM; **Figure 3.4b**). 70 μM sodium acetate enhanced frequency-dependent responses at 30 and 40 Hz, but did not significantly attenuate frequency-dependent responses compared to control (**Figure 3.4a**).

In experiments with perfusion of equimolar substituted NaCl in the Krebs buffer with 30 mM sodium acetate or 30 mM sodium propionate there was a significant main effect observed (**Figure 3.5**). Diminished frequency-dependent responses were observed in the second frequency-response curve of 30 mM sodium acetate at 15 and 20 Hz (**Figure 3.5a**) and the second frequency-response curve of 30 mM sodium propionate at stimulation frequencies of 15 to 40 Hz (**Figure 3.5b**), indicating a possible time-dependent effect of 30 mM sodium acetate and 30 mM sodium propionate under these conditions.

Control experiments were carried out with an increase in NaCl concentration of 150 mM NaCl added to the Krebs buffer compared to 118 mM NaCl usually present. This was done to determine if an increase in NaCl and, thus, an increase in osmolarity may have an effect on frequency-dependent responses. 150 mM NaCl Krebs buffer diminished frequency-dependent responses at 15 and 20 Hz **(Figure 3.6**). These data also indicate there may be a time-dependent amplification of attenuation of responses at 15 and 20 Hz with 150 mM NaCl in the Krebs buffer.

In order to determine the effect of SCFA absorption with Na^+ into the mesenteric vascular bed, perfusion experiments were then done without equimolar substitution of NaCl. Addition of 30 mM sodium acetate (**Figure 3.7a**) and 30 mM sodium propionate (**Figure 3.8a**) to the Krebs buffer perfusate attenuated frequency-dependent responses at 15 and 20 Hz. Significant augmentation of the frequency-dependent responses at 30 and 40 Hz were also observed with 30 mM sodium acetate. However, 30 mM sodium acetate did not significantly alter the mean of the frequency-response curves, thus addition of 30 mM sodium acetate without equimolar substitution of NaCl in the Krebs buffer did not have a statistically significant main effect (**Figure 3.7a**). However, addition of 30 mM sodium propionate without equimolar substitution of NaCl did appear to have a significant main effect (**Figure 3.8a**). In order to determine how these SCFAs may be mediating these effects under increased osmolarity conditions, further experiments were carried out with pharmacological inhibitors.

The effect of sodium acetate, without equimolar substitution of NaCl, on frequency-dependent responses in the perfused mesenteric bed was investigated in the absence and presence of L-NAME, and TRAM-34 and apamin. The frequency-dependent response was significantly attenuated at stimulation frequencies of 15 Hz and 20 Hz in the presence of sodium acetate (30 mM) when compared to control (**Figure 3.7a**). The attenuation of frequency-dependent responses

was lost in the presence of L-NAME (100 μM; **Figure 3.7b**). However, when comparing sodium acetate (30 mM) with L-NAME (100 μM) to L-NAME (100 μM) alone there was a significant difference in the frequency-dependent response at stimulation frequencies of 15 and 20 Hz between these two treatments (**Figure 3.7b**). In the presence of TRAM-34 (1 μM) and apamin (50 nM) the effects of sodium acetate were not significantly lost at 15 Hz stimulation. At 20 Hz there is a significant difference in response between treatment with 30 mM sodium acetate and 30 mM sodium acetate with TRAM-34 (1 μM) and apamin (50 nM) indicating loss of the attenuation effect of 30 mM sodium acetate (**Figure 3.7c**).

The effects of sodium propionate, without equimolar substitution of NaCl, on frequency-dependent responses in the perfused mesenteric vascular bed were also investigated in the absence and presence of L-NAME, and TRAM-34 and apamin. In the presence of sodium propionate (30 mM) the frequency-dependent response was significantly attenuated at stimulation frequencies of 15 and 20 Hz (**Figure 3.8a**). This attenuation of frequency-dependent response was lost in the presence of L-NAME (100 μM; **Figure 3.8b**). When comparing sodium propionate (30 mM) with L-NAME (100 μM) to L-NAME (100 μM) alone there was a significant difference in the frequency-dependent responses at 15 and 20 Hz between these two treatments (**Figure 3.8b**). In the presence of TRAM-34 (1 μM) and apamin (50 nM) the effects of sodium propionate were not lost at 15 and 20 Hz stimulation frequencies (**Figure 3.8c**). There was no significant difference in the means of these frequency-response curves, therefore no statistically significant main effect was observed (**Figure 3.8c**).

Taken together, μM concentrations of sodium acetate and sodium propionate had a minimal overall effect on frequency-response curves. At a higher concentration, 30 mM sodium acetate and sodium propionate have a significant and time-delayed effect on frequency-dependent responses

when included in the Krebs buffer as equimolar substitutions for NaCl. Addition of 30 mM sodium acetate or sodium propionate to the Krebs buffer, without equimolar substitution, provided greater attenuation of frequency-dependent responses at 15 and 20 Hz. This effect appears to be mediated in part through NO production and less significantly through endothelium-dependent hyperpolarization mechanisms in the perfused mesenteric vascular bed. This is contrary to what was observed in the wire myography data, where the effect of sodium propionate did not appear to be mediated by NO production. Therefore, an increase in osmolarity and the presence of shear stress may influence the effects of these SCFAs in this study.

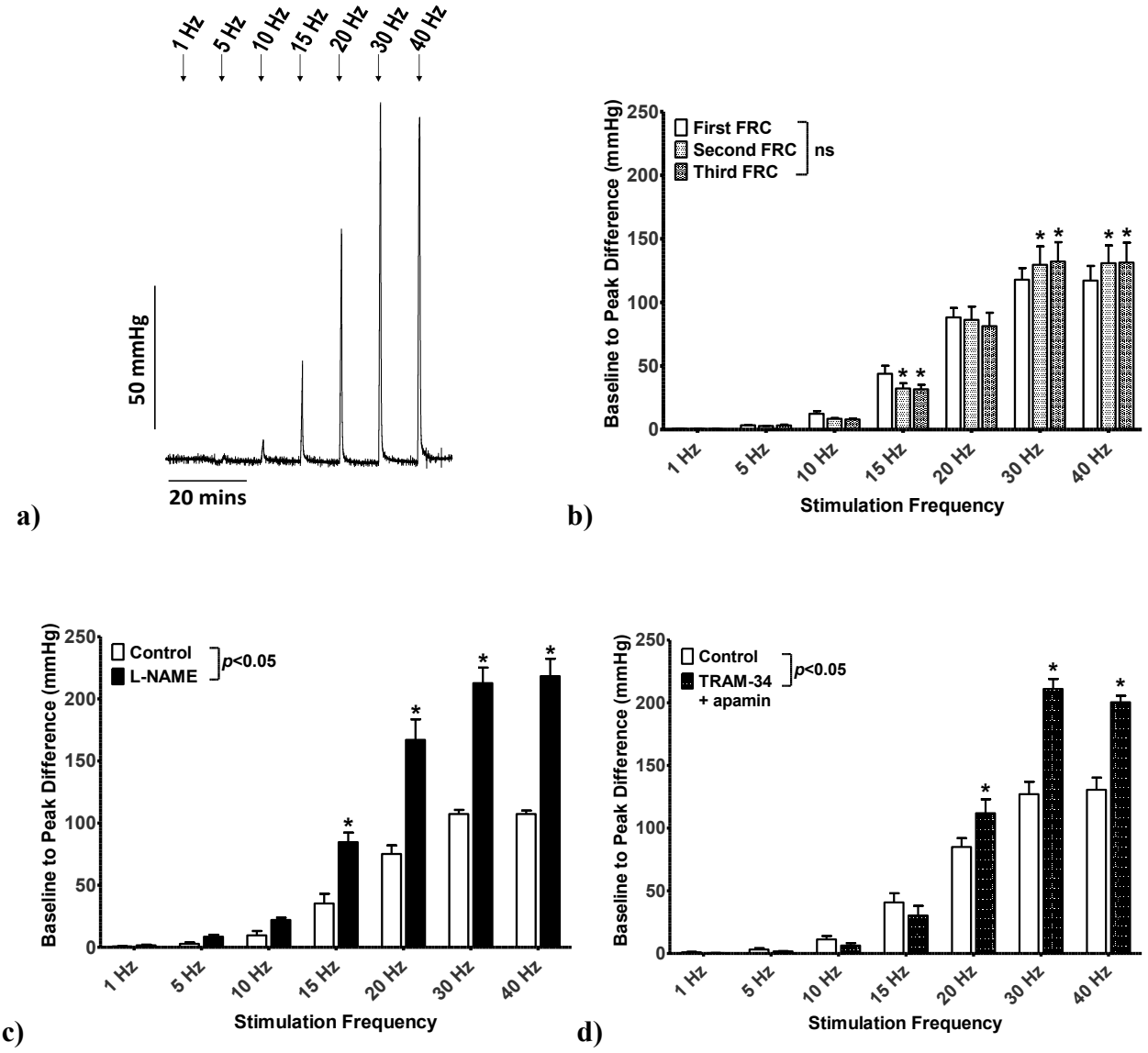

Figure 3.3 Increases in perfusion pressure are frequency-dependent and regulated by NO production and endothelial Ca^{2+}-activated K^+ channels. a) Representative trace of electrical field stimulation (1-40 Hz) of the mesenteric vascular bed presenting a frequency-dependent increase in perfusion pressure. **b)** Mean data of time control frequency-response curves (FRC), n=6. **c)** Mean data of frequency-response curves in the absence and presence of L-NAME (100 μM) with a significant difference between control and L-NAME treatment in the second frequency-response curve, n=4. **d)** Mean data of frequency-response curves in the absence and presence of TRAM-34 (1 μM) and apamin (50 nM) with a significant difference between control and the TRAM-34 and apamin treatment in the second frequency-response curve, n=4. All data are presented as mean ± SEM. *denotes $p<0.05$ for treatment compared to control.

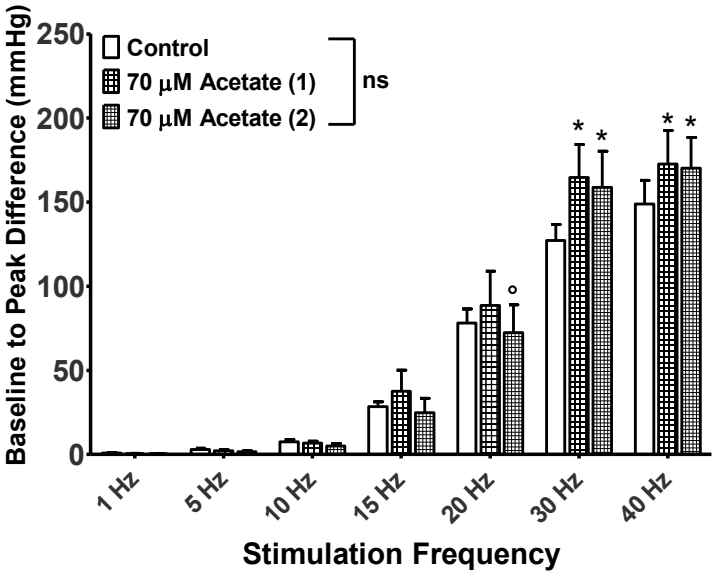

a)

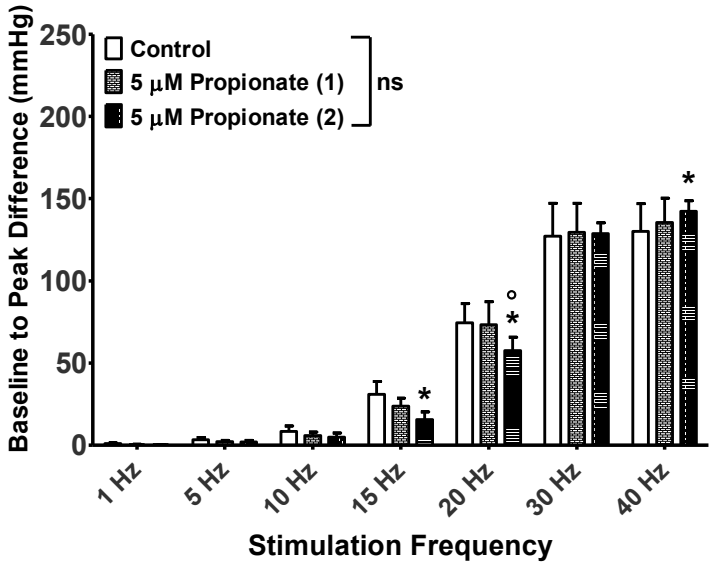

b)

Figure 3.4 Physiological peripheral concentrations of SCFAs acetate and propionate minimally altered mean frequency-dependent responses. a) Mean data of frequency-response curves in the absence and presence of sodium acetate (70 μM), n=4. **b)** Mean data of frequency-response curves in the absence and presence of sodium acetate (5 μM), n=4. All data are presented as mean ± SEM. * denotes $p<0.05$ treatment compared to control; ° denotes $p<0.05$ treatment compared to the first frequency-response curve of SCFA treatment.

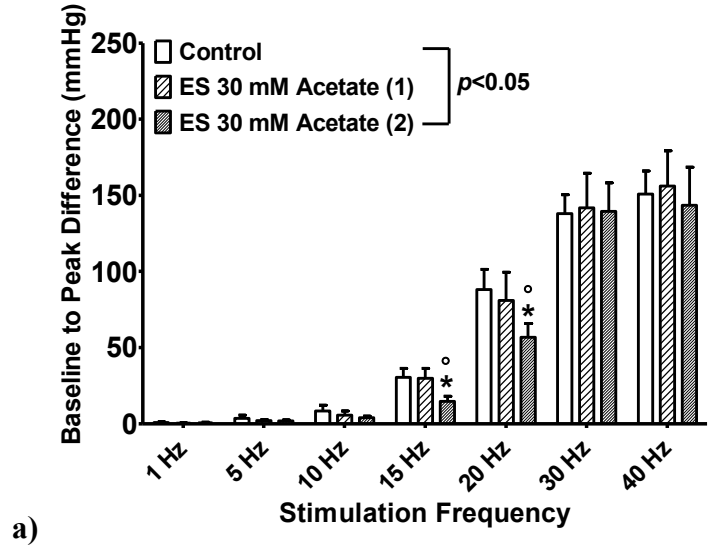

a)

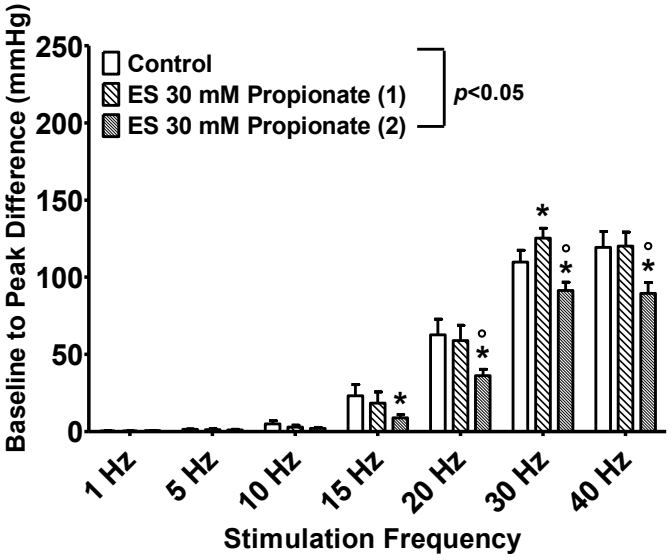

b)

Figure 3.5 Equimolar substitution of NaCl with sodium acetate and sodium propionate diminished frequency-dependent response in a time-dependent manner. a) Mean data of frequency-response curves in the absence and presence of equimolar substitution (ES) of NaCl with sodium acetate (30 mM), n=4. **b)** Mean data of frequency-response curves in the absence and presence of equimolar substitution of NaCl with sodium propionate (30 mM), n=4. All data are presented as mean ± SEM. * denotes $p<0.05$ treatment compared to control; ° denotes $p<0.05$ treatment compared to the first frequency-response curve of SCFA treatment.

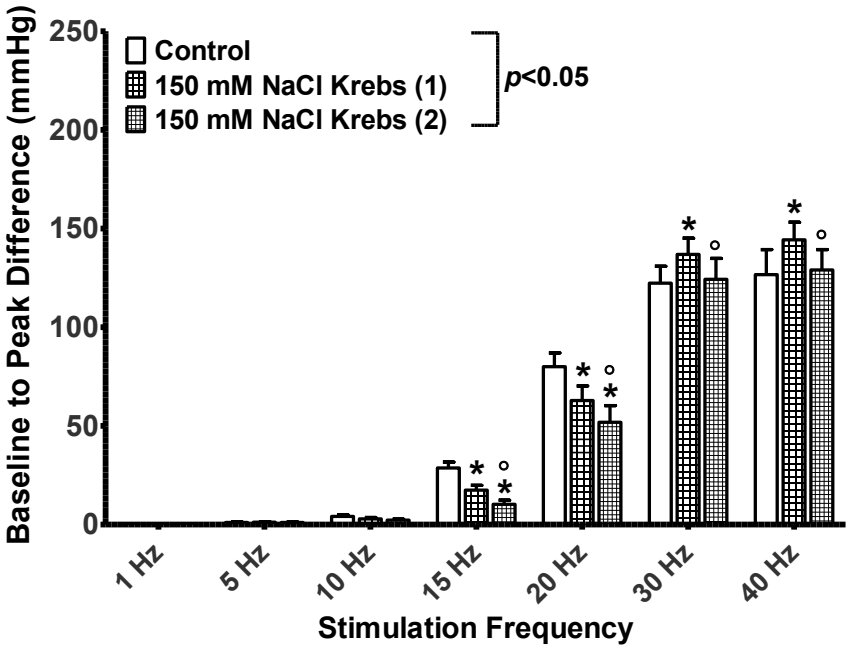

Figure 3.6 An increase in NaCl concentration in the Krebs buffer diminished frequency-dependent responses. a) Mean data of frequency-response curves in the absence and presence of 150 mM NaCl Krebs buffer, n=4. Data are presented as mean ± SEM. * denotes $p<0.05$ treatment compared to control; ° denotes $p<0.05$ treatment compared to the first frequency-response curve of the 150 mM NaCl Krebs buffer treatment.

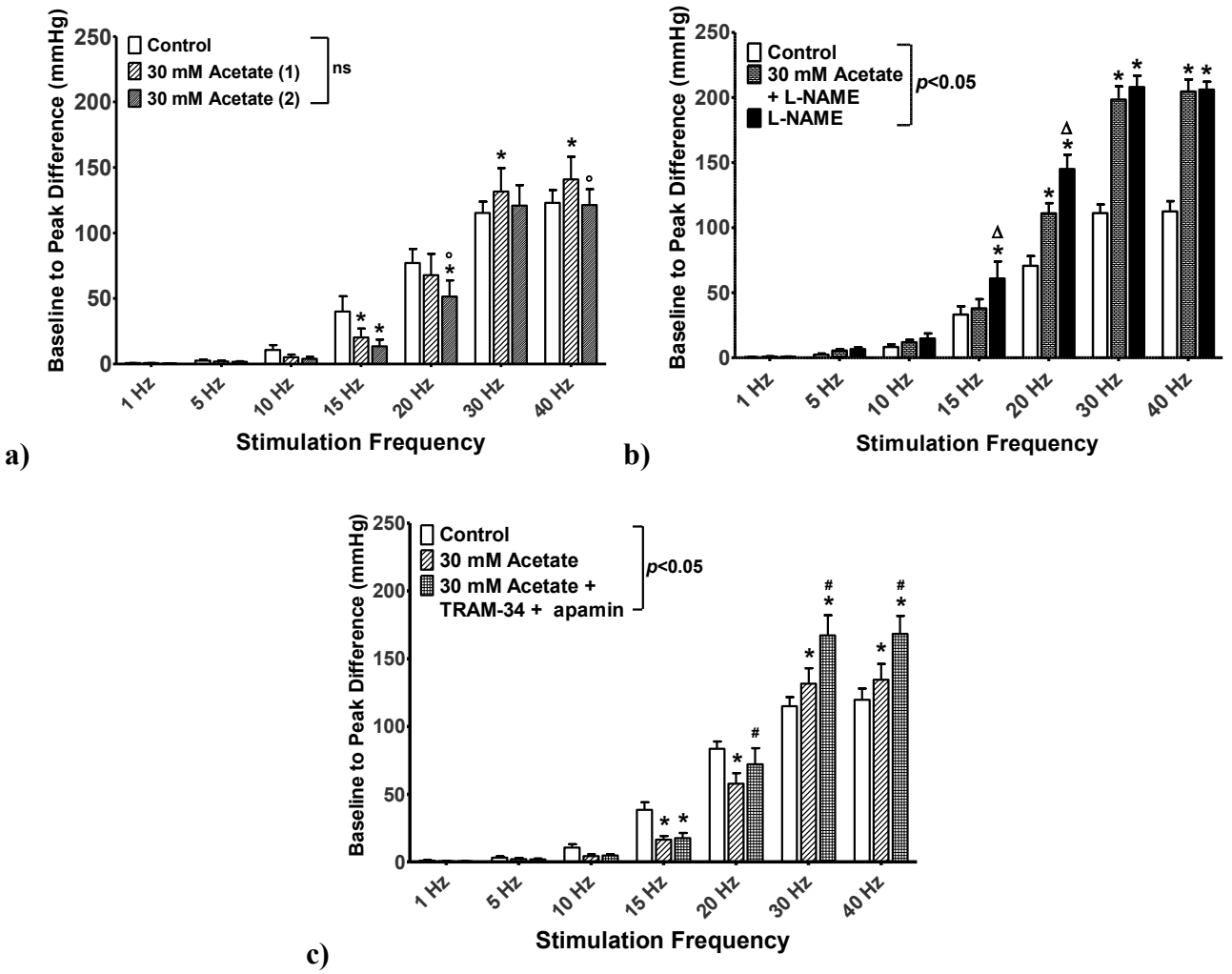

Figure 3.7 Sodium acetate diminished nerve-evoked increases in perfusion pressure in the perfused mesenteric bed at 15 and 20 Hz. a) Mean data of frequency-response curves in the absence and presence of sodium acetate (30 mM), n=4. **b)** Mean data of frequency-response curves of sodium acetate (30 mM) with L-NAME (100 μM), and L-NAME alone (100 μM), n=6. **c)** Mean data of frequency-response curves of sodium acetate (30 mM), and sodium acetate (30 mM) with TRAM-34 (1 μM) and apamin (50 nM), n=6. All data are presented as mean ± SEM. * denotes $p<0.05$ treatment compared to control; ° denotes p<0.05 treatment compared to the first frequency-response curve of 30 mM sodium acetate treatment; **Δ** denotes $p<0.05$ treatment compared to sodium acetate (30 mM) with L-NAME (100 μM) and # denotes $p<0.05$ treatment compared to sodium acetate (30 mM).

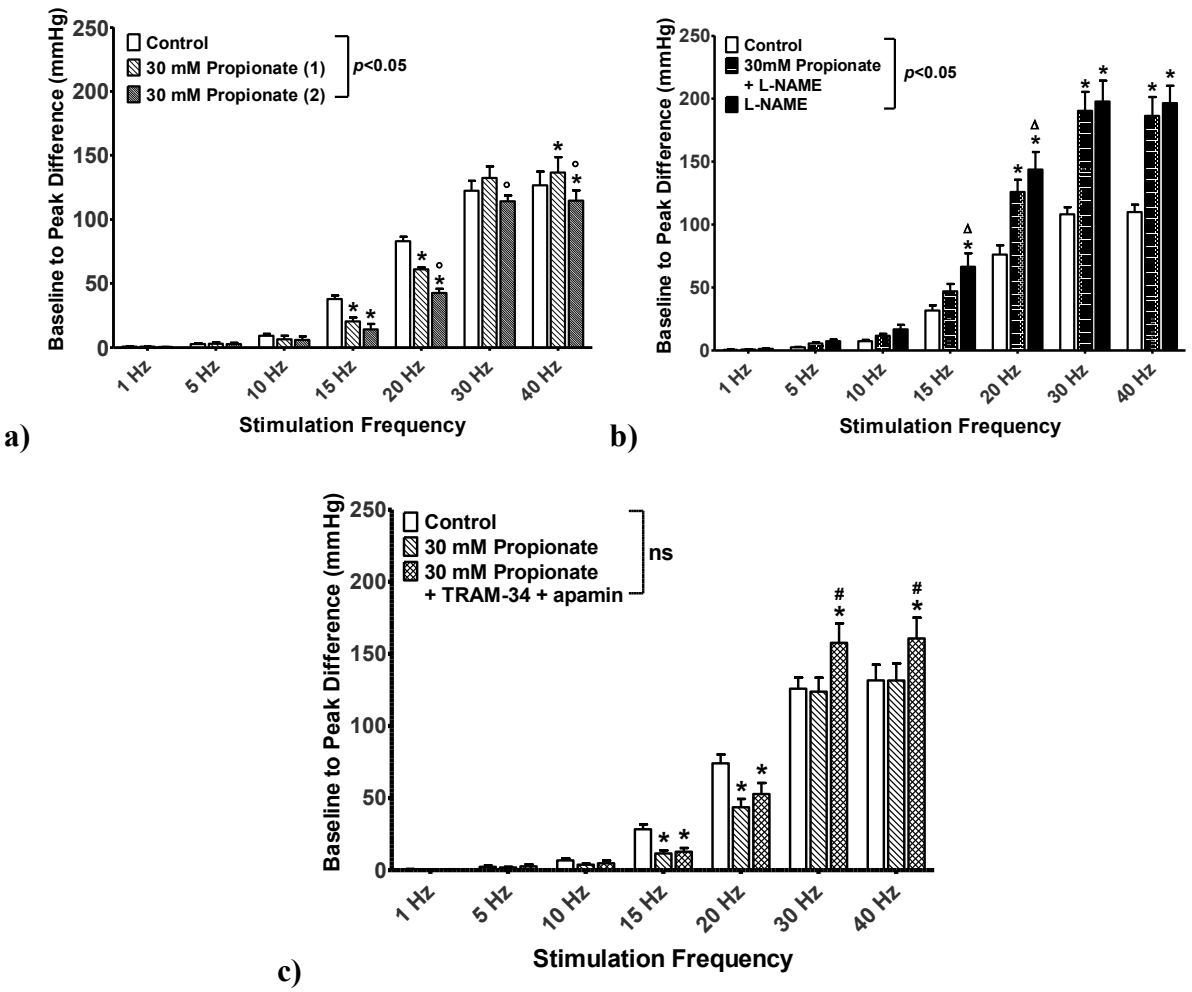

Figure 3.8 Sodium propionate diminished nerve-evoked increases in perfusion pressure in the perfused mesenteric bed at 15 and 20 Hz. a) Mean data of frequency-response curves in the absence and presence of sodium propionate (30 mM), n=4. **b)** Mean data of frequency-response curves of sodium propionate (30 mM) with L-NAME (100 μM), and L-NAME alone (100 μM), n=6; *data contributed by Caitlin Seeger.* **c)** Mean data of frequency-response curves of sodium propionate (30 mM), and sodium propionate (30 mM) with TRAM-34 (1 μM) and apamin (50 nM), n=6. All data are presented as mean ± SEM. * denotes $p<0.05$ treatment compared to control; ° denotes p<0.05 treatment compared to the first frequency-response curve of 30 mM sodium propionate treatment; **Δ** denotes $p<0.05$ treatment compared to sodium propionate (30 mM) with L-NAME and # denotes $p<0.05$ treatment compared to sodium propionate (30 mM).

3.2 Discussion

Previous studies have shown that supplementation and administration of SCFAs to rats and mice *in vivo* decreased blood pressure or prevented hypertension in these animal models (Ganesh et al., 2018; Kaye et al., 2020; Skrzypecki et al., 2018). SCFAs have been reported to induce vasorelaxation in isolated rat and human arteries in the mM concentrations (Aaronson et al., 1996; Mortensen et al., 1990; Nutting et al., 1991). The mechanisms through which these SCFAs produce this effect are still not fully understood. There has been some contention on the role of endothelium-dependent mechanisms in mediating this vasorelaxation effect, with earlier studies reporting that these effects are independent of the endothelium (Aaronson et al., 1996; Mortensen et al., 1990; Nutting et al., 1991) and more recent studies reporting that the effect of SCFAs are endothelium-dependent (Knock et al., 2002; Natarajan et al., 2016). One difference and possible explanation for these discrepancies is the concentration of SCFA used in these studies. Studies that included higher concentrations of SCFAs reported endothelium independent mediation of the effect of SCFAs (Aaronson et al., 1996; Mortensen et al., 1990; Nutting et al., 1991) while studies that included lower concentrations of SCFAs reported that the effect of SCFAs were mediated by endothelium-dependent mechanisms (Knock et al., 2002; Natarajan et al., 2016). Therefore, further work is needed to better understand the mechanism underlying the effect of SCFAs *in vitro*. In my thesis work, I aimed to investigate this by determining the effect of SCFAs at μM concentrations on isolated rat mesenteric resistance arteries in order to provide more insight on the endothelium-dependent mechanisms involved at lower concentrations. This arm of my thesis addresses the hypothesis that SCFAs have a direct vasorelaxation effect on isolated arteries and that this effect is mediated by endothelium-dependent mechanisms.

3.2.1 SCFAs mediate their vasorelaxation effect through different endothelium-dependent mechanisms in isolated rat mesenteric arteries

Wire myography data, presented in **section 3.1,** showed that SCFAs reduced agonist-induced tone in artery segments. These data suggest that these small, gut derived SCFAs have a direct vasorelaxation effect on isolated rat mesenteric resistance arteries. This vasorelaxation effect was seen at SCFA concentrations of 0.3 – 100 μM. This result is supported by the studies mentioned above (Aaronson et al., 1996; Knock et al., 2002; Mortensen et al., 1990; Natarajan et al., 2016; Nutting et al., 1991). SCFA-induced vasorelaxation was attenuated in the presence of a combination of pharmacological inhibitors of eNOS and of SK_{Ca} and IK_{Ca} channels. eNOS is required for NO production and SK_{Ca} and IK_{Ca} channels are required for endothelium-dependent hyperpolarization (EDH), two major endothelium-dependent relaxation pathways (described in **Chapter 1).** This suggests that endothelium-dependent mechanisms are involved in mediating these effects, which supports the work of Knock et al. (2002) and Natarajan et al. (2016) that found that removal of the endothelium attenuated the effect of SCFAs (Knock et al., 2002; Natarajan et al., 2016). However, these three SCFAs had different sensitivities to the pharmacological inhibitors used which may indicate a possible difference in mechanisms mediating the effect of each of these SCFAs.

Acetate: The vasodilation effect of acetate at low concentrations (0.3 – 3 μM) in the wire myography results was significantly attenuated by NOS inhibitor, L-NAME (100 μM), alone and by Ca^{2+}-activated K^{+}-channel blockers, TRAM-34 (1 μM) and apamin (50 nM), with L-NAME (100 μM) suggesting that the NO endothelium-dependent vasodilation pathway plays a role in mediating acetate's effect in isolated mesenteric arteries at these lower concentrations. The involvement of endothelium-dependent mechanisms in acetate induced vasorelaxation is

supported by Natarajan et al. (2016) that reported that the vasodilation effect of acetate (0.3 – 10 mM) was attenuated when the endothelium was removed in isolated rat tail arteries (Natarajan et al., 2016). However, Natarajan et al. (2016) also reported that L-NAME did not significantly attenuate the effect of acetate at 0.3 – 10 mM which appears to contradict the wire myography data presented in **section 3.1.1**. This suggests that the activation of eNOS and the production of NO may play a role in mediating these effects only at lower concentrations of acetate. In addition to this discrepancy in eNOS involvement, the attenuation of acetate's effect by L-NAME, alone, and by TRAM-34, apamin and L-NAME is lost with increasing concentrations of acetate (10 – 100 μM), suggesting that other endothelium-dependent, and independent, mechanisms may be involved in acetate mediated vasorelaxation at higher concentrations. This concentration-dependent involvement of endothelium-dependent mechanisms in SCFA-induced vasorelaxation has also been reported by Knock et al. (2002) with propionate and butyrate (Knock et al., 2002).

Propionate: The wire myography data presented that propionate also produced concentration-dependent vasorelaxation. This effect did not appear to significantly rely on the production of NO as it was not attenuated by 100 μM L-NAME, which is supported by the studies done by Knock et al. (2002) and by Natarajan et al. (2016) (Knock et al., 2002; Natarajan et al., 2016). Both investigators demonstrated that propionate produced a concentration-dependent vasorelaxation effect that was not inhibited by L-NAME (100 μM). These investigators also reported that, although the effect of propionate is not mediated by NO production, it is reliant on other endothelium-dependent mechanisms (Knock et al., 2002; Natarajan et al., 2016). In the presence of apamin (50 nM) with TRAM-34 (1 μM) and all three inhibitors together, there was significant attenuation of the effects of propionate at 10 μM, suggesting the possible involvement of EDH. However, there was no significant difference in the overall effect of propionate in the

presence of the three combinations of inhibitors, indicating the involvement of other endothelium-dependent mediators in the effects of propionate, such as endothelium-derived prostacyclin as proposed by Natarajan et al. (2016) (Natarajan et al., 2016). The role of prostacyclin was not investigated in the work presented in this chapter, however future wire myography work including an inhibitor of prostacyclin production, such as indomethacin, will provide insight on the possible role of prostacyclin in effect of SCFAs (Ding & Triggle, 2000; Edwards et al., 2010). Endothelium-dependent vasorelaxation evoked by propionate is concentration dependent, as Knock et al. (2002) reported that endothelium-dependent mechanisms were involved in vasorelaxation of 10 mM propionate but appeared to be endothelium-independent at 50 mM propionate (Knock et al., 2002).

Butyrate: Butyrate induced the greatest reduction in agonist-induced tone in isolated rat mesenteric arteries. This effect was significantly attenuated by all three combinations of inhibitors added, suggesting that eNOS activation and EDH play a significant role in mediating the effect of butyrate. These results are supported by Onyszkiewicz et al. (2019) that reported vasorelaxation of mesenteric arteries with 50 μM butyrate, and by Knock et al. (2002) that reported vasorelaxation with 10 mM butyrate (Knock et al., 2002; Onyszkiewicz et al., 2019). Aaronson et al. (1996) and Knock et al. (2002) both reported that at higher concentrations of butyrate (50 mM) the vasorelaxation effect persisted in isolated arteries with and without an intact endothelial layer, suggesting that the effect butyrate at 50 mM was not mediated solely by endothelium-dependent mechanisms (Aaronson et al., 1996; Knock et al., 2002). Together this suggests that, like acetate and propionate, the effect of butyrate may be mediated by different endothelium-dependent and independent mechanisms in a concentration-dependent manner.

Given the results presented in this chapter and what has been reported previously, it appears that all three SCFAs mediate their effects through different mechanisms of action with increasing concentrations (Aaronson et al., 1996; Knock et al., 2002; Natarajan et al., 2016; Nutting et al., 1991). It has been proposed that with increasing concentrations of these SCFAs there may be acidification of the endothelium (Aaronson et al., 1996). However, work done by Aaronson et al. (1996) investigating whether endothelial cell acidification accounts for the effect of 50 mM butyrate reported that in isolated arteries the intracellular pH remained within the physiological range with the addition of 50 mM butyrate and that any change in intracellular pH was transient (Aaronson et al., 1996). In addition to this, Aaronson et al. (1996) also reported that the effects of butyrate persisted regardless of intracellular pH (Aaronson et al., 1996). Therefore, this suggests that in the wire myography data presented in this chapter intracellular pH does not play a significant role in mediating the effects of SCFAs at the concentrations investigated (0.1 – 100 μM).

It has been proposed by Pluznick et al. (2013) and Natarajan et al. (2016) that SCFAs may initiate their vasodilation effect through activation of an endogenous SCFA receptor, GPR41. This receptor has been located to the endothelium of vascular tissue and therefore may use endothelium-dependent mechanisms to mediate the effects of SCFAs (Natarajan et al., 2016; Pluznick et al., 2013). Activation of GPR41 has been reported to increase intracellular Ca^{2+} in different cell types (Le Poul et al., 2003; Mizuta et al., 2020; Ulven et al., 2020). This increase in intracellular Ca^{2+} could then promote the activation of endothelium-dependent mechanisms (described in **Chapter 1**) to mediate the effects of SCFAs. Future wire myography work with a GPR41 specific agonist, AR420626, would provide greater understanding on the effect of activation of GPR41 and if GPR41 activation may evoke similar vasorelaxation effects to SCFAs

(Mikami et al., 2020). Furthermore, studies with a selective GPR41 antagonist and SCFAs could be useful in investigating the extent through which SCFAs mediate their effects through this receptor. To date, no selective antagonist for GPR41 is commercially available although a novel patented antagonist was synthesized in a laboratory (Engelstoft et al., 2013). β-hydroxybutyrate has been reported to be a GPR41 antagonist, however, there is some disagreement on its selectiveness and effectiveness (Kimura et al., 2011; Onyszkiewicz et al., 2019, 2020; Won et al., 2013). In addition to this, future studies with GPR41 knock out animals would provide a useful model to further investigate the interaction of SCFAs, GPR41 and blood pressure *in vivo*.

In summary, the three SCFAs, acetate, propionate, and butyrate, have a direct vasorelaxation effect on isolated rat mesenteric resistance arteries. However, it appears that there is a difference in intensity of the effect of these three SCFAs with butyrate having the greatest effect followed by acetate and propionate. In addition to this, there also appears to be a difference in endothelium-dependent mechanisms involved in mediating these effects. Activation of eNOS may have a role in mediating the effect of acetate and butyrate but does not appear to be involved in mediating the effect of propionate. EDH may mediate the effect of propionate and butyrate but does not seem to be significantly involved in mediating the effect of acetate. All together, the mechanisms underlying the vasorelaxation effect of SCFAs appear to be complex, concentration-dependent, and mediated by more than one pathway.

3.2.2 The effects of SCFAs may be influenced by shear stress in the perfused rat mesenteric vascular bed

Data on the effects of SCFAs on isolated rat mesenteric resistance arteries provides insights on the complexity of the relaxation mechanisms involved. To extend these findings into an experimental preparation that utilizes vessel fluid flow, the effects of SCFAs were investigated in

a perfused intact mesenteric arterial vascular bed. As described in **section 1.6.3**, fluid flow along blood vessels acts as a physical stimulus for endothelium activation and so this preparation replicates a normal physiological environment. The time control data presented in this chapter shows attenuation of the frequency-dependent response at 15 Hz and augmentation of response at 30 and 40 Hz over time (**Figure 3.3b**). Time-dependent changes in frequency-dependent responses have not been previously observed in our lab. The time control data in this chapter was collected over the course of my thesis work, which may have influenced the data through variability between animal shipments. The experimental data was collected over shorter periods of time; therefore, interpretation of the data presents some limitations in determining if SCFAs have an effect on frequency-response curves, however, presence of statistically significant main effects and attenuation at several stimulation frequencies likely represents an effect on response.

The statistical analyses I completed on this work included repeated-measures two-way ANOVA followed by Tukey's post hoc test to determine if treatment significantly altered the response at the same stimulation frequencies. Tukey's post hoc test was done whether or not the main effect of the treatment was statistically significant in order to establish whether an effect may be observed at specific stimulation frequencies. This allows comparison of the effect of treatment at different stimulation frequencies where at the greatest stimulation frequencies of 30 and 40 Hz it appears that treatment with the SCFAs has little effect, however, at lower stimulation frequencies of 15 and 20 Hz there was a significant attenuation of response observed. This suggests that the vasodilation effects of SCFAs in the mesenteric vascular bed were overcome by the vasoconstriction induced at higher stimulation frequencies. Although the statistical methods that I used in this work were appropriate and useful, the sample numbers used in these experiments provided low statistical power for the perfusion data presented given the small effect of the SCFAs

observed. Therefore, prior to future experiments a statistical power analysis calculation should be performed given these preliminary observations of the effects of SCFAs in the perfused mesenteric bed. This will ensure an appropriate sample size is used to support greater statistical power, thus providing greater probability that the rejection of the null hypothesis is correct and that the effect of the SCFAs observed has a greater probability of being true. Statistical analysis with other post hoc tests that may better promote statistical power may also be useful, such as Newman-Keuls post hoc test (McHugh, 2011). However, the reduction of the probability of type II errors with this method increases the probability of type I errors, therefore much needs to be considered when finding the most appropriate statistical analysis for these data (McHugh, 2011).

In mesenteric perfusion experiments, the SCFAs, acetate and propionate, did not have a significant main effect on frequency-response curves at μM concentrations, however, in the second frequency-response curve with 5 μM sodium propionate there was a significant attenuation of the frequency-dependent response at 15 and 20 Hz, suggesting a possible time delayed effect (**Figure 3.4b**). In addition to this, 70 μM sodium acetate augments the frequency-dependent response at higher stimulation frequencies of 30 and 40 Hz (**Figure 3.4a**) which may be amplification of the changes seen at these stimulation frequencies in the time control data (**Figure 3.3b**). Equimolar substitution of NaCl in the Krebs buffer with 30 mM sodium acetate or 30 mM sodium propionate induced a time-dependent effect seen in the second frequency-response curve of SCFA treatment, indicating that longer exposure is necessary prior to observation of the effects of SCFAs under these conditions (**Figure 3.5**). Future studies focused on time-dependent effects of SCFAs may provide more insight on how circulation of these SCFAs, and therefore longer exposure to these SCFAs may affect blood vessel function.

To better understand the possible mechanisms through which absorbed SCFAs, acetate and propionate, may act, prefusion experiments were carried out with 30 mM sodium acetate or 30 mM sodium propionate added to the Krebs buffer without equimolar substitution of NaCl. As a control, the effect of increasing osmolarity of the Krebs buffer with 150 mM NaCl was also conducted and found to significantly attenuate frequency-dependent responses at 15 and 20 Hz and had a statistically significant main effect overall (**Figure 3.6**). This is supported by osmolarity induced vasodilation reported in previous studies (F. N. Miller et al., 1981; Steenbergen & Bohlen, 1993; Zakaria et al., 2005). To determine if the presence of both SCFAs and Na^+ further influence frequency-dependent responses, experiments were carried out with addition of SCFAs, sodium acetate and sodium propionate (30 mM) without equimolar substitution of NaCl.

Perfusion data of 30 mM sodium acetate, without equimolar substitution of NaCl, showed significant attenuation of frequency-dependent responses at 15 and 20 Hz. This result is supported by a study by Sakakibara et al. (2010) that investigated the effect of ingestion of a solution containing 15% vinegar (100-120 mM acetic acid) on flow mediated vasodilatation in the forearm of postmenopausal women (Sakakibara et al., 2010). Sakakibara et al. (2010) reported that there was an increase in forearm blood flow after occlusion release with ingestion of the vinegar solution when compared to subjects that did not ingest the vinegar solution (Sakakibara et al., 2010). The augmentation of response at 30 and 40 Hz, as seen with 70 μM sodium acetate, was unexpected and the combination of frequency-dependent attenuation and augmentation of response with treatment has not been previously observed in our lab. To determine if the order of stimulation frequencies may be influencing this effect, future studies with a reversed or an alternative order of stimulation frequencies could be employed. Altering the order of stimulation frequencies may come with limitations that must be considered in the design of these studies, as

stimulation with the higher frequencies first may alter the response of the lower stimulation frequencies to follow. Furthermore, the main effect of 30 mM sodium acetate was not statistically different from control, suggesting that 30 mM sodium acetate may not significantly influence the overall responses of the frequency-response curves.

To investigate mechanisms through which 30 mM sodium acetate, without equimolar substitution of NaCl, induced attenuation of frequency-dependent increases in perfusion pressure at stimulation frequencies of 15 and 20 Hz, perfusion experiments were carried out with eNOS and endothelial Ca^{2+}-activated K^+ channel inhibitors. When comparing treatments of 30 mM sodium acetate with L-NAME (100 μM) to L-NAME (100 μM) alone, there is a significant difference in the frequency-dependent responses at 15 and 20 Hz, suggesting that the effect of sodium acetate may be mediated, in part, through eNOS activation and production of NO, but that other mechanisms may also be involved. To determine if EDH may be another mechanism involved in mediating the effect of sodium acetate in the vascular bed, perfusion was performed in the presence of 30 mM sodium acetate with TRAM-34 (1 μM) and apamin (50 nM). The addition of these two Ca^{2+}-activated K^+ channel inhibitors did not affect the 30 mM sodium acetate attenuation of the frequency-dependent response at 15 Hz, but did inhibit the effect of sodium acetate at 20 Hz. This suggests that EDH may play a role in mediating the effect of 30 mM sodium acetate in the perfused mesenteric bed. Therefore, in this perfusion set up, the effect of sodium acetate may be partially mediated by activation of eNOS and Ca^{2+}-activated K^+ channels along with other yet to be identified mechanisms.

In the perfused rat mesenteric vascular bed, 30 mM sodium propionate, without equimolar substitution of NaCl, significantly attenuated the frequency-dependent responses at 15 and 20 Hz. This effect was lost with the addition of L-NAME (100 μM) and there was a significant difference

between treatment with 30 mM sodium propionate with L-NAME (100 μM) compared to treatment with L-NAME (100 μM) alone. This suggests that activation of eNOS and production of NO may play a role in the effects of propionate on the intact mesenteric vascular bed but may not be the sole mechanism involved under these perfusion conditions. To determine if EDH may play a role in this effect, perfusion was done in the presence of 30 mM sodium propionate with TRAM-34 (1 μM) and apamin (50 nM). There was no significant difference in frequency-dependent responses between 30 mM sodium propionate and 30 mM sodium propionate with TRAM-34 (1 μM) and apamin (50 nM) at 15 and 20 Hz, indicating that EDH may not play a significant role in mediating the effect of sodium propionate in the perfused mesenteric bed. The involvement of NO in the effect of sodium propionate differs from what was seen in the wire myography data and what has been previously reported by other investigators (Knock et al., 2002; Natarajan et al., 2016). However, this may be due to the action of shear stress that can prompt eNOS activation (described in **Chapter 1**) suggesting that shear stress may provide the condition necessary for sodium propionate to mediate an effect through NO release (Ballermann et al., 1998; Joannides et al., 1995; Korenaga et al., 1994; Sprague et al., 2010). The effect of sodium propionate in the perfused mesenteric vascular bed may be significantly influenced by flow-mediated vasodilation. To determine the extent of the influence of flow-mediated vasodilation on the effect of SCFAs, it would be worth investigating the effect of sodium propionate and sodium acetate (30 mM) under conditions where flow-mediated vasodilation could be inhibited through disruption of the glycocalyx with heparin, heparinase or hyaluronidase (Florian et al., 2003; Pahakis et al., 2007; VanTeeffelen et al., 2007), or inhibition of shear stress sensitive TRPV4 channels on the endothelium, with RN-1734 (Mendoza et al., 2010; Vincent et al., 2009). The effect of butyrate on the perfused mesenteric vascular bed was not investigated in my thesis as

butyrate does not enter the mesenteric circulation at the same rate as acetate and propionate, rather it acts as a primary energy source for colonocytes (Bugaut, 1987; Donohoe et al., 2011; Morrison & Preston, 2016).

Together, these results indicate that SCFAs have a direct effect on isolated mesenteric arteries at μM concentrations through endothelium-dependent mechanisms, however SCFAs do not appear to have a significant effect on the intact mesenteric vascular bed at these lower concentrations. Higher concentrations of sodium acetate and sodium propionate (30 mM) added to the perfusate as equimolar substitution of NaCl in Krebs buffer did attenuate some frequency-dependent responses in the perfused mesenteric bed, however, this required longer exposure before evoking an effect. Future studies that focus on investigating length of exposure of SCFAs and the associated effects would provide more insight on how circulating SCFAs may influence blood vessels. Addition of 30 mM sodium acetate and sodium propionate to the Krebs buffer without equimolar substitution of NaCl attenuated frequency-dependent responses, possibly through eNOS activation prompted by shear stress present in this perfusion set up. Furthermore, an increase in osmolarity does appear to play a role in these responses as well. Although the effects of these SCFAs in wire myography results are similar, their mechanisms of action seem to be quite complex. Elucidating their possible mechanism of action in vascular tissue will require further investigation with possible removal of the endothelial cell layer in these set ups or through the use of other antagonists, such as indomethacin to determine the role of prostacyclin in these effects, and GPR41 receptor antagonists as they become more readily available.

In the data I have presented in my thesis, the effects of the SCFAs were investigated independently of each other. However, physiologically, these three predominant SCFAs are produced and absorbed together, and are found together in the blood (Bloemen et al., 2009;

Cummings et al., 1987). These SCFAs may have more significant effects when combined as reported by Mortensen et al. (1990) (Mortensen et al., 1990). Further investigation of the effect of these SCFAs when combined may be useful to better understand how these SCFAs may be interacting with blood vessels under more physiologically relevant parameters. In addition to this limitation, wire myography artery segments are dissected in such a way that the perivascular adipose tissue was removed, eliminating influences from the adipose tissue (Nava & Llorens, 2019). Once set up in the wire myograph, these artery segments also lack hormonal and neural inputs, therefore, these results only provide information on how SCFAs impact vascular tone in the absence of these influences. My investigation also focused on the effects of SCFAs on rat mesenteric resistance arteries only. Onyszkiewicz et al. (2019) found there was some difference in the effect of butyrate at 1 mM on rat mesenteric arteries and garcilis musculus arteries (Onyszkiewicz et al., 2019). Although these results provide information on the effects SCFAs on mesenteric arteries, which would have the greatest exposure to gut derived SCFAs, future studies using other resistance arteries such as garcilis musculus arteries and cerebral arteries may be worthwhile pursuing (Schiffrin, 1992).

This work showed that SCFAs do have a direct vasorelaxation effect on isolated resistance arteries at μM concentrations. In the perfused mesenteric bed, μM concentrations did not evoke a significant main effect, however, did indicate a latency in onset of their effects. At a higher concentration of 30 mM sodium acetate and 30 mM sodium propionate, attenuation of frequency-dependent responses was observed, and a greater effect was observed with the addition of increased osmolarity. These results suggest that direct vasorelaxation effects of SCFAs can be influenced by shear stress and osmolarity, and that there are multiple mechanisms, both endothelium-dependent and independent, that are involved in mediating these effects. Therefore,

in the context of systemic hypertension and portal hypertension, alteration of SCFA production in the lower intestine through the use of antibiotics or changes in diet may play a role in influencing blood pressure or the development of splanchnic vasodilation through direct vasorelaxation action once absorbed. Future *in vivo* studies with colonic administration of SCFAs in different animal models, including GPR41 knock out animals, are required to provide better insight into the effect of these small molecules on blood pressure and blood flow.

Part 2

Chapter 4: Introduction to blood vessel-gut interactions

As outlined in the beginning of **Part 1,** my thesis is focused on investigating the interactions between gut and blood vessels that I have split into two parts. Here, I will present my work on protease-activated receptor 2 activation in the gastrointestinal wall.

Blood and blood vessels allow for movement and circulation of proteins, endocrine signals, and nutrients throughout the body. Blood also contains red blood cells (erythrocytes) to transport oxygen (Pittman, 2013), white blood cells (leukocytes) to mediate immune responses (Carrick & Begg, 2008) and platelets (thrombocytes) to facilitate blood hemostasis (Holinstat, 2017). Of the proteins found in blood plasma, serine proteases such as trypsin (Adrian et al., 1979; Colombo et al., 1989; Dandona et al., 1981; Frier et al., 1980), factor VIIa and factor Xa (Camerer et al., 1996; Isermann, 2017) can activate protease-activated receptor 2 (PAR-2) and may play a role in regulating gut motility (Al-Ani et al., 1995; Corvera et al., 1997; Mulè, Baffi, & Cerra, 2002; Mulè, Baffi, Falzone, et al., 2002; Mulè et al., 2003; Saifeddine et al., 1996).

4.1 Gut motility

Gut motility is necessary for digestion of food and excretion of waste. Regulation of gut motility is complex and is influenced by many factors including enteroendocrine signals and neural inputs (Foong et al., 2020; Wu et al., 2013). Motility is also regulated by several different cell types including smooth muscle cells, interstitial cells, and enteric neurons within the gastrointestinal wall (**Figure 4.1**) (Foong et al., 2020). These cells are responsible for maintenance and initiation of rhythmic and phasic contractions throughout the gastrointestinal tract (reviewed by Foong et al., 2020). This is achieved through the formation of a multicellular syncytium,

composed of smooth muscle cells, interstitial cells of Cajal (ICC) and platelet-derived growth factor receptor alpha positive (PDGFRα+) interstitial cells (Daniel et al., 1998; Koh et al., 1998; Sanders et al., 2016; Sanders, 2019; Takayama et al., 2002; Torihashi et al., 1995). These cells are innervated by enteric motor neurons and express neurotransmitter receptors such as $5HT_{2B}$ and muscarinic acetylcholine receptors on ICC (Garcia-Lopez et al., 2009; B. Jin et al., 2021), and purine receptor (P2Y1) on PDGFRα+ interstitial cells (Lee et al., 2014). ICC also produce intrinsic slow wave depolarizations that are independent of neural or hormonal inputs and influence phasic motility (Sanders, 2019; Ward et al., 2000).

4.1.1 Role of interstitial cells of Cajal in gut motility

Interstitial cells of Cajal (ICC) act as pacemaker cells and are located in the submucosal and myenteric plexuses, as well as intramuscularly in the circular and the longitudinal smooth muscle layers of the gastrointestinal tract (**Figure 4.1**) (Takayama et al., 2002; Torihashi et al., 1995; Ward et al., 2000). In order to properly proliferate and develop within this network, ICC require a surface receptor tyrosine kinase, known as c-kit (Takayama et al., 2002; Torihashi et al., 1995). Development of antibodies against c-kit has allowed for the identification of c-kit positive (c-kit+) ICC and localization of these ICC within the gastrointestinal tract (Foong et al., 2020; Koh et al., 1998; Takayama et al., 2002; Torihashi et al., 1995). ICC in the intramuscular layers are associated with nerves and microvasculature (Hashitani et al., 2015; Liu et al., 2015; Okamoto et al., 2014), and have been found to be electrically coupled with smooth muscle cells via gap junctions (Daniel et al., 1998). Therefore, when ICC generate slow wave depolarizations they then spread to the smooth muscle cells with which they are electrically coupled in the syncytium network (Koh et al., 1998; Takayama et al., 2002).

The generation of slow wave depolarizations in ICC is reported to be initiated by an increase in cytosolic Ca^{2+} from intracellular stores (Pasternak et al., 2016; Ward et al., 2000). Ward et al. (2000) suggested that the rhythmic depolarization of the cell is due to the cyclic Ca^{2+} movement in and out of the endoplasmic reticulum through oscillatory Ca^{2+} release by IP_3 receptors and Ca^{2+} uptake into the endoplasmic reticulum by SERCA (Ward et al., 2000). Koh et al. (1998) proposed that rhythmic Ca^{2+} movement and depolarization were the result of non-selective cation conductance or chloride (Cl^-) conductance (Koh et al., 1998). It was later reported that cytosolic increase in Ca^{2+} can then initiate inward currents via an increase Cl^- conductance through Ca^{2+} activated Cl^- channels such as anoctamin-1 (ANO1) Ca^{2+} activated Cl^- channels expressed on ICC (Hirst et al., 2002; Hwang et al., 2009; Kito & Suzuki, 2003; Zhu et al., 2009)

As the cells in this network are electrically coupled, the slow wave depolarization of ICC influences the excitability of smooth muscle cells, therefore depolarizing smooth muscles cells and increasing the open probability of L-type VGCCs located on the smooth muscle cell (Yamazawa & Iino, 2002). Once these channels open, they allow the entry of Ca^{2+} into the cell and initiates smooth muscle contraction as described in section **1.6.2 Regulation of vascular tone**. As this slow wave depolarization propagates to many smooth muscle cells within the intestinal wall, the resulting contraction contributes to the phasic motility of the gut (Sanders, 2019; Yamazawa & Iino, 2002). Although this depolarization of ICC is initiated by intrinsic and rhythmic Ca^{2+} release, it can also be influenced by neural inputs such as nitrergic nerves that inhibit ICC Ca^{2+} signalling through NO release (Drumm et al., 2020). Studies have also investigated the involvement of protease-activated receptor 2 in mediating the pacemaker activity of ICC (Al-Ani et al., 1995; Corvera et al., 1997; Mulè, Baffi, & Cerra, 2002; Mulè, Baffi, Falzone, et al., 2002; Mulè et al., 2003; Nishikawa et al., 2002; Saifeddine et al., 1996).

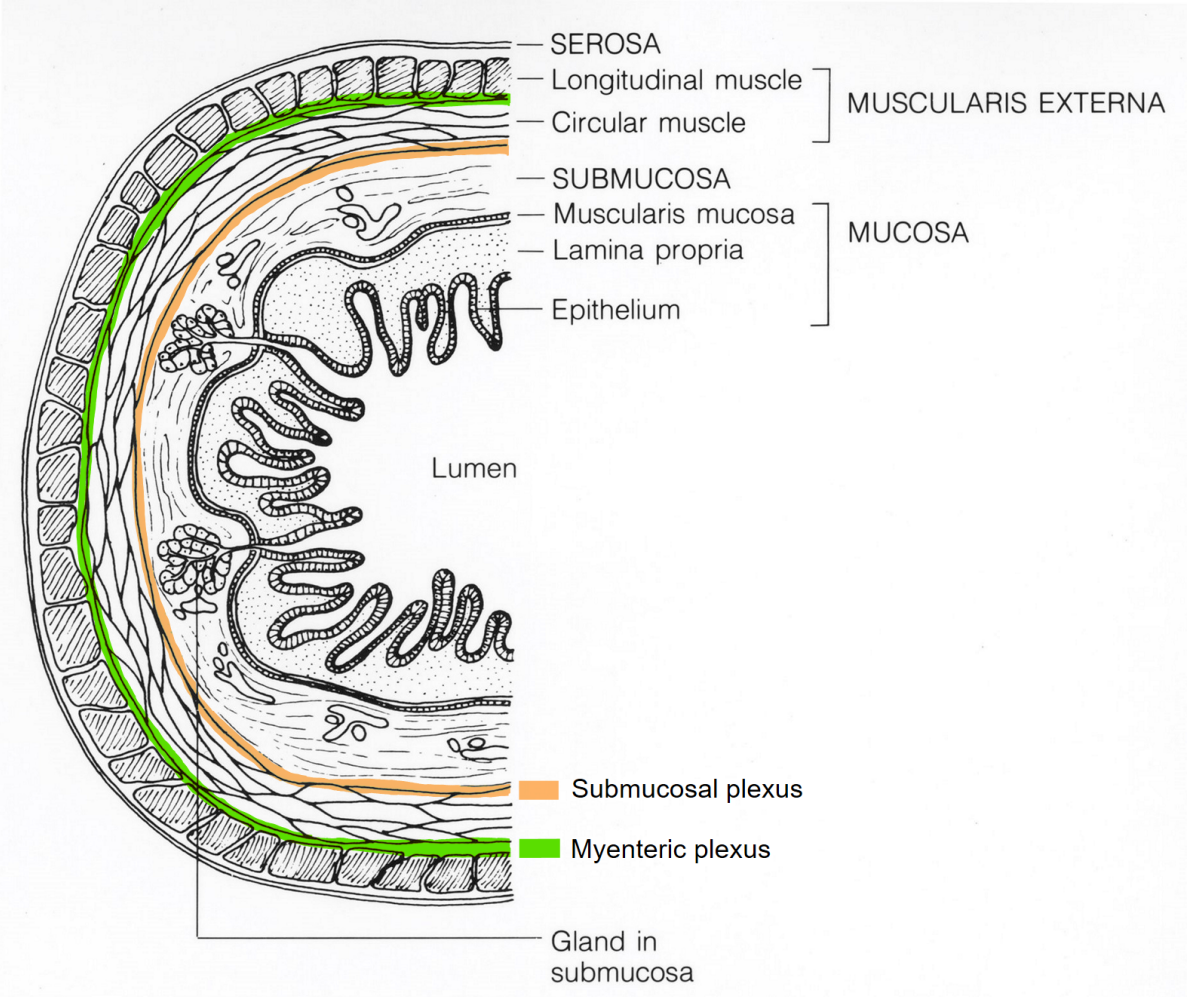

Figure 4.1 Intestinal wall structure. The intestinal lumen is surrounded by the mucosa, followed by the submucosa, then the circular and longitudinal smooth muscle layers. The submucosal plexus is found between the submucosa and muscle layer, and the myenteric plexus is located between the circular and longitudinal smooth muscle layers. This image has been modified to include the myenteric and submucosal plexuses from the original "Mucosa" created by an unknown illustrator from the National Cancer Institute (U.S.), this image is public domain.

4.2 Protease-activated receptor 2

Protease-activated receptors (PARs) are GPCRs, of which there are 4 subtypes: PAR-1 (Vu et al., 1991), PAR-2 (Nystedt et al., 1994), PAR-3 (Ishihara et al., 1997), and PAR-4 (Xu et al., 1998). PAR-2 is a cell surface receptor that is expressed on many tissues throughout the body, including the kidney, the gastrointestinal tract (Nystedt et al., 1994), the endothelium, and vascular smooth muscle (Molino et al., 1998). Within the gastrointestinal tract, PAR-2 has been located to the gastrointestinal epithelium and smooth muscles (Al-Ani et al., 1995; Corvera et al., 1997; Nishikawa et al., 2002; Saifeddine et al., 1996). PAR-2 is activated by serine proteases including: trypsin, tryptase, factor VIIa, and factor Xa (Camerer et al., 1996; Corvera et al., 1997; Isermann, 2017; Mirza et al., 1997; Nystedt et al., 1994). These proteases activate PAR-2 by cleaving a section of the extracellular N-terminal sequence which unmasks an N-terminal receptor-activating sequence (Isermann, 2017; Vu et al., 1991). This exposed sequence acts as a tethered ligand that then binds to the receptor and activates the protein (**Figure 4.2**) (Isermann, 2017; Vu et al., 1991). Activation of PAR-2 can also be achieved through the application of exogenous synthetic mimetic peptides that contain the same amino acid sequence that would be unmasked by cleavage of the N-terminal domain (Nystedt et al., 1994). These mimetic peptides are named after their amino acid sequence in single letter code such as SLIGRL and f-LIGRL (Kawabata et al., 2004; Nystedt et al., 1994).

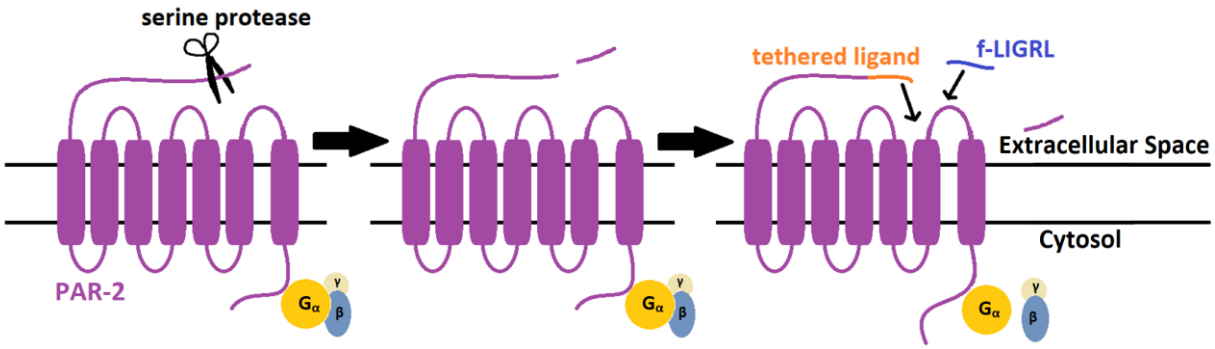

Figure 4.2 PAR-2 activation. Serine proteases cleave the extracellular N-terminal domain and unmask a tethered ligand that can then activate the PAR-2 receptor. PAR-2 can also be activated by peptide mimetics such as f-LIGRL. This image was modified to focus on PAR-2 activation and include the mimetic peptide f-LIGRL from the original "Activation vs silencing of PAR" created by Marta Šlaufová which is licensed under CC BY-SA 4.0.

PAR-2 activation initiates signal transduction through G-protein dependent pathways requiring G_q, G_i, and/or $G_{12/13}$ proteins and through G-protein independent pathways such as the recruitment of β-arrestin (reviewed by Rothmeier & Ruf, 2012, and by Isermann, 2017). Proteases do not all cleave at the same amino acid residue for a given PAR, therefore activation of PARs at different points of cleavage may contribute to differences in signal transduction and secondary messengers activated with respect to the receptor-activating sequence exposed (Isermann, 2017). However, this biased signalling may also be mediated by the location of the receptor to specific tissues and dimerization of PARs (Isermann, 2017; Mulè, Baffi, Falzone, et al., 2002).

Activation of PAR-2 on colonic smooth muscle segments has been reported by Mulè, Baffi, Falzone, et al. (2002) to initiate the PLC secondary messenger signalling pathway, leading to an increase in IP_3 which activates IP_3R on intracellular Ca^{2+} stores to release Ca^{2+} into the cytosol described in section **1.6.2 Regulation of vascular tone** (Mulè, Baffi, Falzone, et al., 2002). Several investigators have also reported that activation of PAR-2 results an increase in Ca^{2+} in the cytosol

of the cell (Kawabata et al., 2004; Mirza et al., 1996; Molino et al., 1998; Mulè, Baffi, & Cerra, 2002; Mulè, Baffi, Falzone, et al., 2002). Mulè, Baffi, Falzone, et al. (2002) report that activation of PAR-2 in the longitudinal smooth muscle of colonic segments resulted in an increase in intracellular Ca^{2+} that they propose is mediated by the opening of L-type VGCCs (Mulè, Baffi, Falzone, et al., 2002). Initiation of the PLC-PKC signalling cascade and an increase in intracellular Ca^{2+} suggests that PAR-2 is likely coupled to G_q-protein in the gastrointestinal tract (Boyer et al., 1992; Kawabata et al., 2004; Mulè, Baffi, Falzone, et al., 2002).

4.2.1 PAR-2 and gut motility

As mentioned above, PAR-2 is expressed in the gastrointestinal smooth muscle and effort has been made to determine how PAR-2 may influence gut motility (Al-Ani et al., 1995; Corvera et al., 1997; Mulè, Baffi, & Cerra, 2002; Mulè, Baffi, Falzone, et al., 2002; Mulè et al., 2003; Nishikawa et al., 2002; Saifeddine et al., 1996). Activation of PAR-2 and its subsequent influence on gut motility has been reported to be quite complex and differs between sections of the gastrointestinal tract. Activation of PAR-2 on circular smooth muscle in the colon induces relaxation in a concentration-dependent manner (Mulè et al., 2003; Mulè, Baffi, & Cerra, 2002; Mulè, Baffi, Falzone, et al., 2002). In longitudinal smooth muscle, stimulation of PAR-2 appears to have a biphasic effect on the smooth muscle in which activation induces transient relaxation followed by contraction (Mulè et al., 2003; Mulè, Baffi, & Cerra, 2002; Mulè, Baffi, Falzone, et al., 2002). However, it has also been reported by Corvera et al. (1997) that stimulation of PAR-2 in colonic muscle strips with trypsin and mimetic peptide, SLIGRL, inhibits spontaneous contractile activity of gastrointestinal smooth muscle cells in a concentration-dependent manner (Corvera et al., 1997).

Previous work in our lab aimed to determine the effect of PAR-2 activation on spontaneous contractile activity of the longitudinal smooth muscle of rat mid-colon. In these experiments the contractile activity of the longitudinal smooth muscle was measured under the initial load of 1 g in organ bath chambers. Area under the curve of the traces measured was used to determine changes in spontaneous activity with the addition of trypsin or a mimetic peptide, f-LIGRL, in the absence and presence of apamin over a 6-minute period (**Figure 4.3**). These functional studies support what Corvera et al. (1997) reported and showed that activation of PAR-2 by addition of trypsin or f-LIGRL inhibits spontaneous colonic smooth muscle activity in a concentration-dependent manner (Corvera et al., 1997). Many investigators have determined the importance of small-conductance Ca^{2+}-activated K^+ channels (SK_{Ca}) in the effects of PAR-2 activation (Cocks et al., 1999; Corvera et al., 1997; Mulè, Baffi, & Cerra, 2002; Mulè, Baffi, Falzone, et al., 2002; Sato et al., 2006). In our lab's previous work, addition of apamin, an inhibitor of SK_{Ca} channels, to these organ baths resulted in an increase in spontaneous contractile activity of longitudinal smooth muscle and inhibited the effects of trypsin and f-LIGRL (**Figure 4.3**). It may be that activation of SK_{Ca} channels inhibits depolarization-dependent contractile activity originating in the ICC network, and that activation of SK_{Ca} channels induce relaxation of the gastrointestinal smooth muscle through hyperpolarization of ICC via efflux of K^+ (Kawabata, 2003). Hyperpolarization of ICC would then spread to smooth muscle cells and decrease the open probability of VGCCs, therefore reducing the influx of Ca^{2+} necessary for smooth muscle contraction as described in **section 1.6.2 Regulation of vascular tone**.

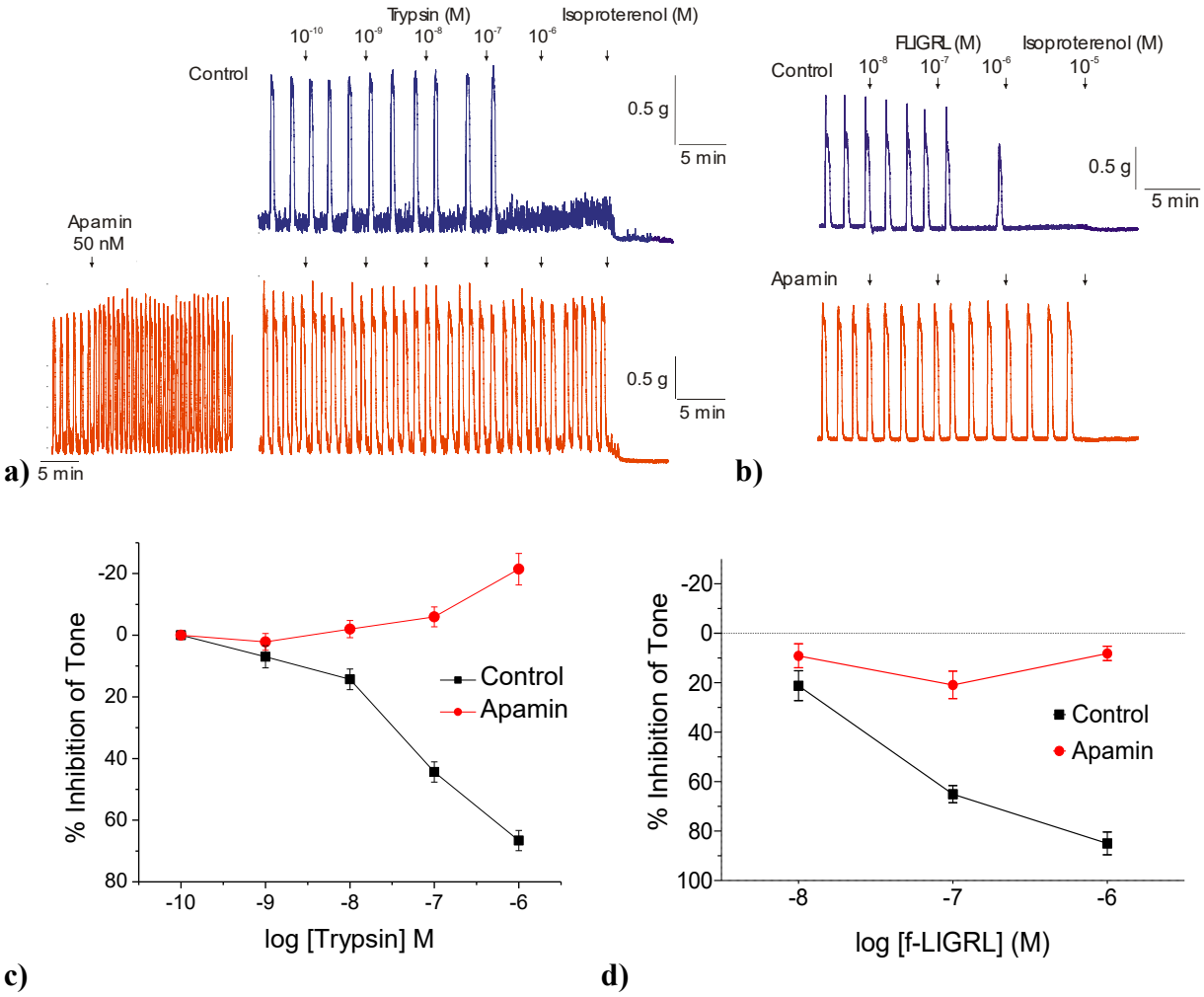

Figure 4.3 Effect of PAR-2 activation on spontaneous contractile activity. a) A representative trace of the effect of trypsin on spontaneous activity in the absence and presence of apamin. **b)** A representative trace of the effect of f-LIGRL on spontaneous activity in the absence and presence of apamin. The effect of **c)** trypsin (n = 8) and **d)** f-LIGRL (n = 6) on spontaneous activity in the absence and presence of 50 nM apamin, presented as % inhibition of activity induced by 10^{-5} M isoproterenol. Data are presented as mean data ± SEM; *data from Dr. Paul Kerr*.

To support the finding that PAR-2 activation may work through ICC directly, determining the location of PAR-2 with respect to ICC is yet to be done. Sung et al. (2015) have reported the presence of a PAR-2-encoding gene in ICC (Sung et al., 2015). More recently, Tomuschat et al. (2020) have reported expression of PAR-2 on ICC and PDGFRα+ cells in human colon samples of very young patients (3-19 months old) (Tomuschat et al., 2020). Both of these studies support the possibility of PAR-2 acting directly through ICC. Investigation of the expression of PAR-2 and c-kit proteins in rat mid-colon tissue with immunofluorescence imaging could support this theory.

4.3 Hypothesis

Activation of PAR-2 inhibits spontaneous contractile activity initiated by ICC in colonic smooth muscle, but how PAR-2 activation may be influencing ICC activity has not yet been well defined. My goal in this arm of my thesis and research was to investigate the expression of PAR-2 proteins with respect to c-kit+ ICC and smooth muscle cells in the rat mid-colon to determine if these PAR-2 proteins may be working on ICC directly to modulate muscle contractile activity. To reach this goal I proposed the following hypothesis:

PAR-2 protein is located on c-kit+ ICC and influences gut motility through direct action on ICC in the rat mid-colon.

Chapter 5: Materials and methods

5.1 Tissue collection

Animal care and use was approved by the University of Alberta Animal Care and Use Committee Health Sciences 1 (AUP 312). Animal husbandry and care were as described in **section 2.1**. Sections of rat mid-colon were collected from male Sprague-Dawley rats (250-300g; Charles River Canada).

5.2 Tissue preparation and imaging

Tissue fixing and paraffin embedding

Sections of the mid-colon were collected and cleaned prior to being submerged an BD Pharmingen™ immunohistochemistry zinc fixative solution (BD Biosciences) for 24-48 hours before paraffin embedding at the Alberta Diabetes Institute HistoCore at the University of Alberta. Paraffin embedding was done by first sequentially immersing the samples in 70%, 85% and 95% ethanol for 90 mins each. The samples were then placed in 70% Butanol for 24 hours, followed by 85% Butanol for 24 hours. The samples were then submerged in paraffin wax in a vacuum chamber kept at 52°C for 5 hours. The paraffin was then left to cool and harden on a cold plate. The paraffin embedded tissue was then cut into sections 5 μm thick and placed onto a microscope slide.

Sample deparaffinization

To remove the paraffin from the tissue slices, the microscope slides were placed in an oven at 60°C for 2 hours. The warm slides were then sequentially immersed into 3 fresh xylene containers for 10 minutes each. Rehydration of the samples were done by immersing the slides in decreasing concentrations of ethanol for 5 minutes beginning with 100% ethanol twice, then followed by 95%, 70%, and 50% ethanol. The slides were then submerged sequentially in 2 containers of distilled water for 5 minutes each.

Antigen retrieval

Sodium citrate buffer solution (0.01mM trisodium citrate dihydrate and 0.05% tween-20 pH 6 in distilled water) was pre-heated to a rolling boiling in a microwave. The microscope slides were then placed in the hot buffer solution and microwaved again for 10 mins. The slides were then rinsed with water for 5 minutes and allowed to cool before immunofluorescence staining.

Immunofluorescence staining

Prior to staining, the samples were washed three times for 5 mins with 1X Tris-buffered saline (TBS) composed of 10% 10X TBS stock buffer (200 mM Tris Base;1500 mM NaCl; pH 7.5), 90% distilled water and 0.1% Tween-20. A blocking solution composed of 5% fish gelatin (Sigma-Aldrich) and 20% goat serum (Sigma-Aldrich) in Dako Antibody Diluent (Agilent) was placed on the samples for 1 hour in a humid chamber at room temperature. The blocking solution was then removed, and the primary antibodies were added (**Table 5.1**). For PAR-2 and α smooth muscle actin staining, PAR-2 antibodies were added at a dilution of 1:50 and α-smooth muscle actin antibodies were added at a dilution of 1:320 in Dako Antibody Diluent solution. In PAR-2 and c-kit staining, PAR-2 antibodies were added at a dilution of 1:50 and c-kit antibodies were added at a dilution of 1:500 in Dako Antibody Diluent solution. Once primary antibodies were added to the samples the slides were placed in a humid chamber and kept at 4°C overnight.

After incubating overnight, the slides were then washed with TBS 0.1% Tween-20 solution 3 times. Secondary antibodies were then added to the samples with both secondary antibodies added at a dilution of 1:1000 in Dako Antibody Diluent solution. The samples were then left to incubate in a humid chamber at room temperature for 1 hour. The samples were then washed with TBS 0.1% Tween-20 solution 3 times and diluted 4′,6-diamidino-2-phenylindole (DAPI; 1:1000) in phosphate-buffered saline (Gibco) was then added to the samples and left to incubate for 3

minutes. Any excess diluted DAPI solution was then removed, and the samples were temporarily dried prior to the application of mounting media (ProLong Gold antifade reagent; Invitrogen) and a cover slip. The negative controls were included in all staining protocols to ensure that the primary antibodies or the secondary antibodies showed no significant non-specific binding or staining.

Antibodies and stain

Table 5.1 Antibodies and Stain			
Primary Antibodies	**Source**	**Dilution**	**Company and Catalogue #**
Anti-PAR-2 (SAM11)	Mouse monoclonal	1:50	Santa Cruz Biotechnology Cat # Sc-13504
Anti-α smooth muscle actin	Rabbit monoclonal	1:320	Cell Signaling Technology Cat # 19245S
Anti-c-kit	Rabbit Recombinant monoclonal	1:500	Abcam Cat # ab256345
Secondary Antibodies			
Alexa Fluor 488 Anti-mouse	Goat	1:1000	Invitrogen Cat # A11029
Alexa Fluor 594 Anti-rabbit	Donkey	1:1000	Invitrogen Cat # A21207
Stain			
4′,6-diamidino-2-phenylindole (DAPI)	n/a	1:1000	Sigma Cat # 32670-5MG-F

Immunofluorescence imaging

Immunofluorescence images were taken using with a Leica DM IRB Fluorescence Microscope (Leica; Germany) at 200x magnification using Open Lab software, version 4.0.2.

Chapter 6: Expression of PAR-2 in the rat mid-colon

Previous work done in our lab demonstrated that activation of PAR-2 inhibited spontaneous contractile activity originating from ICC, described in **Chapter 4**. Although Sung et al. (2015) have investigated the presence of transcriptional expression of a PAR-2-encoding gene in ICC immunofluorescence imaging is yet to be done to determine expression of PAR-2 proteins on ICC in the rat mid-colon (Sung et al., 2015). Therefore, using immunofluorescence staining, I looked for the expression of PAR-2 and c-kit proteins on cross-sections of the rat mid-colon to determine if PAR-2 is expressed on c-kit+ ICC.

6.1 Results

As described in **Chapter 5**, immunofluorescence staining utilized PAR-2 antibodies, to bind to PAR-2, and α smooth muscle actin antibodies, to bind α-actin in smooth muscles cells. By using a co-staining approach, I could identify whether these proteins are present in the same cell types. **Figure 6.1(a,b,c)** present immunofluorescence images of PAR-2 staining, in green, and α-actin staining, in red. These images also present DAPI staining in blue, a fluorophore that binds to adenine and thymine in DNA. PAR-2 staining in **Figure 6.1a** is present in the mucosa, where it plays a role in intestinal permeability (Bueno & Fioramonti, 2008; Pontarollo et al., 2020), as well as the endothelium of blood vessels (Molino et al., 1998) and in the circular and longitudinal smooth muscle layers. The staining of smooth muscle α-actin (**Figure 6.1b**) appears on the circular and the longitudinal smooth muscle cells of the intestinal wall, as well as the mucosal and vascular smooth muscle. The merged image (**Figure 6.1c**) shows the staining of both PAR-2 and α-actin in the circular and longitudinal smooth muscle areas. Control staining experiments were carried out to determine if the colon tissues displayed any auto-fluorescence or if the antibodies had any non-

specific binding **(Figure 6.1 d,e,f).** These controls showed minimal auto-fluorescence and minimal non-specific binding.

Next, the possible localization of PAR-2 on ICC was investigated with the use of PAR-2 antibodies and c-kit antibodies that bind to c-kit positive ICC (Koh et al., 1998; Torihashi et al., 1995). Presented in **Figure 6.2 (a,b,c)** are the immunofluorescence images showing the staining of PAR-2 (green), of c-kit+ cells (red), and of DAPI (blue). PAR-2 staining is present in the mucosa, the endothelium of blood vessels, and the circular and longitudinal smooth muscle layers of the rat mid-colon (**Figure 6.2a**). **Figure 6.2b** presents red staining of c-kit in the intestinal wall along the myenteric and submucosal plexuses and within the circular smooth muscle layer. A merged image of PAR-2 and c-kit staining is presented in **Figure 6.2c** showing staining of PAR-2 and c-kit in the intestinal smooth muscle layers and in the intestinal plexuses, respectively. Crucially, there appears to be no significant areas of co-staining with these antibodies. Control experiments demonstrated that there was no significant auto-fluorescence or non-specific binding (**Figure 6.2 d,e,f**).

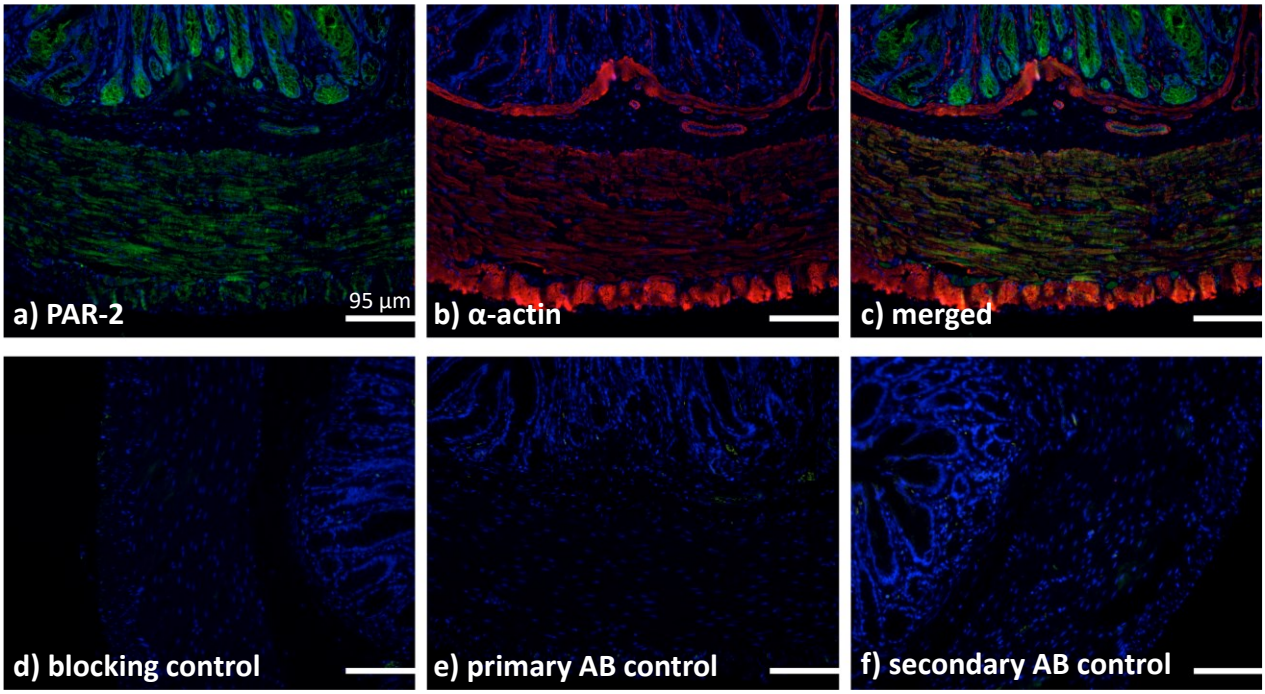

Figure 6.1. Immunofluorescence imaging of rat mid colon cross-sections for PAR-2 and smooth muscle α-actin. Image **a)** shows PAR-2 staining, in green, in the colon mucosa, and in the circular and longitudinal smooth muscle layers. **b)** shows α smooth muscle actin staining, in red, in the mucosa muscularis, and the circular and longitudinal smooth muscle layers. **c)** a merged image of PAR-2 and α smooth muscle actin staining showing the presence of PAR-2 within the circular and longitudinal smooth muscle layers. Control experiments **d)** DAPI and blocking solution, **e)** DAPI and primary antibodies, and **f)** DAPI and secondary antibodies. Scale bar = 95 µm.

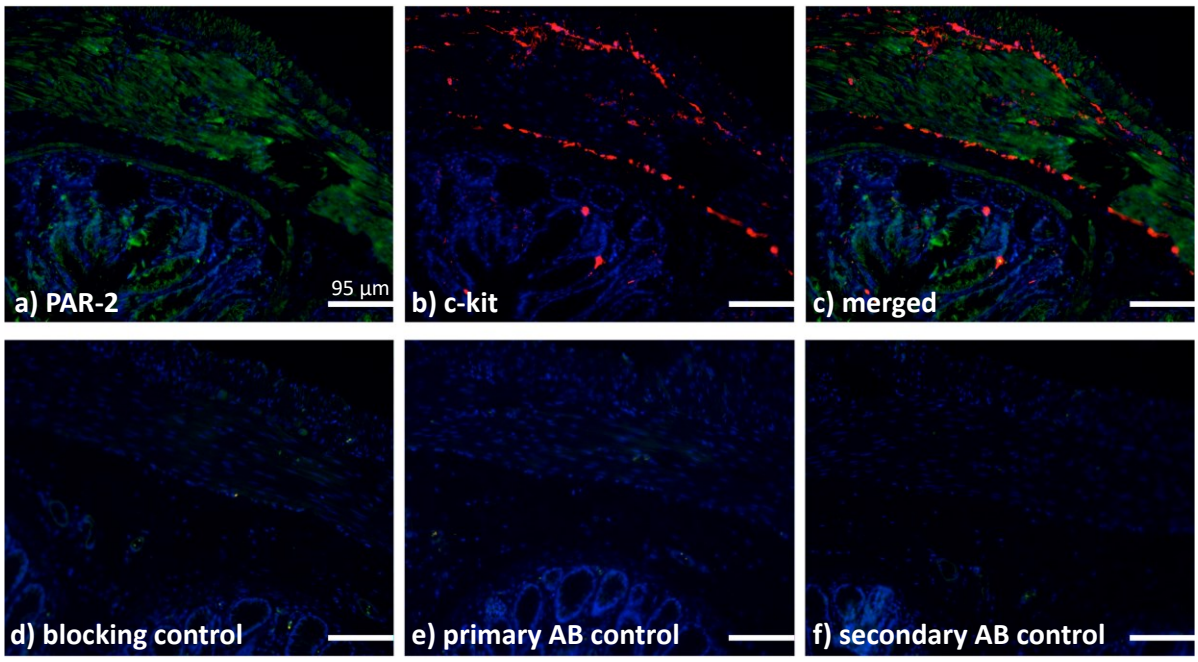

Figure 6.2 Immunofluorescence imaging of rat mid colon cross-sections for PAR-2 and c-kit. Image **a)** shows PAR-2 staining, in green, in the colon mucosa, and the smooth muscle layers. **b)** shows c-kit staining, in red, on mast cells in the mucosa, and along the submucosal plexus and myenteric plexus between the circular and longitudinal smooth muscle layers. **c)** a merged image of PAR-2 and c-kit staining showing distinct staining of PAR-2 and c-kit. Control experiments **d)** DAPI and blocking solution, **e)** DAPI and primary antibodies, and **f)** DAPI and secondary antibodies. Scale bar = 95 µm.

6.2 Discussion

6.2.1 PAR-2 may not inhibit colonic spontaneous contractile activity through direct action on ICC

Previous work in our lab has shown that activation of PAR-2 on rat colonic smooth muscle inhibits ICC induced spontaneous contractile activity. Therefore, to determine if PAR-2 mediates this effect through direct action on ICC, I investigated the location of PAR-2 in rat mid-colon cross sections with respect to smooth muscle cells and ICC. These images clearly show that PAR-2 stains in the circular and the longitudinal smooth muscle layers, in addition to the epithelial cells of the rat colon. The presence of PAR-2 on smooth muscle cells is supported by previous studies that have reported the presence of PAR-2 mRNA in rat gastrointestinal smooth muscle (Al-Ani et al., 1995; Nishikawa et al., 2002; Saifeddine et al., 1996) and by Corvera et al. (1997) that reported PAR-2 protein localization on circular and longitudinal smooth muscle cells in rat colon (Corvera et al., 1997). Staining of c-kit to identify ICC indicates that these cells are restricted to areas that are likely to be the submucosal plexus and myenteric plexus of the colon (Takayama et al., 2002; Torihashi et al., 1995; Ward et al., 2000). Overlay of the PAR-2 and c-kit images showed that there was no significant overlap of the areas of the colon wall that expressed both of these proteins indicating ICC do not express PAR-2 on their cell surface. This finding contrasts with Sung et al. (2015) who reported transcriptional expression of PAR-2 in ICC and PDGFRα+ interstitial cells in murine colon (Sung et al., 2015). However, it may be that PAR-2 genes present in murine colon ICC (Sung et al., 2015) are not transcribed to mRNA, that the mRNA is not translated to form the receptor protein, or that the receptor protein may not be translocated to the cell membrane on c-kit+ ICC.

Based on the present studies, activation of PAR-2 in rat mid colon is not likely to inhibit spontaneous contractile activity through direct action on ICC and, therefore, further research is

necessary to determine how PAR-2 may be mediating its inhibitory effect on ICC-dependent spontaneous contractile activity. The effects of PAR-2 activation were blocked by apamin, a SK_{Ca} channel inhibitor, suggesting that SK_{Ca} channels play a role in mediating PAR-2 responses (Cocks et al., 1999; Mulè, Baffi, & Cerra, 2002; Sato et al., 2006; Sung et al., 2015, 2018). ICC have been reported to express SK_{Ca} channels (Fujita et al., 2001), but this was contradicted by Vanderwinden et al. (2002) and Iino et al. (2009) (Iino et al., 2009; Vanderwinden et al., 2002). These results further suggest that inhibition of ICC activity by PAR-2 activation may involve other cells in the syncytium network. c-kit+ ICC are electrically coupled with smooth muscle cells and PDGFRα+ interstitial cells and, therefore, may be influenced by the excitability of these other cells in the network (Daniel et al., 1998; Koh et al., 1998; Sanders, 2019; Sanders et al., 2016; Takayama et al., 2002). Sung et al. (2015) reported that application of trypsin on PDGFRα+ cells induced hyperpolarization, an effect that was inhibited by apamin (Sung et al., 2015). SK_{Ca} channels have been found to be expressed on PDGFRα+ interstitial cells within the gastrointestinal wall (Iino et al., 2009; Vanderwinden et al., 2002). Furthermore, Hashitani et al. (2015) reported that SK_{Ca} channels were not located to the gastric smooth muscle (Hashitani et al., 2015). Therefore, PAR-2 activation may lead to hyperpolarization of PDGFRα+ interstitial cells through opening of apamin-sensitive SK_{Ca} channels that then spreads to ICC rather than direct hyperpolarization of ICC (Kurahashi et al., 2012; Sung et al., 2015). Further investigation and immunofluorescence imaging of PAR-2 with respect to PDGFRα+ interstitial cells and SK_{Ca} channels could assist in determining if hyperpolarization of PDGFRα+ interstitial cells may be involved in the inhibitory effect of PAR-2 on spontaneous contractile activity. It could also confirm the localization of SK_{Ca} channels on PDGFRα+ interstitial cells previously reported (Iino et al., 2009; Vanderwinden et al., 2002).

The images presented in this study were obtained using a Leica DM IRB Fluorescence Microscope. Obtaining images with a confocal microscope with greater resolution would provide a clearer location of the proteins of interest. However, in the images presented there does not appear to be an overlap of PAR-2 and c-kit staining, and additional imaging with a confocal microscope may not provide further insights. The interpretation of the images presented here depends upon the specificity of the primary antibodies for PAR-2 and c-kit. Although care was taken when choosing the quality and specificity of the antibodies used in these experiments, these antibodies were not directly tested for specificity in this work. Therefore, testing the specificity of these antibodies or replicating of these images with antibodies from other sources in future work would further support these findings.

Chapter 7: General discussion

The influence of diet and the gut microbiota on cardiovascular health has been highlighted over the last 30 years (Appel et al., 1997; Chiu et al., 2016; Dolmatova et al., 2018; Kaye et al., 2020; Mills et al., 2020; Najjar et al., 2018; Nardocci et al., 2019; Rabi et al., 2020; Rouse et al., 1984; Saneei et al., 2014; Schwingshackl et al., 2019). These studies report an association between fiber-rich and plant-based diets and promotion of cardiovascular health and blood pressure management. SCFAs, that rely on both diet and microbial diversity for their production, have been proposed to influence blood pressure regulation (Natarajan et al., 2016; Onyszkiewicz et al., 2019; Pluznick et al., 2013; Skrzypecki et al., 2018). The effect of SCFAs in isolated arteries show that these small molecules induce vasorelaxation through endothelium-dependent pathways supported by the wire myography results presented in **Chapter 3**. However, within the perfused mesenteric vascular bed these SCFAs do not have a significant effect at physiological μM concentrations. It is not clear if physiological μM concentrations may evoke direct vasorelaxation significant enough to influence blood pressure. SCFAs at mM concentrations, that were not subject to equimolar substitution of NaCl in the Krebs buffer, significantly attenuated frequency-dependent increases in perfusion pressure at 15 and 20 Hz stimulation frequencies. This suggests that the effect of SCFAs may be influenced by shear stress and osmolarity under conditions better resembling physiological parameters as seen in the perfusion data presented in **Chapter 3**. The influence of SCFAs on blood pressure regulation, as seen in *in vivo* studies, may also be influenced by osmolarity and shear stress. It is necessary that future work be completed to further elucidate the ways in which SCFAs influence blood pressure. This may also inform the possibility of a role of SCFAs in treatment in systemic hypertension and if any limitation of these SCFAs should be considered in other conditions such as portal hypertension.

Digestion and production of SCFAs can be impacted by transit time through the gastrointestinal tract and, therefore, gut motility (Titgemeyer et al., 1991). Regulation and maintenance of gut motility are influenced by many factors (described in **Chapter 4**) that may alter digestion and production of these gut-derived molecules. Serine proteases such as trypsin, factor VIIa and factor Xa can be transported in the blood (Adrian et al., 1979; Camerer et al., 1996; Colombo et al., 1989; Dandona et al., 1981; Frier et al., 1980; Isermann, 2017). Of these serine proteases, trypsin, has been reported to influence intestinal smooth muscle contractility through activation of PAR-2 in the intestinal wall (Al-Ani et al., 1995; Corvera et al., 1997; Mulè, Baffi, & Cerra, 2002; Saifeddine et al., 1996). Although I hypothesized that PAR-2 activation directly inhibits ICC initiated spontaneous contractile activity, the results presented in **Chapter 6** suggest otherwise as PAR-2 and c-kit+ ICC did not appear to stain together in immunofluorescence imaging. Further work is required to determine if PAR-2 may be working through another interstitial cell in the electrically coupled syncytium, such as PDGFRα+ interstitial cells, to influence ICC activity. These PDGFRα+ interstitial cells have been reported to express SK_{Ca} channels and therefore could mediate the apamin-sensitive PAR-2 inhibition of ICC pacemaker activity (Iino et al., 2009; Vanderwinden et al., 2002). Future imaging and functional studies focusing on PDGFRα+ interstitial cells may provide insight into the mechanisms and cells involved in mediating PAR-2 inhibition of spontaneous contractile activity.

Together, this work supports the notion that gut health and nutrition can influence cardiovascular health, and further demonstrates the complexity of interactions between the gastrointestinal tract and the cardiovascular system, as the cardiovascular system may also be involved in influencing gut motility and, thus, nutrient breakdown. The health of the cardiovascular system and the gastrointestinal tract appear to be linked through complex

interactions. However, the depth and extent of these interactions are still to be uncovered in future studies. Further research to continue the efforts to better understand how SCFAs may be influencing blood pressure regulation, how PAR-2 activation may be influencing gastrointestinal motility, and how gut and blood vessel interactions influence each other may be useful in building knowledge that could be applied to treating hypertension and maintaining cardiovascular and gastrointestinal health.

References

Aalkjær, C. (2002). Short chained fatty acids and the colon: how do they cause vasodilatation? *The Journal of Physiology*, *538*(3), 674–674. https://doi.org/10.1113/jphysiol.2001.015115

Aaronson, P. I., McKinnon, W., & Poston, L. (1996). Mechanism of butyrate-induced vasorelaxation of rat mesenteric resistance artery. *British Journal of Pharmacology*, *117*(2), 365–371. https://doi.org/10.1111/j.1476-5381.1996.tb15200.x

Adak, A., & Khan, M. R. (2019). An insight into gut microbiota and its functionalities. *Cellular and Molecular Life Sciences*, *76*(3), 473–493. https://doi.org/10.1007/s00018-018-2943-4

Adrian, T. E., Besterman, H. S., Mallinson, C. N., Pera, A., Redshaw, M. R., Wood, T. P., & Bloom, S. R. (1979). Plasma trypsin in chronic pancreatitis and pancreatic adenocarcinoma. *Clinica Chimica Acta*, *97*(2–3), 205–212. https://doi.org/10.1016/0009-8981(79)90417-0

Al-Ani, B., Saifeddine, M., & Hollenberg, M. D. (1995). Detection of functional receptors for the proteinase-activated-receptor-2-activating polypeptide, SLIGRL-NH 2 , in rat vascular and gastric smooth muscle. *Canadian Journal of Physiology and Pharmacology*, *73*(8), 1203–1207. https://doi.org/10.1139/y95-172

Allen, B. G., & Walsh, M. P. (1994). The biochemical basis of the regulation of smooth-muscle contraction. *Trends in Biochemical Sciences*, *19*(9), 362–368. https://doi.org/10.1016/0968-0004(94)90112-0

Appel, L. J., Moore, T. J., Obarzanek, E., Vollmer, W. M., Svetkey, L. P., Sacks, F. M., Bray, G. A., Vogt, T. M., Cutler, J. A., Windhauser, M. M., Lin, P.-H. H., Karanja, N., Simons-Morton, D., McCullough, M., Swain, J., Steele, P., Evans, M. A., Miller, E. R., & Harsha, D. W. (1997). A clinical trial of the effects of dietary patterns on blood pressure. DASH Collaborative Research Group. *The New England Journal of Medicine*, *336*(16), 1117–1124. https://doi.org/10.1056/NEJM199704173361601

Bachmann, O., Juric, M., Seidler, U., Manns, M. P., & Yu, H. (2011). Basolateral ion transporters involved in colonic epithelial electrolyte absorption, anion secretion and cellular homeostasis. *Acta Physiologica*, *201*(1), 33–46. https://doi.org/10.1111/j.1748-1716.2010.02153.x

Ballermann, B. J., Dardik, A., Eng, E., & Liu, A. (1998). Shear stress and the endothelium. *Kidney International*, *54*(67), S100–S108. https://doi.org/10.1046/j.1523-1755.1998.06720.x

Bao, J. X., Eriksson, I. E., & Stjärne, L. (1990). Neurotransmitters and pre- and post-junctional receptors involved in the vasoconstrictor response to sympathetic nerve stimulation in rat tail artery. *Acta Physiologica Scandinavica*, *140*(4), 467–479. https://doi.org/10.1111/j.1748-1716.1990.tb09023.x

Batenburg, W. W., Tom, B., Schuijt, M. P., & Danser, A. H. J. (2005). Angiotensin II type 2 receptor-mediated vasodilation. Focus on bradykinin, NO and endothelium-derived hyperpolarizing factor(s). *Vascular Pharmacology*, *42*(3), 109–118. https://doi.org/10.1016/j.vph.2005.01.005

Bean, B. P., Sturek, M., Puga, A., & Hermsmeyer, K. (1986). Calcium channels in muscle cells isolated from rat mesenteric arteries: Modulation by dihydropyridine drugs. *Circulation Research*, *59*(2), 229–235. https://doi.org/10.1161/01.RES.59.2.229

Behuliak, M., Bencze, M., Vaněčková, I., Kuneš, J., & Zicha, J. (2017). Basal and Activated Calcium Sensitization Mediated by RhoA/Rho Kinase Pathway in Rats with Genetic and Salt Hypertension. *BioMed Research International*, *2017*, 8029728. https://doi.org/10.1155/2017/8029728

Bennett, M. R. (1998). Transmission at Sympathetic Varicosities. *News in Physiological Sciences*, *13*(2), 79–84. https://doi.org/10.1152/physiologyonline.1998.13.2.79

Bishop, J. J., Nance, P. R., Popel, A. S., Intaglietta, M., & Johnson, P. C. (2000). Diameter changes in skeletal muscle venules during arterial pressure reduction. *American Journal of Physiology-Heart and Circulatory Physiology*, *279*(1), H47–H57. https://doi.org/10.1152/ajpheart.2000.279.1.H47

Blatz, A. L., & Magleby, K. L. (1986). Single apamin-blocked Ca-activated K+ channels of small conductance in cultured rat skeletal muscle. *Nature*, *323*(6090), 718–720. https://doi.org/10.1038/323718a0

Blausen.com staff. (2014). Medical gallery of Blausen Medical 2014. *WikiJournal of Medicine*, *1*(2). https://doi.org/10.15347/wjm/2014.010

Bloemen, J. G., Venema, K., van de Poll, M. C., Olde Damink, S. W., Buurman, W. A., & Dejong, C. H. (2009). Short chain fatty acids exchange across the gut and liver in humans measured at surgery. *Clinical Nutrition*, *28*(6), 657–661. https://doi.org/10.1016/j.clnu.2009.05.011

Bosman, J., Tangelder, G. J., Oude Egbrink, M. G., Reneman, R. S., & Slaaf, D. W. (1995). Capillary diameter changes during low perfusion pressure and reactive hyperemia in rabbit skeletal muscle. *American Journal of Physiology-Heart and Circulatory Physiology*, *269*(3), H1048–H1055. https://doi.org/10.1152/ajpheart.1995.269.3.H1048

Boyer, J. L., Waldo, G. L., & Harden, T. K. (1992). Beta gamma-subunit activation of G-protein-regulated phospholipase C. *Journal of Biological Chemistry*, *267*(35), 25451–25456. https://doi.org/10.1016/S0021-9258(19)74062-9

Bradley, E., Law, A., Bell, D., & Johnson, C. D. (2003). Effects of varying impulse number on cotransmitter contributions to sympathetic vasoconstriction in rat tail artery. *American Journal of Physiology-Heart and Circulatory Physiology*, *284*(6), H2007–H2014. https://doi.org/10.1152/ajpheart.01061.2002

Brain, S. D., Tippins, J. R., & Williams, T. J. (1988). Endothelin induces potent microvascular constriction. *British Journal of Pharmacology*, *95*(4), 1005–1007. https://doi.org/10.1111/j.1476-5381.1988.tb11731.x

Braunstein, T. H., Inoue, R., Cribbs, L., Oike, M., Ito, Y., Holstein-Rathlou, N. H., & Jensen, L. J. (2009). The role of L- and T-type calcium channels in local and remote calcium responses in rat mesenteric terminal arterioles. *Journal of Vascular Research*, *46*(2), 138–151. https://doi.org/10.1159/000151767

Broadley, K., & Kelly, D. (2001). Muscarinic Receptor Agonists and Antagonists. *Molecules*, *6*(3), 142–193. https://doi.org/10.3390/60300142

Brown, A. J., Goldsworthy, S. M., Barnes, A. A., Eilert, M. M., Tcheang, L., Daniels, D., Muir, A. I., Wigglesworth, M. J., Kinghorn, I., Fraser, N. J., Pike, N. B., Strum, J. C., Steplewski, K. M., Murdock, P. R., Holder, J. C., Marshall, F. H., Szekeres, P. G., Wilson, S., Ignar, D. M., … Dowell, S. J. (2003). The orphan G protein-coupled receptors GPR41 and GPR43 are activated by propionate and other short chain carboxylic acids. *Journal of Biological Chemistry*, *278*(13), 11312–11319. https://doi.org/10.1074/jbc.M211609200

Brown, B. M., Shim, H., Christophersen, P., & Wulff, H. (2020). Pharmacology of Small- and Intermediate-Conductance Calcium-Activated Potassium Channels. *Annual Review of Pharmacology and Toxicology*, *60*, 219–240. https://doi.org/10.1146/annurev-pharmtox-010919-023420

Brown, I. A. M., Diederich, L., Good, M. E., DeLalio, L. J., Murphy, S. A., Cortese-Krott, M. M., Hall, J. L., Le, T. H., & Isakson, B. E. (2018). Vascular smooth muscle remodeling in conductive and resistance arteries in hypertension. *Arteriosclerosis, Thrombosis, and Vascular Biology*, *38*(9), 1969–1985. https://doi.org/10.1161/ATVBAHA.118.311229

Bueno, l., & Fioramonti, J. (2008). Protease-activated receptor 2 and gut permeability: a review. *Neurogastroenterology & Motility*, *20*(6), 580–587. https://doi.org/10.1111/j.1365-2982.2008.01139.x

Bugaut, M. (1987). Occurrence, absorption and metabolism of short chain fatty acids in the digestive tract of mammals. *Comparative Biochemistry and Physiology Part B: Comparative Biochemistry*, *86*(3), 439–472. https://doi.org/10.1016/0305-0491(87)90433-0

Burnstock, G. (2018). Purine and purinergic receptors. *Brain and Neuroscience Advances*, *2*, 239821281881749. https://doi.org/10.1177/2398212818817494

Callaghan, B., Koh, S. D., & Keef, K. D. (2004). Muscarinic M2 Receptor Stimulation of Cav1.2b Requires Phosphatidylinositol 3-Kinase, Protein Kinase C, and c-Src. *Circulation Research*, *94*(5), 626–633. https://doi.org/10.1161/01.RES.0000118248.17466.B7

Camerer, E., Røttingen, J. A., Iversen, J. G., & Prydz, H. (1996). Coagulation factors VII and X induce Ca2+ oscillations in Madin-Darby canine kidney cells only when proteolytically active. *Journal of Biological Chemistry*, *271*(46), 29034–29042. https://doi.org/10.1074/jbc.271.46.29034

Carrick, J. B., & Begg, A. P. (2008). Peripheral blood leukocytes. *Veterinary Clinics of North America - Equine Practice*, *24*(2), 239–259. https://doi.org/10.1016/j.cveq.2008.05.003

Chang, Y., Chen, Y., Zhou, Q., Wang, C., Chen, L., Di, W., & Zhang, Y. (2020). Short-chain fatty acids accompanying changes in the gut microbiome contribute to the development of hypertension in patients with preeclampsia. *Clinical Science*, *134*(2), 289–302. https://doi.org/10.1042/CS20191253

Chen, L., Soo, M. K., Oppermann, M., Faulhaber-Walter, R., Huang, Y., Mizel, D., Chen, M., Lopez, M. L. S., Weinstein, L. S., Gomez, R. A., Briggs, J. P., & Schnermann, J. (2007). Regulation of renin in mice with Cre recombinase-mediated deletion of G protein Gsα in

juxtaglomerular cells. *American Journal of Physiology - Renal Physiology*, *292*(1), 27–37. https://doi.org/10.1152/ajprenal.00193.2006

Chilian, W. M., Eastham, C. L., & Marcus, M. L. (1986). Microvascular distribution of coronary vascular resistance in beating left ventricle. *American Journal of Physiology - Heart and Circulatory Physiology*, *251*(4), 779–788. https://doi.org/10.1152/ajpheart.1986.251.4.h779

Chiu, S., Bergeron, N., Williams, P. T., Bray, G. A., Sutherland, B., & Krauss, R. M. (2016). Comparison of the DASH (Dietary Approaches to Stop Hypertension) diet and a higher-fat DASH diet on blood pressure and lipids and lipoproteins: a randomized controlled trial. *The American Journal of Clinical Nutrition*, *103*(2), 341–347. https://doi.org/10.3945/ajcn.115.123281

Cocks, T. M., Sozzi, V., Moffatt, J. D., & Selemidis, S. (1999). Protease-activated receptors mediate apamin-sensitive relaxation of mouse and guinea pig gastrointestinal smooth muscle. *Gastroenterology*, *116*(3), 586–592. https://doi.org/10.1016/S0016-5085(99)70180-0

Cole, W. C., & Welsh, D. G. (2011). Role of myosin light chain kinase and myosin light chain phosphatase in the resistance arterial myogenic response to intravascular pressure. *Archives of Biochemistry and Biophysics*, *510*(2), 160–173. https://doi.org/10.1016/j.abb.2011.02.024

Colombo, C., Maiavacca, R., Ronchi, M., Bottani, P., Stripparo, L., Corbetta, C., & Sereni, L. P. (1989). Serum levels of immunoreactive trypsin during development: Comparison with levels of lipase and amylase. *Journal of Pediatric Gastroenterology and Nutrition*, *9*(2), 194–199. https://doi.org/10.1097/00005176-198908000-00011

Colyer, J. (1998). Phosphorylation states of phospholamban. *Annals of the New York Academy of Sciences*, *853*, 79–91. https://doi.org/10.1111/j.1749-6632.1998.tb08258.x

Corvera, C. U., Déry, O., McConalogue, K., Böhm, S. K., Khitin, L. M., Caughey, G. H., Payan, D. G., & Bunnett, N. W. (1997). Mast cell tryptase regulates rat colonic myocytes through proteinase- activated receptor 2. *Journal of Clinical Investigation*, *100*(6), 1383–1393. https://doi.org/10.1172/JCI119658

Cowan, C. L., Palacino, J. J., Najibi, S., & Cohen, R. A. (1993). Potassium channel-mediated relaxation to acetylcholine in rabbit arteries. *Journal of Pharmacology and Experimental Therapeutics*, *266*(3), 1482–1489.

Cummings, J. H., Pomare, E. W., Branch, W. J., Naylor, C. P., & Macfarlane, G. T. (1987). Short chain fatty acids in human large intestine, portal, hepatic and venous blood. *Gut*, *28*(10), 1221–1227. https://doi.org/10.1136/gut.28.10.1221

Dandona, P., Hodson, M., Bell, J., Ramdial, L., Beldon, I., & Batten, J. C. (1981). Serum immunoreactive trypsin in cystic fibrosis. *Thorax*, *36*(1), 60–62. https://doi.org/10.1136/thx.36.1.60

Daniel, E. E., Wang, Y.-F., & Cayabyab, F. S. (1998). Role of gap junctions in structural arrangements of interstitial cells of Cajal and canine ileal smooth muscle. *American Journal of Physiology-Gastrointestinal and Liver Physiology*, *274*(6), G1125–G1141. https://doi.org/10.1152/ajpgi.1998.274.6.G1125

Danser, A. H. J., Tom, B., De Vries, R., & Saxena, P. R. (2000). L-NAME-resistant bradykinin-induced relaxation in porcine coronary arteries is NO-dependent: Effect of ACE inhibition. *British Journal of Pharmacology*, *131*(2), 195–202. https://doi.org/10.1038/sj.bjp.0703555

DeLorey, D. S., Hamann, J. J., Kluess, H. A., Clifford, P. S., & Buckwalter, J. B. (2006). α-Adrenergic receptor-mediated restraint of skeletal muscle blood flow during prolonged exercise. *Journal of Applied Physiology*, *100*(5), 1563–1568. https://doi.org/10.1152/japplphysiol.01035.2005

Dewey, C. F., Bussolari, S. R., Gimbrone, M. A., & Davies, P. F. (1981). The dynamic response of vascular endothelial cells to fluid shear stress. *Journal of Biomechanical Engineering*, *103*(3), 177–185. https://doi.org/10.1115/1.3138276

Ding, H., & Triggle, C. R. (2000). Novel endothelium-derived relaxing factors: Identification of factors and cellular targets. *Journal of Pharmacological and Toxicological Methods*, *44*(2), 441–452. https://doi.org/10.1016/S1056-8719(00)00127-1

Docherty, J. R. (2019). The pharmacology of α1-adrenoceptor subtypes. *European Journal of Pharmacology*, *855*, 305–320. https://doi.org/10.1016/j.ejphar.2019.04.047

Dolmatova, E. V., Moazzami, K., & Bansilal, S. (2018). Dietary sodium intake among US adults with hypertension, 1999–2012. *Journal of Hypertension*, *36*(2), 237–242. https://doi.org/10.1097/HJH.0000000000001558

Donohoe, D. R., Garge, N., Zhang, X., Sun, W., O'Connell, T. M., Bunger, M. K., & Bultman, S. J. (2011). The Microbiome and Butyrate Regulate Energy Metabolism and Autophagy in the Mammalian Colon. *Cell Metabolism*, *13*(5), 517–526. https://doi.org/10.1016/j.cmet.2011.02.018

Drumm, B. T., Rembetski, B. E., Messersmith, K., Manierka, M. S., Baker, S. A., & Sanders, K. M. (2020). Pacemaker function and neural responsiveness of subserosal interstitial cells of Cajal in the mouse colon. *The Journal of Physiology*, *598*(4), 651–681. https://doi.org/10.1113/JP279102

Duncan, S. H., Barcenilla, A., Stewart, C. S., Pryde, S. E., & Flint, H. J. (2002). Acetate utilization and butyryl coenzyme A (CoA):acetate-CoA transferase in butyrate-producing bacteria from the human large intestine. *Applied and Environmental Microbiology*, *68*(10), 5186–5190. https://doi.org/10.1128/AEM.68.10.5186-5190.2002

Durgan, D. J., Ganesh, B. P., Cope, J. L., Ajami, N. J., Phillips, S. C., Petrosino, J. F., Hollister, E. B., & Bryan, R. M. (2016). Role of the gut microbiome in obstructive sleep apnea–induced hypertension. *Hypertension*, *67*(2), 469–474. https://doi.org/10.1161/HYPERTENSIONAHA.115.06672

Eckburg, P. B., Bik, E. M., Bernstein, C. N., Purdom, E., Dethlefsen, L., Sargent, M., Gill, S. R., Nelson, K. E., & Relman, D. A. (2005). Diversity of the human intestinal microbial flora. *Science (New York, N.Y.)*, *308*(5728), 1635–1638. https://doi.org/10.1126/science.1110591

Edwards, G., Dora, K. A., Gardener, M. J., Garland, C. J., & Weston, A. H. (1998). K+ is an endothelium-derived hyperpolarizing factor in rat arteries. *Nature*, *396*(6708), 269–272. https://doi.org/10.1038/24388

Edwards, G., Félétou, M., & Weston, A. H. (2010). Endothelium-derived hyperpolarising factors and associated pathways: a synopsis. *Pflügers Archiv - European Journal of Physiology*, *459*(6), 863–879. https://doi.org/10.1007/s00424-010-0817-1

Engelstoft, M. S., Park, W., Sakata, I., Kristensen, L. V., Husted, A. S., Osborne-Lawrence, S., Piper, P. K., Walker, A. K., Pedersen, M. H., Nøhr, M. K., Pan, J., Sinz, C. J., Carrington, P. E., Akiyama, T. E., Jones, R. M., Tang, C., Ahmed, K., Offermanns, S., Egerod, K. L., … Schwartz, T. W. (2013). Seven transmembrane G protein-coupled receptor repertoire of gastric ghrelin cells. *Molecular Metabolism*, *2*(4), 376–392. https://doi.org/10.1016/j.molmet.2013.08.006

Etter, E. F., Eto, M., Wardle, R. L., Brautigan, D. L., & Murphy, R. A. (2001). Activation of myosin light chain phosphatase in intact arterial smooth muscle during nitric oxide-induced relaxation. *Journal of Biological Chemistry*, *276*(37), 34681–34685. https://doi.org/10.1074/jbc.M104737200

Faussner, A., Wennerberg, G., Schüssler, S., Feierler, J., Seidl, C., Jochum, M., & Proud, D. (2009). Alanine screening of the intracellular loops of the human bradykinin B 2 receptor - Effects on receptor maintenance, G protein activation and internalization. *FEBS Journal*, *276*(13), 3491–3503. https://doi.org/10.1111/j.1742-4658.2009.07071.x

Ferro, A., Gilbert, R., & Krum, H. (2006). Importance of renin in blood pressure regulation and therapeutic potential of renin inhibition. *International Journal of Clinical Practice*, *60*(5), 577–581. https://doi.org/10.1111/j.1368-5031.2006.00920.x

Fleming, S. E., Choi, S. Y., & Fitch, M. D. (1991). Absorption of Short-Chain Fatty Acids from the Rat Cecum in Vivo. *The Journal of Nutrition*, *121*(11), 1787–1797. https://doi.org/10.1093/jn/121.11.1787

Flint, H. J., Duncan, S. H., Scott, K. P., & Louis, P. (2015). Links between diet, gut microbiota composition and gut metabolism. *Proceedings of the Nutrition Society*, *74*(1), 13–22. https://doi.org/10.1017/S0029665114001463

Florian, J. A., Kosky, J. R., Ainslie, K., Pang, Z., Dull, R. O., & Tarbell, J. M. (2003). Heparan sulfate proteoglycan is a mechanosensor on endothelial cells. *Circulation Research*, *93*(10), e136-42. https://doi.org/10.1161/01.RES.0000101744.47866.D5

Foong, D., Zhou, J., Zarrouk, A., Ho, V., & O'Connor, M. D. (2020). Understanding the biology of human interstitial cells of Cajal in gastrointestinal motility. *International Journal of Molecular Sciences*, *21*(12), 4540. https://doi.org/10.3390/ijms21124540

Förstermann, U., & Münzel, T. (2006). Endothelial nitric oxide synthase in vascular disease. *Circulation*, *113*(13), 1708–1714. https://doi.org/10.1161/CIRCULATIONAHA.105.602532

Frier, B. M., Adrian, T. E., Saunders, J. H. B., & Bloom, S. R. (1980). Serum trypsin concentration and pancreatic trypsin secretion in insulin-dependent diabetes mellitus. *Clinica Chimica Acta*, *105*(2), 297–300. https://doi.org/10.1016/0009-8981(80)90472-6

Fujita, A., Takeuchi, T., Saitoh, N., Hanai, J., & Hata, F. (2001). Expression of Ca2+-activated K+ channels, SK3, in the interstitial cells of Cajal in the gastrointestinal tract. *American*

Journal of Physiology - Cell Physiology, *281*(5), C1727–C1733. https://doi.org/10.1152/ajpcell.2001.281.5.c1727

Furukawa, K. I., Tawada-iwata, Y., & Shigekawa, M. (1989). Modulation of plasma membrane Ca2+ pump by membrane potential in cultured vascular smooth muscle cells. *Journal of Biochemistry*, *106*(6), 1068–1073. https://doi.org/10.1093/oxfordjournals.jbchem.a122966

Ganesh, B. P., Nelson, J. W., Eskew, J. R., Ganesan, A., Ajami, N. J., Petrosino, J. F., Bryan, R. M., & Durgan, D. J. (2018). Prebiotics, probiotics, and acetate supplementation prevent hypertension in a model of obstructive sleep apnea. *Hypertension*, *72*(5), 1141–1150. https://doi.org/10.1161/HYPERTENSIONAHA.118.11695

Garcia-Lopez, P., Garcia-Marin, V., Martínez-Murillo, R., & Freire, M. (2009). Updating old ideas and recent advances regarding the Interstitial Cells of Cajal. *Brain Research Reviews*, *61*(2), 154–169. https://doi.org/10.1016/j.brainresrev.2009.06.001

Gibson, G. R., & Roberfroid, M. B. (1995). Dietary modulation of the human colonic microbiota: Introducing the concept of prebiotics. *Journal of Nutrition*, *125*(6), 1401–1412. https://doi.org/10.1093/jn/125.6.1401

Gomez-Arango, L. F., Barrett, H. L., McIntyre, H. D., Callaway, L. K., Morrison, M., Dekker Nitert, M., & SPRING Trial Group. (2016). Increased systolic and diastolic blood pressure is associated with altered gut microbiota composition and butyrate production in early pregnancy. *Hypertension*, *68*(4), 974–981. https://doi.org/10.1161/HYPERTENSIONAHA.116.07910

Gonzalez-Montelongo, M. D. C., & Fountain, S. J. (2021). Neuropeptide Y facilitates P2X1 receptor-dependent vasoconstriction via Y1 receptor activation in small mesenteric arteries during sympathetic neurogenic responses. *Vascular Pharmacology*, *136*, 106810. https://doi.org/10.1016/j.vph.2020.106810

Grundy, D. (2015). Principles and standards for reporting animal experiments in The Journal of Physiology and Experimental Physiology. *Experimental Physiology*, *100*(7), 755–758. https://doi.org/10.1113/EP085299

Hackenthal, E., Paul, M., Ganten, D., & Taugner, R. (1990). Morphology, physiology, and molecular biology of renin secretion. *Physiological Reviews*, *70*(4), 1067–1116. https://doi.org/10.1152/physrev.1990.70.4.1067

Hashitani, H., Mitsui, R., Masaki, S., & Van Helden, D. F. (2015). Pacemaker role of pericytes in generating synchronized spontaneous Ca2+ transients in the myenteric microvasculature of the guinea-pig gastric antrum. *Cell Calcium*, *58*(5), 442–456. https://doi.org/10.1016/j.ceca.2015.06.012

Hepler, J. R., & Gilman, A. G. (1992). G proteins. *Trends in Biochemical Sciences*, *17*(10), 383–387. https://doi.org/10.1016/0968-0004(92)90005-T

Hirst, G. D. S., Bramich, N. J., Teramoto, N., Suzuki, H., & Edwards, F. R. (2002). Regenerative component of slow waves in the guinea-pig gastric antrum involves a delayed increase in [Ca2+]i and Cl- channels. *Journal of Physiology*, *540*(3), 907–919. https://doi.org/10.1113/jphysiol.2001.014803

Holinstat, M. (2017). Normal platelet function. *Cancer Metastasis Reviews*, *36*(2), 195–198. https://doi.org/10.1007/s10555-017-9677-x

Hu, J., Luo, H., Wang, J., Tang, W., Lu, J., Wu, S., Xiong, Z., Yang, G., Chen, Z., Lan, T., Zhou, H., Nie, J., Jiang, Y., & Chen, P. (2017). Enteric dysbiosis-linked gut barrier disruption triggers early renal injury induced by chronic high salt feeding in mice. *Experimental & Molecular Medicine*, *49*(8), e370. https://doi.org/10.1038/emm.2017.122

Hudson, B. D., Tikhonova, I. G., Pandey, S. K., Ulven, T., & Milligan, G. (2012). Extracellular ionic locks determine variation in constitutive activity and ligand potency between species orthologs of the free fatty acid receptors FFA2 and FFA3. *Journal of Biological Chemistry*, *287*(49), 41195–41209. https://doi.org/10.1074/jbc.M112.396259

Hwang, S. J., Blair, P. J. A., Britton, F. C., O'Driscoll, K. E., Hennig, G., Bayguinov, Y. R., Rock, J. R., Harfe, B. D., Sanders, K. M., & Ward, S. M. (2009). Expression of anoctamin 1/TMEM16A by interstitial cells of Cajal is fundamental for slow wave activity in gastrointestinal muscles. *Journal of Physiology*, *587*(20), 4887–4904. https://doi.org/10.1113/jphysiol.2009.176198

Iino, S., Horiguchi, K., Horiguchi, S., & Nojyo, Y. (2009). C-Kit-negative fibroblast-like cells express platelet-derived growth factor receptor α in the murine gastrointestinal musculature. *Histochemistry and Cell Biology*, *131*(6), 691–702. https://doi.org/10.1007/s00418-009-0580-6

Illiano, P., Brambilla, R., & Parolini, C. (2020). The mutual interplay of gut microbiota, diet and human disease. *FEBS Journal*, *287*(5), 833–855. https://doi.org/10.1111/febs.15217

Isermann, B. (2017). Homeostatic effects of coagulation protease-dependent signaling and protease activated receptors. *Journal of Thrombosis and Haemostasis*, *15*(7), 1273–1284. https://doi.org/10.1111/jth.13721

Ishihara, H., Connolly, A. J., Zeng, D., Kahn, M. L., Zheng, Y. W., Timmons, C., Tram, T., & Coughlin, S. R. (1997). Protease-activated receptor 3 is a second thrombin receptor in humans. *Nature*, *386*(6624), 502–506. https://doi.org/10.1038/386502a0

Iwakiri, Y. (2014). Pathophysiology of portal hypertension. *Clinics in Liver Disease*, *18*(2), 281–291. https://doi.org/10.1016/j.cld.2013.12.001

Jensen, L. J., Salomonsson, M., Jensen, B. L., & Holstein-Rathlou, N. H. (2004). Depolarization-induced calcium influx in rat mesenteric small arterioles is mediated exclusively via mibefradil-sensitive calcium channels. *British Journal of Pharmacology*, *142*(4), 709–718. https://doi.org/10.1038/sj.bjp.0705841

Jin, B., Ha, S. E., Wei, L., Singh, R., Zogg, H., Clemmensen, B., Heredia, D. J., Gould, T. W., Sanders, K. M., & Ro, S. (2021). Colonic motility is improved by the activation of 5-HT2B receptors on interstitial cells of Cajal in diabetic mice. *Gastroenterology*, *161*(2), 608-622.e7. https://doi.org/10.1053/j.gastro.2021.04.040

Jin, H., Koyama, T., Hatanaka, Y., Akiyama, S., Takayama, F., & Kawasaki, H. (2006). Histamine-induced vasodilation and vasoconstriction in the mesenteric resistance artery of the rat. *European Journal of Pharmacology*, *529*(1–3), 136–144.

https://doi.org/10.1016/j.ejphar.2005.10.060

Joannides, R., Haefeli, W. E., Linder, L., Richard, V., Bakkali, E. H., Thuillez, C., & Lüscher, T. F. (1995). Nitric oxide is responsible for flow-dependent dilatation of human peripheral conduit arteries in vivo. *Circulation*, *91*(5), 1314–1319. https://doi.org/10.1161/01.CIR.91.5.1314

Just, T. P., Cooper, I. R., & DeLorey, D. S. (2016). Sympathetic vasoconstriction in skeletal muscle: Adaptations to exercise training. *Exercise and Sport Sciences Reviews*, *44*(4), 137–143. https://doi.org/10.1249/JES.0000000000000085

Kawabata, A. (2003). Gastrointestinal functions of proteinase-activated receptors. *Life Sciences*, *74*(2–3), 247–254. https://doi.org/10.1016/j.lfs.2003.09.011

Kawabata, A., Kanke, T., Yonezawa, D., Ishiki, T., Saka, M., Kabeya, M., Sekiguchi, F., Kubo, S., Kuroda, R., Iwaki, M., Katsura, K., & Plevin, R. (2004). Potent and metabolically stable agonists for protease-activated receptor-2: Evaluation of activity in multiple assay systems in vitro and in vivo. *Journal of Pharmacology and Experimental Therapeutics*, *309*(3), 1098–1107. https://doi.org/10.1124/jpet.103.061010

Kaye, D. M., Shihata, W. A., Jama, H. A., Tsyganov, K., Ziemann, M., Kiriazis, H., Horlock, D., Vijay, A., Giam, B., Vinh, A., Johnson, C., Fiedler, A., Donner, D., Snelson, M., Coughlan, M. T., Phillips, S., Du, X.-J., El-Osta, A., Drummond, G., … Marques, F. Z. (2020). Deficiency of prebiotic fiber and insufficient signaling through gut metabolite-sensing receptors leads to cardiovascular disease. *Circulation*, *141*(17), 1393–1403. https://doi.org/10.1161/CIRCULATIONAHA.119.043081

Keef, K. D., Hume, J. R., & Zhong, J. (2001). Regulation of cardiac and smooth muscle Ca 2+ channels (Ca V 1.2a,b) by protein kinases. *American Journal of Physiology-Cell Physiology*, *281*(6), C1743–C1756. https://doi.org/10.1152/ajpcell.2001.281.6.C1743

Kenner, T. (1988). Arterial blood pressure and its measurement. *Basic Research in Cardiology*, *83*(2), 107–121. https://doi.org/10.1007/BF01907264

Kerr, P. M., Tam, R., Narang, D., Potts, K., McMillan, D., McMillan, K., & Plane, F. (2012). Endothelial calcium-activated potassium channels as therapeutic targets to enhance availability of nitric oxide. *Canadian Journal of Physiology and Pharmacology*, *90*(6), 739–752. https://doi.org/10.1139/Y2012-075

Kerr, P. M., Wei, R., Tam, R., Sandow, S. L., Murphy, T. V., Ondrusova, K., Lunn, S. E., Tran, C. H. T., Welsh, D. G., & Plane, F. (2015). Activation of endothelial IK Ca channels underlies NO-dependent myoendothelial feedback. *Vascular Pharmacology*, *74*, 130–138. https://doi.org/10.1016/j.vph.2015.09.001

Kimura, I., Ichimura, A., Ohue-Kitano, R., & Igarashi, M. (2020). Free fatty acid receptors in health and disease. *Physiological Reviews*, *100*(1), 171–210. https://doi.org/10.1152/physrev.00041.2018

Kimura, I., Inoue, D., Maeda, T., Hara, T., Ichimura, A., Miyauchi, S., Kobayashi, M., Hirasawa, A., & Tsujimoto, G. (2011). Short-chain fatty acids and ketones directly regulate sympathetic nervous system via G protein-coupled receptor 41 (GPR41). *Proceedings of the*

National Academy of Sciences, *108*(19), 8030–8035. https://doi.org/10.1073/pnas.1016088108

Kito, Y., & Suzuki, H. (2003). Properties of pacemaker potentials recorded from myenteric interstitial cells of Cajal distributed in the mouse small intestine. *Journal of Physiology*, *553*(3), 803–818. https://doi.org/10.1113/jphysiol.2003.051334

Knock, G., Psaroudakis, D., Abbot, S., & Aaronson, P. I. (2002). Propionate-induced relaxation in rat mesenteric arteries: a role for endothelium-derived hyperpolarising factor. *The Journal of Physiology*, *538*(3), 879–890. https://doi.org/10.1113/jphysiol.2001.013105

Kobayashi, S., Kitazawa, T., Somlyo, A. V., & Somlyo, A. P. (1989). Cytosolic heparin inhibits muscarinic and α-adrenergic Ca2+ release in smooth muscle. Physiological role of inositol 1,4,5-trisphosphate in pharmacomechanical coupling. *Journal of Biological Chemistry*, *264*(30), 17997–18004. https://doi.org/10.1016/S0021-9258(19)84670-7

Koh, S. D., Sanders, K. M., & Ward, S. M. (1998). Spontaneous electrical rhythmicity in cultured interstitial cells of Cajal from the murine small intestine. *Journal of Physiology*, *513*(1), 203–213. https://doi.org/10.1111/j.1469-7793.1998.203by.x

Komalavilas, P., & Lincoln, T. M. (1996). Phosphorylation of the inositol 1,4,5-trisphosphate receptor: Cyclic GMP-dependent protein kinase mediates cAMP and cGMP dependent phosphorylation in the intact rat aorta. *Journal of Biological Chemistry*, *271*(36), 21933–21938. https://doi.org/10.1074/jbc.271.36.21933

Korenaga, R., Ando, J., Tsuboi, H., Yang, W. D., Sakuma, I., Toyooka, T., & Kamiya, A. (1994). Laminar flow stimulates ATP- and shear stress-dependent nitric oxide production in cultured bovine endothelial cells. *Biochemical and Biophysical Research Communications*, *198*(1), 213–219. https://doi.org/10.1006/bbrc.1994.1030

Kurahashi, M., Nakano, Y., Hennig, G. W., Ward, S. M., & Sanders, K. M. (2012). Platelet-derived growth factor receptor α-positive cells in the tunica muscularis of human colon. *Journal of Cellular and Molecular Medicine*, *16*(7), 1397–1404. https://doi.org/10.1111/j.1582-4934.2011.01510.x

Lamy, C., Goodchild, S. J., Weatherall, K. L., Jane, D. E., Liégeois, J. F., Seutin, V., & Marrion, N. V. (2010). Allosteric block of KCa2 channels by apamin. *Journal of Biological Chemistry*, *285*(35), 27067–27077. https://doi.org/10.1074/jbc.M110.110072

Le Poul, E., Loison, C., Struyf, S., Springael, J. Y., Lannoy, V., Decobecq, M. E., Brezillon, S., Dupriez, V., Vassart, G., Van Damme, J., Parmentier, M., & Detheux, M. (2003). Functional characterization of human receptors for short chain fatty acids and their role in polymorphonuclear cell activation. *Journal of Biological Chemistry*, *278*(28), 25481–25489. https://doi.org/10.1074/jbc.M301403200

Lee, H., Koh, B. H., Peri, L. E., Sanders, K. M., & Koh, S. D. (2014). Purinergic inhibitory regulation of murine detrusor muscles mediated by PDGFRα+ interstitial cells. *Journal of Physiology*, *592*(6), 1283–1293. https://doi.org/10.1113/jphysiol.2013.267989

Lepretre, N., Mironneau, J., & Morel, J. L. (1994). Both α(1A)- and α(2A)-adrenoreceptor subtypes stimulate voltage-operated L-type calcium channels in rat portal vein myocytes.

Evidence for two distinct transduction pathways. *Journal of Biological Chemistry*, *269*(47), 29546–29552. https://doi.org/10.1016/s0021-9258(18)43914-2

Liu, Y.-A., Chung, Y.-C., Shen, M.-Y., Pan, S.-T., Kuo, C.-W., Peng, S.-J., Pasricha, P. J., & Tang, S.-C. (2015). Perivascular Interstitial Cells of Cajal in Human Colon. *Cellular and Molecular Gastroenterology and Hepatology*, *1*(1), 102–119. https://doi.org/10.1016/j.jcmgh.2014.11.003

Louis, P., & Flint, H. J. (2017). Formation of propionate and butyrate by the human colonic microbiota. *Environmental Microbiology*, *19*(1), 29–41. https://doi.org/10.1111/1462-2920.13589

Marletta, M. A. (1993). Nitric oxide synthase structure and mechanism. *Journal of Biological Chemistry*, *268*(17), 12231–12234. https://doi.org/10.1016/s0021-9258(18)31375-9

McConnell, M., & Iwakiri, Y. (2018). Biology of portal hypertension. *Hepatology International*, *12*(s1), 11–23. https://doi.org/10.1007/s12072-017-9826-x

McHugh, M. L. (2011). Multiple comparison analysis testing in ANOVA. *Biochemia Medica*, *21*(3), 203–209. https://doi.org/10.11613/bm.2011.029

Mendoza, S. A., Fang, J., Gutterman, D. D., Wilcox, D. A., Bubolz, A. H., Li, R., Suzuki, M., & Zhang, D. X. (2010). TRPV4-mediated endothelial Ca2+ influx and vasodilation in response to shear stress. *American Journal of Physiology - Heart and Circulatory Physiology*, *298*(2), 466–476. https://doi.org/10.1152/ajpheart.00854.2009

Mikami, D., Kobayashi, M., Uwada, J., Yazawa, T., Kamiyama, K., Nishimori, K., Nishikawa, Y., Nishikawa, S., Yokoi, S., Taniguchi, T., & Iwano, M. (2020). AR420626, a selective agonist of GPR41/FFA3, suppresses growth of hepatocellular carcinoma cells by inducing apoptosis via HDAC inhibition. *Therapeutic Advances in Medical Oncology*, *12*, 1758835920913432. https://doi.org/10.1177/1758835920913432

Miller, F. N., Nolph, K. D., Joshua, I. G., Wiegman, D. L., Harris, P. D., & Andersen, D. B. (1981). Hyperosmolality, acetate, and lactate: Dilatory factors during peritoneal dialysis. *Kidney International*, *20*(3), 397–402. https://doi.org/10.1038/ki.1981.152

Miller, T. L., & Wolin, M. J. (1996). Pathways of acetate, propionate, and butyrate formation by the human fecal microbial flora. *Applied and Environmental Microbiology*, *62*(5), 1589–1592. https://doi.org/10.1128/aem.62.5.1589-1592.1996

Mills, K. T., Bundy, J. D., Kelly, T. N., Reed, J. E., Kearney, P. M., Reynolds, K., Chen, J., & He, J. (2016). Global disparities of hypertension prevalence and control: A systematic analysis of population-based studies from 90 countries. *Circulation*, *134*(6), 441–450. https://doi.org/10.1161/CIRCULATIONAHA.115.018912

Mills, K. T., Stefanescu, A., & He, J. (2020). The global epidemiology of hypertension. *Nature Reviews Nephrology*, *16*(4), 223–237. https://doi.org/10.1038/s41581-019-0244-2

Mironneau, J., & Macrez-Leprêtre, N. (1995). Modulation of Ca2+ channels by α2A-and α2A-adrenoceptors in vascular myocytes: Involvement of different transduction pathways. *Cellular Signalling*, *7*(5), 471–479. https://doi.org/10.1016/0898-6568(95)00014-G

Mirza, H., Schmidt, V. A., Derian, C. K., Jesty, J., & Bahou, W. F. (1997). Mitogenic responses mediated through the proteinase-activated receptor-2 are induced by expressed forms of mast cell α- or β-tryptases. *Blood*, *90*(10), 3914–3922. https://doi.org/10.1182/blood.V90.10.3914

Mirza, H., Yatsula, V., & Bahou, W. F. (1996). The proteinase activated receptor-2 (PAR-2) mediates mitogenic responses in human vascular endothelial cells. *Journal of Clinical Investigation*, *97*(7), 1705–1714. https://doi.org/10.1172/JCI118597

Mishra, R. C., Mitchell, J. R., Gibbons-Kroeker, C., Wulff, H., Belenkie, I., Tyberg, J. V., & Braun, A. P. (2016). A pharmacologic activator of endothelial KCa channels increases systemic conductance and reduces arterial pressure in an anesthetized pig model. *Vascular Pharmacology*, *79*, 24–31. https://doi.org/10.1016/j.vph.2015.07.016

Mizuta, K., Sasaki, H., Zhang, Y., Matoba, A., & Emala, C. W. (2020). The short-chain free fatty acid receptor FFAR3 is expressed and potentiates contraction in human airway smooth muscle. *American Journal of Physiology-Lung Cellular and Molecular Physiology*, *318*(6), L1248–L1260. https://doi.org/10.1152/ajplung.00357.2019

Molino, M., Raghunath, P. N., Kuo, A., Ahuja, M., Hoxie, J. A., Brass, L. F., & Barnathan, E. S. (1998). Differential expression of functional protease-activated receptor-2 (PAR-2) in human vascular smooth muscle cells. *Arteriosclerosis, Thrombosis, and Vascular Biology*, *18*(5), 825–832. https://doi.org/10.1161/01.ATV.18.5.825

Moncada, S., Gryglewski, R., Bunting, S., & Vane, J. R. (1976). An enzyme isolated from arteries transforms prostaglandin endoperoxides to an unstable substance that inhibits platelet aggregation. *Nature*, *263*(5579), 663–665. https://doi.org/10.1038/263663a0

Moreau, N. M., Goupry, S. M., Antignac, J. P., Monteau, F. J., Le Bizec, B. J., Champ, M. M., Martin, L. J., & Dumon, H. J. (2003). Simultaneous measurement of plasma concentrations and 13C-enrichment of short-chain fatty acids, lactic acid and ketone bodies by gas chromatography coupled to mass spectrometry. *Journal of Chromatography B: Analytical Technologies in the Biomedical and Life Sciences*, *784*(2), 395–403. https://doi.org/10.1016/S1570-0232(02)00827-9

Morrison, D. J., & Preston, T. (2016). Formation of short chain fatty acids by the gut microbiota and their impact on human metabolism. *Gut Microbes*, *7*(3), 189–200. https://doi.org/10.1080/19490976.2015.1134082

Mortensen, F. V, Nielsen, H., Mulvany, M. J., & Hessov, I. (1990). Short chain fatty acids dilate isolated human colonic resistance arteries. *Gut*, *31*(12), 1391–1394. https://doi.org/10.1136/gut.31.12.1391

Mulè, F., Baffi, M. C., Capparelli, A., & Pizzuti, R. (2003). Involvement of nitric oxide and tachykinins in the effects induced by protease-activated receptors in rat colon longitudinal muscle. *British Journal of Pharmacology*, *139*(3), 598–604. https://doi.org/10.1038/sj.bjp.0705273

Mulè, F., Baffi, M. C., & Cerra, M. C. (2002). Dual effect mediated by protease-activated receptors on the mechanical activity of rat colon. *British Journal of Pharmacology*, *136*(3), 367–374. https://doi.org/10.1038/sj.bjp.0704746

Mulè, F., Baffi, M. C., Falzone, M., & Cerra, M. C. (2002). Signal transduction pathways involved in the mechanical responses to protease-activated receptors in rat colon. *The Journal of Pharmacology and Experimental Therapeutics*, *303*(3), 1265–1272. https://doi.org/10.1124/jpet.102.041301

Mulvany, M. J., & Aalkjaer, C. (1990). Structure and function of small arteries. *Physiological Reviews*, *70*(4), 921–961. https://doi.org/10.1152/physrev.1990.70.4.921

Murthy, K. S., & Zhou, H. (2003). Selective phosphorylation of the IP3R-I in vivo by cGMP-dependent protein kinase in smooth muscle. *American Journal of Physiology - Gastrointestinal and Liver Physiology*, *284*(2), 221–230. https://doi.org/10.1152/ajpgi.00401.2002

Musch, M. W., Bookstein, C., Xie, Y., Sellin, J. H., & Chang, E. B. (2001). SCFA increase intestinal Na absorption by induction of NHE3 in rat colon and human intestinal C2/bbe cells. *American Journal of Physiology-Gastrointestinal and Liver Physiology*, *280*(4), G687–G693. https://doi.org/10.1152/ajpgi.2001.280.4.G687

Nair, H., Berzigotti, A., & Bosch, J. (2016). Emerging therapies for portal hypertension in cirrhosis. *Expert Opinion on Emerging Drugs*, *21*(2), 167–181. https://doi.org/10.1080/14728214.2016.1184647

Najjar, R. S., Moore, C. E., & Montgomery, B. D. (2018). A defined, plant-based diet utilized in an outpatient cardiovascular clinic effectively treats hypercholesterolemia and hypertension and reduces medications. *Clinical Cardiology*, *41*(3), 307–313. https://doi.org/10.1002/clc.22863

Nakamura, K., Koga, Y., Sakai, H., Homma, K., & Ikebe, M. (2007). cGMP-dependent relaxation of smooth muscle is coupled with the change in the phosphorylation of myosin phosphatase. *Circulation Research*, *101*(7), 712–722. https://doi.org/10.1161/CIRCRESAHA.107.153981

Narang, D., Kerr, P. M., Lunn, S. E., Beaudry, R., Sigurdson, J., Lalies, M. D., Hudson, A. L., Light, P. E., Holt, A., & Plane, F. (2014). Modulation of resistance artery tone by the trace amine β-phenylethylamine: Dual indirect sympathomimetic and α1-adrenoceptor blocking actions. *Journal of Pharmacology and Experimental Therapeutics*, *351*(1), 164–171. https://doi.org/10.1124/jpet.114.216523

Nardocci, M., Leclerc, B. S., Louzada, M. L., Monteiro, C. A., Batal, M., & Moubarac, J. C. (2019). Consumption of ultra-processed foods and obesity in Canada. *Canadian Journal of Public Health*, *110*(1), 4–14. https://doi.org/10.17269/s41997-018-0130-x

Natarajan, N., Hori, D., Flavahan, S., Steppan, J., Flavahan, N. A., Berkowitz, D. E., & Pluznick, J. L. (2016). Microbial short chain fatty acid metabolites lower blood pressure via endothelial G protein-coupled receptor 41. *Physiological Genomics*, *48*(11), 826–834. https://doi.org/10.1152/physiolgenomics.00089.2016

Nava, E., & Llorens, S. (2019). The Local Regulation of Vascular Function: From an Inside-Outside to an Outside-Inside Model. *Frontiers in Physiology*, *10*, 1–15. https://doi.org/10.3389/fphys.2019.00729

Négrerie, M., Bouzhir, L., Martin, J. L., & Liebl, U. (2001). Control of nitric oxide dynamics by guanylate cyclase in its activated state. *The Journal of Biological Chemistry*, *276*(50), 46815–46821. https://doi.org/10.1074/jbc.M102224200

Nishikawa, H., Kawai, K., Nishimura, S., Tanaka, S., Araki, H., Al-Ani, B., Hollenberg, M. D., Kuroda, R., & Kawabata, A. (2002). Suppression by protease-activated receptor-2 activation of gastric acid secretion in rats. *European Journal of Pharmacology*, *447*(1), 87–90. https://doi.org/10.1016/S0014-2999(02)01892-7

Nutting, C. W., Islam, S., & Daugirdas, J. T. (1991). Vasorelaxant effects of short chain fatty acid salts in rat caudal artery. *American Journal of Physiology-Heart and Circulatory Physiology*, *261*(2), H561–H567. https://doi.org/10.1152/ajpheart.1991.261.2.H561

Nystedt, S., Emilsson, K., Wahlestedt, C., & Sundelin, J. (1994). Molecular cloning of a potential proteinase activated receptor. *Proceedings of the National Academy of Sciences of the United States of America*, *91*(20), 9208–9212. https://doi.org/10.1073/pnas.91.20.9208

O'Neil, A., Quirk, S. E., Housden, S., Brennan, S. L., Williams, L. J., Pasco, J. A., Berk, M., & Jacka, F. N. (2014). Relationship between diet and mental health in children and adolescents: A systematic review. *American Journal of Public Health*, *104*(10), e31–e42. https://doi.org/10.2105/AJPH.2014.302110

Okamoto, T., Barton, M. J., Hennig, G. W., Birch, G. C., Grainger, N., Corrigan, R. D., Koh, S. D., Sanders, K. M., & Smith, T. K. (2014). Extensive projections of myenteric serotonergic neurons suggest they comprise the central processing unit in the colon. *Neurogastroenterology and Motility*, *26*(4), 556–570. https://doi.org/10.1111/nmo.12302

Onyszkiewicz, M., Gawrys-Kopczynska, M., Konopelski, P., Aleksandrowicz, M., Sawicka, A., Koźniewska, E., Samborowska, E., & Ufnal, M. (2019). Butyric acid, a gut bacteria metabolite, lowers arterial blood pressure via colon-vagus nerve signaling and GPR41/43 receptors. *Pflügers Archiv - European Journal of Physiology*, *471*(11–12), 1441–1453. https://doi.org/10.1007/s00424-019-02322-y

Onyszkiewicz, M., Gawrys-Kopczynska, M., Sałagaj, M., Aleksandrowicz, M., Sawicka, A., Koźniewska, E., Samborowska, E., & Ufnal, M. (2020). Valeric acid lowers arterial blood pressure in rats. *European Journal of Pharmacology*, *877*, 173086. https://doi.org/10.1016/j.ejphar.2020.173086

Padwal, R. S., Bienek, A., McAlister, F. A., Campbell, N. R. C., & Outcomes Research Task Force of the Canadian Hypertension Education Program. (2016). Epidemiology of hypertension in Canada: An update. *The Canadian Journal of Cardiology*, *32*(5), 687–694. https://doi.org/10.1016/j.cjca.2015.07.734

Pahakis, M. Y., Kosky, J. R., Dull, R. O., & Tarbell, J. M. (2007). The role of endothelial glycocalyx components in mechanotransduction of fluid shear stress. *Biochemical and Biophysical Research Communications*, *355*(1), 228–233. https://doi.org/10.1016/j.bbrc.2007.01.137

Palmer, R. M. J., Ferrige, A. G., & Moncada, S. (1987). Nitric oxide release accounts for the biological activity of endothelium-derived relaxing factor. *Nature*, *327*(6122), 524–526. https://doi.org/10.1038/327524a0

Pasternak, A., Szura, M., Gil, K., & Matyja, A. (2016). Interstitial cells of Cajal — systematic review. *Folia Morphologica*, *75*(3), 281–286. https://doi.org/10.5603/FM.a2016.0002

Paul, R. J. (1998). The role of phospholamban and SERCA3 in regulation of smooth muscle-endothelial cell signalling mechanisms: evidence from gene-ablated mice. *Acta Physiologica Scandinavica*, *164*(4), 589–597. https://doi.org/10.1111/j.1365-201x.1998.tb10704.x

Pease, J. H. B., & Wemmer, D. E. (1988). Solution Structure of Apamin Determined by Nuclear Magnetic Resonance and Distance Geometry. *Biochemistry*, *27*(22), 8491–8498. https://doi.org/10.1021/bi00422a029

Perry, R. J., Peng, L., Barry, N. A., Cline, G. W., Zhang, D., Cardone, R. L., Petersen, K. F., Kibbey, R. G., Goodman, A. L., & Shulman, G. I. (2016). Acetate mediates a microbiome–brain–β-cell axis to promote metabolic syndrome. *Nature*, *534*(7606), 213–217. https://doi.org/10.1038/nature18309

Phan, T. X., Ton, H. T., Gulyás, H., Pórszász, R., Tóth, A., Russo, R., Kay, M. W., Sahibzada, N., & Ahern, G. P. (2020). TRPV1 expressed throughout the arterial circulation regulates vasoconstriction and blood pressure. *Journal of Physiology*, *598*(24), 5639–5659. https://doi.org/10.1113/JP279909

Pittman, R. N. (2013). Oxygen transport in the microcirculation and its regulation. *Microcirculation*, *20*(2), 117–137. https://doi.org/10.1111/micc.12017

Pluznick, J. L., Protzko, R. J., Gevorgyan, H., Peterlin, Z., Sipos, A., Han, J., Brunet, I., Wan, L. X., Rey, F., Wang, T., Firestein, S. J., Yanagisawa, M., Gordon, J. I., Eichmann, A., Peti-Peterdi, J., & Caplan, M. J. (2013). Olfactory receptor responding to gut microbiota-derived signals plays a role in renin secretion and blood pressure regulation. *Proceedings of the National Academy of Sciences of the United States of America*, *110*(11), 4410–4415. https://doi.org/10.1073/pnas.1215927110

Pontarollo, G., Mann, A., Brandão, I., Malinarich, F., Schöpf, M., & Reinhardt, C. (2020). Protease-activated receptor signaling in intestinal permeability regulation. *FEBS Journal*, *287*(4), 645–658. https://doi.org/10.1111/febs.15055

Pórszász, R., Porkoláb, Á., Ferencz, A., Pataki, T., Szilvássy, Z., & Szolcsányi, J. (2002). Capsaicin-induced nonneural vasoconstriction in canine mesenteric arteries. *European Journal of Pharmacology*, *441*(3), 173–175. https://doi.org/10.1016/S0014-2999(01)01596-5

Pugsley, M. K., & Tabrizchi, R. (2000). The vascular system. An overview of structure and function. *Journal of Pharmacological and Toxicological Methods*, *44*(2), 333–340. https://doi.org/10.1016/S1056-8719(00)00125-8

Rabi, D. M., McBrien, K. A., Sapir-Pichhadze, R., Nakhla, M., Ahmed, S. B., Dumanski, S. M., Butalia, S., Leung, A. A., Harris, K. C., Cloutier, L., Zarnke, K. B., Ruzicka, M., Hiremath, S., Feldman, R. D., Tobe, S. W., Campbell, T. S., Bacon, S. L., Nerenberg, K. A., Dresser, G. K., … Daskalopoulou, S. S. (2020). Hypertension Canada's 2020 Comprehensive guidelines for the prevention, diagnosis, risk assessment, and treatment of hypertension in adults and children. *Canadian Journal of Cardiology*, *36*(5), 596–624.

https://doi.org/10.1016/j.cjca.2020.02.086

Raffai, G., Lódi, C., Illyés, G., Nádasy, G., & Monos, E. (2008). Increased diameter and enhanced myogenic response of saphenous vein induced by two-week experimental orthostasis are reversible. *Physiological Research*, *57*(2), 175–183. https://doi.org/10.33549/physiolres.931175

Ratz, P. H., & Miner, A. S. (2009). Role of protein kinase Cζ and calcium entry in KCl-induced vascular smooth muscle calcium sensitization and feedback control of cellular calcium levels. *Journal of Pharmacology and Experimental Therapeutics*, *328*(2), 399–408. https://doi.org/10.1124/jpet.108.142422

Rees, D. D., Palmer, R. M. J., Hodson, H. F., & Moncada, S. (1989). A specific inhibitor of nitric oxide formation from l-arginine attenuates endothelium-dependent relaxation. *British Journal of Pharmacology*, *96*(2), 418–424. https://doi.org/10.1111/j.1476-5381.1989.tb11833.x

Rees, D. D., Palmer, R. M. J., Schulz, R., Hodson, H. F., & Moncada, S. (1990). Characterization of three inhibitors of endothelial nitric oxide synthase in vitro and in vivo. *British Journal of Pharmacology*, *101*(3), 746–752. https://doi.org/10.1111/j.1476-5381.1990.tb14151.x

Rothmeier, A. S., & Ruf, W. (2012). Protease-activated receptor 2 signaling in inflammation. *Seminars in Immunopathology*, *34*(1), 133–149. https://doi.org/10.1007/s00281-011-0289-1

Rouse, I. L., Beilin, L. J., Armstrong, B. K., & Vandongen, R. (1984). Vegetarian diet, blood pressure and cardiovascular risk. *Australian and New Zealand Journal of Medicine*, *14*(4), 439–443. https://doi.org/10.1111/j.1445-5994.1984.tb03611.x

Rübsamen, K., & von Engelhardt, W. (1981). Absorption of Na, H ions and short chain fatty acids from the sheep colon. *Pflügers Archiv - European Journal of Physiology*, *391*(2), 141–146. https://doi.org/10.1007/BF00657005

Russell-Puleri, S., dela Paz, N. G., Adams, D., Chattopadhyay, M., Cancel, L., Ebong, E., Orr, A. W., Frangos, J. A., & Tarbell, J. M. (2017). Fluid shear stress induces upregulation of COX-2 and PGI2 release in endothelial cells via a pathway involving PECAM-1, PI3K, FAK, and p38. *American Journal of Physiology - Heart and Circulatory Physiology*, *312*(3), H485–H500. https://doi.org/10.1152/ajpheart.00035.2016

Saifeddine, M., Al-Ani, B., Cheng, C. H., Wang, L., & Hollenberg, M. D. (1996). Rat proteinase-activated receptor-2 (PAR-2): cDNA sequence and activity of receptor-derived peptides in gastric and vascular tissue. *British Journal of Pharmacology*, *118*(3), 521–530. https://doi.org/10.1111/j.1476-5381.1996.tb15433.x

Sakakibara, S., Murakami, R., Takahashi, M., Fushimi, T., Murohara, T., Kishi, M., Kajimoto, Y., Kitakaze, M., & Kaga, T. (2010). Vinegar intake enhances flow-mediated vasodilatation via upregulation of endothelial nitric oxide synthase activity. *Bioscience, Biotechnology, and Biochemistry*, *74*(5), 1055–1061. https://doi.org/10.1271/bbb.90953

Samuel, B. S., Shaito, A., Motoike, T., Rey, F. E., Backhed, F., Manchester, J. K., Hammer, R. E., Williams, S. C., Crowley, J., Yanagisawa, M., & Gordon, J. I. (2008). Effects of the gut

microbiota on host adiposity are modulated by the short-chain fatty-acid binding G protein-coupled receptor, Gpr41. *Proceedings of the National Academy of Sciences*, *105*(43), 16767–16772. https://doi.org/10.1073/pnas.0808567105

Sanders, K. M. (2019). Spontaneous Electrical Activity and Rhythmicity in Gastrointestinal Smooth Muscles. *Advances in Experimental Medicine and Biology*, *1124*, 3–46. https://doi.org/10.1007/978-981-13-5895-1_1

Sanders, K. M., Kito, Y., Hwang, S. J., & Ward, S. M. (2016). Regulation of gastrointestinal smooth muscle function by interstitial cells. *Physiology*, *31*(5), 316–326. https://doi.org/10.1152/physiol.00006.2016

Sandow, S. L., Neylon, C. B., Chen, M. X., & Garland, C. J. (2006). Spatial separation of endothelial small- and intermediate-conductance calcium-activated potassium channels (K(Ca)) and connexins: Possible relationship to vasodilator function? *Journal of Anatomy*, *209*(5), 689–698. https://doi.org/10.1111/j.1469-7580.2006.00647.x

Saneei, P., Salehi-Abargouei, A., Esmaillzadeh, A., & Azadbakht, L. (2014). Influence of Dietary Approaches to Stop Hypertension (DASH) diet on blood pressure: A systematic review and meta-analysis on randomized controlled trials. *Nutrition, Metabolism and Cardiovascular Diseases*, *24*(12), 1253–1261. https://doi.org/10.1016/j.numecd.2014.06.008

Sato, K., Ninomiya, H., Ohkura, S., Ozaki, H., & Nasu, T. (2006). Impairment of PAR-2-mediated relaxation system in colonic smooth muscle after intestinal inflammation. *British Journal of Pharmacology*, *148*(2), 200–207. https://doi.org/10.1038/sj.bjp.0706717

Schermuly, R. T., Ghofrani, H. A., Wilkins, M. R., & Grimminger, F. (2011). Mechanisms of disease: Pulmonary arterial hypertension. *Nature Reviews Cardiology*, *8*(8), 443–455. https://doi.org/10.1038/nrcardio.2011.87

Schiffrin, E. L. (1992). Reactivity of small blood vessels in hypertension: Relation with structural changes. *Hypertension*, *19*(2 Suppl), II1–II9. https://doi.org/10.1161/01.HYP.19.2_Suppl.II1-a

Schiffrin, E. L. (2004). Remodeling of resistance arteries in essential hypertension and effects of antihypertensive treatment. *American Journal of Hypertension*, *17*(12), 1192–1200. https://doi.org/10.1016/j.amjhyper.2004.05.023

Schlossmann, J., Feil, R., & Hofmann, F. (2003). Signaling through NO and cGMP-dependent protein kinases. *Annals of Medicine*, *35*(1), 21–27. https://doi.org/10.1080/07853890310004093

Schwiertz, A., Taras, D., Schäfer, K., Beijer, S., Bos, N. A., Donus, C., & Hardt, P. D. (2010). Microbiota and SCFA in Lean and Overweight Healthy Subjects. *Obesity*, *18*(1), 190–195. https://doi.org/10.1038/oby.2009.167

Schwingshackl, L., Chaimani, A., Schwedhelm, C., Toledo, E., Pünsch, M., Hoffmann, G., & Boeing, H. (2019). Comparative effects of different dietary approaches on blood pressure in hypertensive and pre-hypertensive patients: A systematic review and network meta-analysis. *Critical Reviews in Food Science and Nutrition*, *59*(16), 2674–2687.

https://doi.org/10.1080/10408398.2018.1463967

Seitz, B. M., Krieger-Burke, T., Fink, G. D., & Watts, S. W. (2016). Serial measurements of splanchnic vein diameters in rats using high-frequency ultrasound. *Frontiers in Pharmacology*, *7*, 116. https://doi.org/10.3389/fphar.2016.00116

Sekirov, I., Russell, S. L., Caetano M Antunes, L., & Finlay, B. B. (2010). Gut microbiota in health and disease. *Physiological Reviews*, *90*(3), 859–904. https://doi.org/10.1152/physrev.00045.2009

Shi, H., Zhang, B., Abo-Hamzy, T., Nelson, J. W., Ambati, C. S. R., Petrosino, J. F., Bryan, R. M., & Durgan, D. J. (2021). Restructuring the gut microbiota by intermittent fasting lowers blood pressure. *Circulation Research*, *128*(9), 1240–1254. https://doi.org/10.1161/CIRCRESAHA.120.318155

Shoukas, A. A., & Bohlen, H. G. (1990). Rat venular pressure-diameter relationships are regulated by sympathetic activity. *American Journal of Physiology-Heart and Circulatory Physiology*, *259*(3), H674–H680. https://doi.org/10.1152/ajpheart.1990.259.3.H674

Skrzypecki, J., Niewęgłowska, K., & Samborowska, E. (2020). Valeric acid, a gut microbiota product, penetrates to the eye and lowers intraocular pressure in rats. *Nutrients*, *12*(2), 387. https://doi.org/10.3390/nu12020387

Skrzypecki, J., Żera, T., & Ufnal, M. (2018). Butyrate, a gut bacterial metabolite, lowers intraocular pressure in normotensive but not in hypertensive rats. *Journal of Glaucoma*, *27*(9), 823–827. https://doi.org/10.1097/IJG.0000000000001025

Sprague, B., Chesler, N. C., & Magness, R. R. (2010). Shear stress regulation of nitric oxide production in uterine and placental artery endothelial cells: Experimental studies and hemodynamic models of shear stresses on endothelial cells. *International Journal of Developmental Biology*, *54*(2–3), 331–339. https://doi.org/10.1387/ijdb.082832bs

Staszyk, C., Bohnet, W., Gasse, H., & Hackbarth, H. (2003). Blood vessels of the rat tail: A histological re-examination with respect to blood vessel puncture methods. *Laboratory Animals*, *37*(2), 121–125. https://doi.org/10.1258/00236770360563750

Steenbergen, J. M., & Bohlen, H. G. (1993). Sodium hyperosmolarity of intestinal lymph causes arteriolar vasodilation in part mediated by EDRF. *American Journal of Physiology-Heart and Circulatory Physiology*, *265*(1), H323–H328. https://doi.org/10.1152/ajpheart.1993.265.1.H323

Stumpff, F. (2018). A look at the smelly side of physiology: transport of short chain fatty acids. *Pflügers Archiv - European Journal of Physiology*, *470*(4), 571–598. https://doi.org/10.1007/s00424-017-2105-9

Stumpff, F., Georgi, M. I., Mundhenk, L., Rabbani, I., Fromm, M., Martens, H., & Günzel, D. (2011). Sheep rumen and omasum primary cultures and source epithelia: Barrier function aligns with expression of tight junction proteins. *Journal of Experimental Biology*, *214*(17), 2871–2882. https://doi.org/10.1242/jeb.055582

Sukumaran, S. V., Singh, T. U., Parida, S., Narasimha Reddy, C. E., Thangamalai, R., Kandasamy, K., Singh, V., & Mishra, S. K. (2013). TRPV4 channel activation leads to

endothelium-dependent relaxation mediated by nitric oxide and endothelium-derived hyperpolarizing factor in rat pulmonary artery. *Pharmacological Research*, *78*, 18–27. https://doi.org/10.1016/j.phrs.2013.09.005

Sung, T. S., Kim, H. U., Kim, J. H., Lu, H., Sanders, K. M., & Koh, S. D. (2015). Protease-activated receptors modulate excitability of murine colonic smooth muscles by differential effects on interstitial cells. *The Journal of Physiology*, *593*(5), 1169–1181. https://doi.org/10.1113/jphysiol.2014.285148

Sung, T. S., Lu, H., Sung, J., Yeom, J. H., Perrino, B. A., & Koh, S. D. (2018). The functional role of protease-activated receptors on contractile responses by activation of Ca2+ sensitization pathways in simian colonic muscles. *American Journal of Physiology - Gastrointestinal and Liver Physiology*, *315*(6), G921–G931. https://doi.org/10.1152/ajpgi.00255.2018

Takano, H., Dora, K. A., & Garland, C. J. (2005). Spreading vasodilatation in resistance arteries. *Journal of Smooth Muscle Research*, *41*(6), 303–311. https://doi.org/10.1540/jsmr.41.303

Takayama, I., Horiguchi, K., Daigo, Y., Mine, T., Fujino, M. A., & Ohno, S. (2002). The interstitial cells of Cajal and a gastroenteric pacemaker system. *Archives of Histology and Cytology*, *65*(1), 1–26. https://doi.org/10.1679/aohc.65.1

Tazoe, H., Otomo, Y., Karaki, S., Kato, I., Fukami, Y., Terasaki, M., & Kuwahara, A. (2009). Expression of short-chain fatty acid receptor GPR41 in the human colon. *Biomedical Research*, *30*(3), 149–156. https://doi.org/10.2220/biomedres.30.149

Tertyshnikova, S., Yan, X., & Fein, A. (1998). cGMP inhibits IP3-induced Ca2+ release in intact rat megakaryocytes via cGMP- and cAMP-dependent protein kinases. *Journal of Physiology*, *512*(1), 89–96. https://doi.org/10.1111/j.1469-7793.1998.089bf.x

Tian, Z., Zhuang, X., Luo, M., Yin, W., & Xiong, L. (2020). The propionic acid and butyric acid in serum but not in feces are increased in patients with diarrhea-predominant irritable bowel syndrome. *BMC Gastroenterology*, *20*(1), 73. https://doi.org/10.1186/s12876-020-01212-3

Timmermans, P. B., Van Meel, J. C., & Van Zwieten, P. A. (1980). Evaluation of the selectivity of alpha-adrenoreceptor blocking drugs for postsynaptic alpha 1- and alpha 2-adrenoreceptors in a simple animal model. *Journal of Autonomic Pharmacology*, *1*(1), 53–60. https://doi.org/10.1111/j.1474-8673.1980.tb00441.x

Titgemeyer, E. C., Bourquin, L. D., Fahey, G. C., & Garleb, K. A. (1991). Fermentability of various fiber sources by human fecal bacteria in vitro. *The American Journal of Clinical Nutrition*, *53*(6), 1418–1424. https://doi.org/10.1093/ajcn/53.6.1418

Tomuschat, C., O'Donnell, A. M., Coyle, D., & Puri, P. (2020). Increased protease activated receptors in the colon of patients with Hirschsprung's disease. *Journal of Pediatric Surgery*, *55*(8), 1488–1494. https://doi.org/10.1016/j.jpedsurg.2019.11.009

Toral, M., Robles-Vera, I., de la Visitación, N., Romero, M., Sánchez, M., Gómez-Guzmán, M., Rodriguez-Nogales, A., Yang, T., Jiménez, R., Algieri, F., Gálvez, J., Raizada, M. K., & Duarte, J. (2019). Role of the immune system in vascular function and blood pressure control induced by faecal microbiota transplantation in rats. *Acta Physiologica*, *227*(1),

e13285. https://doi.org/10.1111/apha.13285

Torihashi, S., Ward, S. M., Nishikawa, S., Nishi, K., Kobayashi, S., & Sanders, K. M. (1995). c-kit-Dependent development of interstitial cells and electrical activity in the murine gastrointestinal tract. *Cell and Tissue Research*, *280*(1), 97–111. https://doi.org/10.1007/BF00304515

Touyz, R. M., Alves-Lopes, R., Rios, F. J., Camargo, L. L., Anagnostopoulou, A., Arner, A., & Montezano, A. C. (2018). Vascular smooth muscle contraction in hypertension. *Cardiovascular Research*, *114*(4), 529–539. https://doi.org/10.1093/cvr/cvy023

Tran, Q. K., Ohashi, K., & Watanabe, H. (2000). Calcium signalling in endothelial cells. *Cardiovascular Research*, *48*(1), 13–22. https://doi.org/10.1016/S0008-6363(00)00172-3

Turnbaugh, P. J., Bäckhed, F., Fulton, L., & Gordon, J. I. (2008). Diet-induced obesity is linked to marked but reversible alterations in the mouse distal gut microbiome. *Cell Host & Microbe*, *3*(4), 213–223. https://doi.org/10.1016/j.chom.2008.02.015

Tykocki, N. R., Boerman, E. M., & Jackson, W. F. (2017). Smooth muscle ion channels and regulation of vascular tone in resistance arteries and arterioles. *Comprehensive Physiology*, *7*(2), 485–581. https://doi.org/10.1002/cphy.c160011

Uehata, M., Ishizaki, T., Satoh, H., Ono, T., Kawahara, T., Morishita, T., Tamakawa, H., Yamagami, K., Inui, J., Maekawa, M., & Narumiya, S. (1997). Calcium sensitization of smooth muscle mediated by a Rho-associated protein kinase in hypertension. *Nature*, *389*(6654), 990–994. https://doi.org/10.1038/40187

Ulven, E. R., Quon, T., Sergeev, E., Barki, N., Brvar, M., Hudson, B. D., Dutta, P., Hansen, A. H., Bielefeldt, L. Ø., Tobin, A. B., McKenzie, C. J., Milligan, G., & Ulven, T. (2020). Structure–Activity Relationship Studies of Tetrahydroquinolone Free Fatty Acid Receptor 3 Modulators. *Journal of Medicinal Chemistry*, *63*(7), 3577–3595. https://doi.org/10.1021/acs.jmedchem.9b02036

Underbakke, E. S., Iavarone, A. T., Chalmers, M. J., Pascal, B. D., Novick, S., Griffin, P. R., & Marletta, M. A. (2014). Nitric oxide-induced conformational changes in soluble guanylate cyclase. *Structure*, *22*(4), 602–611. https://doi.org/10.1016/j.str.2014.01.008

VanBavel, E., Sorop, O., Andreasen, D., Pfaffendorf, M., & Jensen, B. L. (2002). Role of T-type calcium channels in myogenic tone of skeletal muscle resistance arteries. *American Journal of Physiology-Heart and Circulatory Physiology*, *283*(6), H2239–H2243. https://doi.org/10.1152/ajpheart.00531.2002

Vanderwinden, J. M., Rumessen, J. J., De Kerchove d'Exaerde, A., Gillard, K., Panthier, J. J., Laet, M. H. De, & Schiffmann, S. N. (2002). Kit-negative fibroblast-like cells expressing SK3, a Ca2+-activated K+ channel, in the gut musculature in health and disease. *Cell and Tissue Research*, *310*(3), 349–358. https://doi.org/10.1007/s00441-002-0638-4

Vanhoutte, P. M., Shimokawa, H., Feletou, M., & Tang, E. H. C. (2017). Endothelial dysfunction and vascular disease - a 30th anniversary update. *Acta Physiologica*, *219*(1), 22–96. https://doi.org/10.1111/apha.12646

VanTeeffelen, J. W. G. E., Brands, J., Jansen, C., Spaan, J. A. E., & Vink, H. (2007). Heparin

impairs glycocalyx barrier properties and attenuates shear dependent vasodilation in mice. *Hypertension*, *50*(1), 261–267. https://doi.org/10.1161/HYPERTENSIONAHA.107.089250

Vincent, F., Acevedo, A., Nguyen, M. T., Dourado, M., DeFalco, J., Gustafson, A., Spiro, P., Emerling, D. E., Kelly, M. G., & Duncton, M. A. J. (2009). Identification and characterization of novel TRPV4 modulators. *Biochemical and Biophysical Research Communications*, *389*(3), 490–494. https://doi.org/10.1016/j.bbrc.2009.09.007

Vu, T. K. H., Hung, D. T., Wheaton, V. I., & Coughlin, S. R. (1991). Molecular cloning of a functional thrombin receptor reveals a novel proteolytic mechanism of receptor activation. *Cell*, *64*(6), 1057–1068. https://doi.org/10.1016/0092-8674(91)90261-V

Vuorinen, P., Pörsti, I., Metsä-Ketelä, T., Manninen, V., Vapaatalo, H., & Laustiola, K. E. (1992). Endothelium-dependent and -independent effects of exogenous ATP, adenosine, GTP and guanosine on vascular tone and cyclic nucleotide accumulation of rat mesenteric artery. *British Journal of Pharmacology*, *105*(2), 279–284. https://doi.org/10.1111/j.1476-5381.1992.tb14246.x

Wang, G., Kostidis, S., Tiemeier, G. L., Sol, W. M. P. J., de Vries, M. R., Giera, M., Carmeliet, P., van den Berg, B. M., & Rabelink, T. J. (2020). Shear Stress Regulation of Endothelial Glycocalyx Structure Is Determined by Glucobiosynthesis. *Arteriosclerosis, Thrombosis, and Vascular Biology*, *40*(2), 350–364. https://doi.org/10.1161/ATVBAHA.119.313399

Ward, S. M., Ördög, T., Koh, S. D., Baker, S. A., Jun, J. Y., Amberg, G., Monaghan, K., & Sanders, K. M. (2000). Pacemaking in interstitial cells of Cajal depends upon calcium handling by endoplasmic reticulum and mitochondria. *Journal of Physiology*, *525*(2), 355–361. https://doi.org/10.1111/j.1469-7793.2000.t01-1-00355.x

Watanabe, H., Vriens, J., Prenen, J., Droogmans, G., Voets, T., & Nillus, B. (2003). Anandamide and arachidonic acid use epoxyeicosatrienoic acids to activate TRPV4 channels. *Nature*, *424*(6947), 434–438. https://doi.org/10.1038/nature01807

Won, Y.-J. J., Lu, V. B., Puhl, H. L., & Ikeda, S. R. (2013). β-Hydroxybutyrate modulates N-type calcium channels in rat sympathetic neurons by acting as an agonist for the G-protein-coupled receptor FFA3. *Journal of Neuroscience*, *33*(49), 19314–19325. https://doi.org/10.1523/JNEUROSCI.3102-13.2013

Wu, T., Rayner, C. K., Young, R. L., & Horowitz, M. (2013). Gut motility and enteroendocrine secretion. *Current Opinion in Pharmacology*, *13*(6), 928–934. https://doi.org/10.1016/j.coph.2013.09.002

Wulff, H., & Köhler, R. (2013). Endothelial small-conductance and intermediate-conductance KCa channels: An update on their pharmacology and usefulness as cardiovascular targets. *Journal of Cardiovascular Pharmacology*, *61*(2), 102–112. https://doi.org/10.1097/FJC.0b013e318279ba20

Wulff, H., Miller, M. J., Hänsel, W., Grissmer, S., Cahalan, M. D., & Chandy, K. G. (2000). Design of a potent and selective inhibitor of the intermediate- conductance Ca2+-activated K+ channel, IKCa1: A potential immunosuppressant. *Proceedings of the National Academy of Sciences of the United States of America*, *97*(14), 8151–8156. https://doi.org/10.1073/pnas.97.14.8151

Xia, C., Bao, Z., Yue, C., Sanborn, B. M., & Liu, M. (2001). Phosphorylation and regulation of G-protein-activated phospholipase C-beta 3 by cGMP-dependent protein kinases. *The Journal of Biological Chemistry*, *276*(23), 19770–19777. https://doi.org/10.1074/jbc.M006266200

Xu, W. F., Andersen, H., Whitmore, T. E., Presnell, S. R., Yee, D. P., Ching, A., Gilbert, T., Davie, E. W., & Foster, D. C. (1998). Cloning and characterization of human protease-activated receptor 4. *Proceedings of the National Academy of Sciences of the United States of America*, *95*(12), 6642–6646. https://doi.org/10.1073/pnas.95.12.6642

Yamazawa, T., & Iino, M. (2002). Simultaneous imaging of Ca2+ signals in interstitial cells of Cajal and longitudinal smooth muscle cells during rhythmic activity in mouse ileum. *Journal of Physiology*, *538*(3), 823–835. https://doi.org/10.1113/jphysiol.2001.013045

Yang, T., Santisteban, M. M., Rodriguez, V., Li, E., Ahmari, N., Carvajal, J. M., Zadeh, M., Gong, M., Qi, Y., Zubcevic, J., Sahay, B., Pepine, C. J., Raizada, M. K., & Mohamadzadeh, M. (2015). Gut dysbiosis is linked to hypertension. *Hypertension*, *65*(6), 1331–1340. https://doi.org/10.1161/HYPERTENSIONAHA.115.05315

Zaharia, V., Varzescu, M., Djavadi, I., Newman, E., Egnor, R. W., Alexander-Chacko, J., & Charney, A. N. (2001). Effects of short chain fatty acids on colonic Na+ absorption and enzyme activity. *Comparative Biochemistry and Physiology Part A: Molecular & Integrative Physiology*, *128*(2), 335–347. https://doi.org/10.1016/S1095-6433(00)00318-4

Zakaria, E. R., Hunt, C. M., Li, N., Harris, P. D., & Garrison, R. N. (2005). Disparity in osmolarity-induced vascular reactivity. *Journal of the American Society of Nephrology*, *16*(10), 2931–2940. https://doi.org/10.1681/ASN.2004090764

Zhang, T., Yang, Y., Liang, Y., Jiao, X., & Zhao, C. (2018). Beneficial effect of intestinal fermentation of natural polysaccharides. *Nutrients*, *10*(8), 1055. https://doi.org/10.3390/nu10081055

Zheng, Y. M., Wang, Q. S., Liu, Q. H., Rathore, R., Yadav, V., & Wang, Y. X. (2008). Heterogeneous gene expression and functional activity of ryanodine receptors in resistance and conduit pulmonary as well as mesenteric artery smooth muscle cells. *Journal of Vascular Research*, *45*(6), 469–479. https://doi.org/10.1159/000127438

Zhu, M. H., Kim, T. W., Ro, S., Yan, W., Ward, S. M., Koh, S. D., & Sanders, K. M. (2009). A Ca2+-activated Cl- conductance in interstitial cells of Cajal linked to slow wave currents and pacemaker activity. *Journal of Physiology*, *587*(20), 4905–4918. https://doi.org/10.1113/jphysiol.2009.176206